Title

Moving cargo, keeping whales: Investigating solutions for ocean noise pollution

Journal

The Journal of the Acoustical Society of America, 155(3_Supplement)

ISSN

0001-4966

Authors

ZoBell, Vanessa M

Hildebrand, John

Frasier, Kait

Publication Date

2024-03-01

DOI

10.1121/10.0027065

Peer reviewed

UNIVERSITY OF CALIFORNIA SAN DIEGO

Moving Cargo, Keeping Whales: Investigating Solutions for Ocean Noise Pollution

A Dissertation submitted in partial satisfaction of the requirements
for the degree Doctor of Philosophy

in

Oceanography

by

Vanessa Mary Smith ZoBell

Committee in charge:
Professor John Hildebrand, Chair
Professor Kaitlin Frasier, Co-Chair
Professor John Ahlquist
Professor Simone Baumann-Pickering
Professor William Hodgkiss

2023

The Dissertation of Vanessa Mary Smith ZoBell is approved, and it is acceptable in quality and form for publication on microfilm and electronically.

University of California San Diego

2023

DEDICATION

to all of the female scientists, ship crew, staff, mentors, and students who have paved the way in scientific research for current and future female scientists

to my family, friends, and mentors who supported me through the high highs and low lows of the past five years

EPIGRAPH

To save wildlife and wild places the traction has to come not from the regurgitation of bad-news data but from the poets, prophets, preachers, professors, and presidents who have always dared to inspire.

– Dr. Drew Lanham

TABLE OF CONTENTS

LIST OF FIGURES

LIST OF TABLES

ACKNOWLEDGEMENTS

I wish to extend my deepest gratitude to my co-advisers, John Hildebrand and Kaitlin Frasier for their support and guidance throughout my PhD. I first met John as an intern in his lab when I was in high school. He set me up on a computer where I analyzed the signature whistle theory of bottlenose dolphins. Although I was at first intimidated by the acoustic terminology he used, his enthusiasm about animals and science made me realize how great of an adviser and scientist he was, and I knew I wanted to continue learning from him if given the opportunity. I kept in touch with John over the years about my scientific endeavors and then began as an MS student in his lab. John linked me with Kaitlin Frasier during my first year. To be under her wing my first year was a gift. Kait is so humble you would never know how brilliant of a scientist she is. She has provided so much mentorship to not only me but every grad student in the Marine Bioacoustics Research Collaborative, even when they are not her students. She has been a caring and patient listening throughout the many versions, failures, bumps, and plot twists that have occurred throughout my graduate school experience. As John puts it, “Getting a zoom invite from Kait is like getting a zoom invite from God!” I am excited to keep learning from Kait as a post-doctoral scholar in her lab. I would also like to thank my committee, Simone Baumann-Pickering, William Hodgkiss and John Ahlquist. Simone is a powerhouse. I loved learning from her during her week- long cruise on the R/V Sproul. She was so comfortable on the ship and ran the operations like a boss. It was one of the huge inspirations for me to apply for a UC Ship Funds Grant and lead a cruise on the same ship. William Hodgkiss single-handedly taught me signal processing during my second year of graduate school. When COVID hit and we were all working from home, he explained the homework to me (which I got wrong 7 times in a row) over the phone for two hours. I will always appreciate his patience and enthusiasm for signal

processing. I got paired with John Ahlquist during the UCSD Science Policy Fellows Program. I immediately admired him for his quick wit and woke energy. Every time I came to him with an idea for how to make my thesis more applied to policy, he challenged me with many more ideas. These conversations made my research more multi-disciplinary, and I hope to continue learning from him in the future.

I would also like to thank the fellow graduate students in our lab that not only provided guidance on the PhD process but also in staying sane throughout a difficult five years, especially with the onset of COVID. Thank you to my first officemate, Jessica Sportelli, for starting off graduate school with a bang with me in our office (that was also an e-waste closet). I will never forget reading our horoscopes every Friday before TG. You will be a life-long friend of mine. Natalie Posdaljian was a mentor for me since the SIO open house when I met with her and went for a rainy walk. She never fails to give me the truth and tell me straight up how to fix a problem both in research and in my personal life. You are my work-wife and I consider you a sister. Thank you to Morgan Ziegenhorn for making our lab belly laugh constantly. You are creative and quick-witted. I love to be around you just to witness the hilarious things you say and do. I will be your bridesmaid any day. Thank you to Rebecca Cohen for paving the way in our lab and showing us all the ropes when we began. Thanks to Ella Bea Kim for being my friend for over ten years, after we first met as MPL interns with John and Simone. Our younger selves would be so proud of us now! You are my ocean sister and daily dip queen. Thanks to my current office mate, Michaela Alksne, for always making me laugh and not judging me when I leave food in the refrigerator too long. Thank you to the many other graduate students: Eric Snyder, Margaret Morris, Joe Walker, Eva Hidalgo, Regina Guazzo, and all SWAL graduate student alumni who have provided so much guidance and mentorship for me throughout the years. Thank you to the

staff members in SWAL: Bruce Thayre, John Hurwitz, and Jenny Trickey who brought me to sea and taught me how to build instruments. Special shout out to Kieran Lenssen, thank you for your friendship, our HARP trips are some of my best memories of graduate school. I will never forget our magical trip to the Azores where we were both mooring technicians on the R/V Pelagia!

I would not have made it to this point without my family and friends. Thank you to my dad, who taught me about Darwin's finches when we were at Subway eating spicy Italian subs. You have always inspired me to stay curious about the natural world, ask questions, and be kind and creative in the workplace. Thank you to my mom, who jumped in every body of water we came across growing up. Seeing you jump off of every rock and dock guided me to my own love of water. Your deep connection to the ocean is something I admire and hope to continue in my own life. Thank you to my sister, who is the smartest person I know. You make me strive to be my best self every day. I am thankful for you and Peter for letting me cry on your couch when grad school got really hard, and for housing me when I couldn't walk after ACL surgery. Thank you to my friends, mentors, teachers, classmates, and students, I would not be here without you all!

Chapter 1, in full, is a reprint of the material as it appears in Scientific Reports, ZoBell, Vanessa M., Kaitlin E. Frasier, Jessica A. Morten, Sean P. Hastings, Lindsey E. Peavey Reeves, Sean M. Wiggins, and John A. Hildebrand. "Underwater noise mitigation in the Santa Barbara Channel through incentive-based vessel speed reduction." The dissertation author was the primary investigator and author of this paper.

Chapter 2, in full, is a reprint of the material as it appears in PLOS One. ZoBell, Vanessa M., Martin Gassmann, Lee B. Kindberg, Sean M. Wiggins, John A. Hildebrand, and Kaitlin E.

Frasier. "Retrofit-induced changes in the radiated noise and monopole source levels of container ships." The dissertation author was the primary investigator and author of this paper.

Chapter 3 contains unpublished material coauthored with ZoBell, Vanessa M., John A. Hildebrand, and Kaitlin E. Frasier. The dissertation author was the primary author of this chapter.

Chapter 4, in part is currently being prepared for submission for publication of the material. ZoBell, Vanessa M., John A. Hildebrand, and Kaitlin E. Frasier. The dissertation author was the primary researcher and author of this material.

VITA

2017 Bachelor of Science in Wildlife, Fish, and Conservation Biology, University of California, Davis

2020 Master of Science in Marine Biology, University of California, San Diego

2023 Doctor of Philosophy in Oceanography, University of California, San Diego

PUBLICATIONS

ZoBell, Vanessa M., and Brett J. Furnas. "Impacts of land use and invasive species on native avifauna of Mo'orea, French Polynesia." *PeerJ* 5 (2017): e3761.

ZoBell, Vanessa M., Kaitlin E. Frasier, Jessica A. Morten, Sean P. Hastings, Lindsey E. Peavey Reeves, Sean M. Wiggins, and John A. Hildebrand. "Underwater noise mitigation in the Santa Barbara Channel through incentive-based vessel speed reduction." *Scientific reports* 11, no. 1 (2021): 18391.

ZoBell, Vanessa M., Martin Gassmann, Lee B. Kindberg, Sean M. Wiggins, John A. Hildebrand, and Kaitlin E. Frasier. "Retrofit-induced changes in the radiated noise and monopole source levels of container ships." *Plos one* 18, no. 3 (2023): e0282677.

ZoBell, Vanessa M., John A. Hildebrand, Kaitlin E. Frasier. Ship Noise Modeling in the Santa Barbara Channel: Establishing baselines and Effective Noise Reduction Efforts for Critical Habitats (in prep).

Walker, Joe, Zeng Zheng, **Vanessa M. ZoBell,** Kaitlin E. Frasier. Underwater sound speed profile estimation from vessel traffic recordings and multi-view neural networks. Journal of the Acoustical Society of America (2023, submitted).

FIELD OF STUDY

Major Field: Oceanography

Studies in marine bioacoustics, ocean acoustics, conservation biology
Professors John Hildebrand and Kaitlin Frasier

ABSTRACT OF THE DISSERTATION

Moving cargo, keeping whales: Investigating solutions for ocean noise pollution

by

Vanessa Mary Smith ZoBell

Doctor of Philosophy in Oceanography

University of California San Diego, 2023

Professor John Hildebrand, Chair
Professor Kaitlin Frasier, Co-Chair

Low-frequency (< 500 Hz) noise in the ocean is made up of natural abiotic sounds such as wind, biological sounds such as whale song, and anthropogenic noise such as sound radiated by ships (Wenz 1962; Hildebrand 2009). In areas exposed to commercial shipping, ship noise overtakes other sound sources in amplitude and is the dominant source of low-frequency noise. Over the past several decades, increases in the number, gross tonnage, and horsepower of

commercial vessels have led to higher ambient sound levels in the ocean (McDonald, Hildebrand, and Wiggins 2006; Ross 2005). Sound travels extremely efficiently in the ocean and marine organisms use sound for vital life functions including communication, foraging, and mating (Simpson et al. 2008; Bass and McKibben 2003; Wartzok and Ketten 2014). Because of this, increases in anthropogenic noise have profound impacts on marine organisms (Weilgart 2018; Erbe et al. 2019).

In Chapter 1, I partnered with a coalition of government agencies, non-profits, and environmental organizations to investigate an approach to noise reduction through incentive based vessel speed reduction. I share evidence for an operational approach to reducing the source level and sound exposure levels of vessels that participated voluntarily in the program. In Chapter 2, I collaborated with the largest container shipping company in the world, Maersk, to analyze changes in monopole source level and radiated noise level from a retrofitting initiative. I found that there were reductions below 100 Hz for monopole source levels post-retrofitting. For Chapter 3, I trained a fully connected neural network to predict source levels when provided with a suite of automatic identification system information. In Chapter 4, I mapped sound pressure levels for modern and primeval times. I analyzed different approaches to reducing noise and simulated the sound pressure level across the region to identify the most effective techniques to reduce noise.

Chapter 0: Introduction

Human-activities introduce high levels of noise into the ocean (Hildebrand et al., 2021). Commercial shipping, in particular, has increased to the point that ships make a larger contribution to ocean noise than natural noise sources for most ocean locations and over a broad range of frequencies. Studies of anthropogenic noise impacts on marine organisms have identified acoustic communication masking, increased stress hormone levels, decreased reproductive success, behavioral changes, and mortality as direct results of noise generated by ships (Erbe et al., 2019; Weilgart, 2018). The majority of the known impacts on marine invertebrates, fish, and mammals can be grouped into four categories: communication masking, behavioral changes, altered communication, and physiological impacts. When combined, these cumulative impacts can decrease fitness and may impact populations, negatively affecting the marine organisms that connect food webs, help build ecosystems, as well as provide sustenance, livelihood and cultural importance.

1. Communication masking- anthropogenic noise at similar frequencies to those used by a species can decrease communication ranges for these species (Blackwell et al., 2007; Cummings & Thompson, 1971; Guazzo et al., 2017; McIver et al., 2014; Munger et al., 2008; Payne & Webb, 1971; Schärer et al., 2013; Širović et al., 2004; Stimpert et al., 2011; Tellechea et al., 2011).

2. Behavioral changes- observed responses to anthropogenic noise include increased hiding behavior, changes in predator avoidance, decreased dive duration, altered breathing rates, and cessation of foraging (Blair et al., 2016; Christiansen et al., 2010; Dunlop et al., 2018; Filiciotto et al., 2014; Frankel & Clark, 2002; Lemon et al., 2006; Lusseau et al., 2009; Marley et al., 2017; Noren et al., 2009; Nowacek et al., 2001; Tsujii et al., 2018; Williams et al., 2014).

3. Altered communication behavior- noise can increase call rate and amplitude, and cause cessation of calling (Azzara et al., 2013; Cecilia Krahforst & Luczkovich, 2017; Dahlheim & Castellote, 2016; Guazzo et al., 2020; Helble et al., 2020; Kastelein et al., 2019; May-Collado & Quiñones-Lebrón, 2014; Thode et al., 2007; Tsujii et al., 2018; Williams et al., 2014).

4. Physiological impacts- noise can impair development of larvae, increase cortisol levels, and cause permanent or temporary damage to hearing (Anderson et al., 2011; Caiger et al., 2012; Jolivet et al., 2016; Kastelein et al., 2019; Nedelec et al., 2014, 2015; Nichols et al., 2015; Rolland et al., 2012; Wysocki et al., 2006).

With ample evidence that ship noise is detrimental to marine organisms, many organizations and agencies have stressed the need for mitigation strategies (Chou et al., 2021). These organizations include the International Maritime Organization (IMO), International Whaling Commission (IWC), European Union (EU), National Oceanic and Atmospheric Administration (NOAA), Convention of Migratory Species (CMS), and International Union for Conservation of Nature (IUCN).

Past studies indicate that reducing vessel speed may be an effective strategy for reducing noise in biologically sensitive areas (Gassmann et al., 2017; McKenna et al., 2013; Veirs et al., 2016) and as a result some regions have implemented speed reduction programs. One such program (ECHO) focused on noise reduction in Haro Strait, an important killer whale habitat at the U.S.-Canada border in the U.S. Pacific Northwest (MacGillivray et al., 2019). The effort, implemented by the Port of Vancouver, resulted in significant reductions in vessel noise source levels, which is the noise level 1 m away from the source (MacGillivray et al., 2019). Vessel speed reduction regulations were also implemented on the U.S. East Coast with the goal of reducing ship strikes with the North Atlantic Right Whale, although vessel noise reduction was

not a priority and therefore not quantified. Apart from the ECHO effort, there are no other vessel speed reduction programs that have quantified the effectiveness of this approach to noise reduction.

The Santa Barbara Channel, off southern California, is a highly trafficked shipping lane supporting transits to and from the port of Los Angeles, the busiest shipping port in the United States. In 2014, the Protecting Blue Whales and Blue Skies Program was implemented in the Santa Barbara Channel to allow vessels to voluntarily slow their speed in the hopes of reducing air pollution emissions and ship strikes. The effect of the program on vessel noise levels has not been investigated. For Chapter 1, I analyzed the effectiveness of this vessel speed reduction program in the Santa Barbara Channel in reducing underwater noise generated by participating vessels.

Speed reduction efforts may allow for regional reductions in vessel noise levels, but marine organisms are not restricted to these boundaries and may only benefit from these efforts for the portion of the year that they are in a managed area. The International Maritime Organization identified approaches to reduce noise generated from vessels independent of vessel speed, including design specifications and regular vessel maintenance, as an international approach to vessel noise reduction that could extend across boundaries. Specific propeller and bow designs that can be implemented while the vessel is being manufactured or during a retrofit (change after the vessel has been manufactured) have been identified as a tactic to potentially reduce cavitation, thereby reducing noise production during vessel operations in any region and at all speeds. Although these designs have been identified as potential approaches to reduce noise, their effectiveness for underwater noise reduction has not been studied. For Chapter 2, I

quantified the changes in ship sound levels before and after a retrofitting effort to identify whether the design is effective in reducing noise.

Speed reduction and retrofitting are both efforts that may reduce noise generation at the source, but the impacts of vessel noise are not equally harmful across all habitats. Spatial analysis is needed to target ecologically sensitive regions that should be prioritized for noise reduction. Mapping anthropogenic noise has been identified as a management approach for protecting marine organisms, with the goal of reducing noise in sensitive habitats that may be used for breeding or feeding (Erbe et al., 2012, 2021; Farcas et al., 2020). However, such mapping can be complicated by a number of unknown variables, such as the source levels of differing vessel types under a variety of operational conditions (Erbe et al., 2021; Macgillivray & de Jong, 2021). Sound level maps are highly dependent on accurate estimation of source levels. Source level models have proven to be difficult to create, with discrepancies between measurements of up to 30 dB for vessels within the same class in similar operating conditions (Chion et al., 2019). These differences are likely due to differences in propagation loss models and testing configurations used to estimate source levels, and can be mitigated by creating a source level model generated from measurements taken at high inclination angles and corrected for with robust propagation loss models. For Chapter 3, I established a source level model that incorporates ship type and speed by compiling ship transit data and using Lloyd's mirror model to account for propagation loss.

For Chapter 4, I modeled the natural ocean soundscape in the absence of ship noise using a wind-driven ocean noise model, to identify regions most significantly impacted by vessel noise, which can then be targeted for noise reduction management efforts. Without an estimate for what baseline noise levels in the ocean were historically and what marine organisms' auditory

and vocal systems evolved to thrive in, it is difficult to understand the extent that noise levels have changed and what management targets we should strive for. In order to understand the difference between the ship noise map and what a natural soundscape may have looked like prior to modern commercial shipping, I created a map of wind-driven ocean noise (the dominant source of natural low-frequency ocean noise) with an empirical wind noise model (Hildebrand et al., 2021) to be overlaid with an ocean noise map including the reality of anthropogenic noise in the modern ocean. In order to have a spatial understanding of noise reduction approaches, I then modeled a variety of different noise reduction simulations to investigate which approach was the most effective in reducing areas in three critical habitats: the blue whale Biologically Important Feeding Area (BIA), the humpback whale BIA, and the Channel Islands National Marine Sanctuary (CINMS).

Chapter 1: Underwater noise mitigation in the Santa Barbara Channel through Incentive Based Vessel Speed Reduction

1.1 Abstract

Commercial shipping is the dominant source of low-frequency noise in the ocean. It has been shown that the noise radiated by an individual vessel depends upon the vessel's speed. This study quantified the reduction in source levels (SLs) and sound exposure levels (SELs) for ships participating in two variations of a vessel speed reduction (VSR) program. SLs and SELs of individual ships participating in the program between 2014 and 2017 were statistically lower than non-participating ships ($p < 0.001$). In the 2018 fleet-based program, there were statistical differences between the SLs and SELs of fleets that participated with varying degrees of cooperation. Significant reductions in SL and SEL relied on cooperation of 25% or more in slowing vessel speed. This analysis highlights how slowing vessel speed to 10 knots or less is an effective method in reducing underwater noise emitted from commercial ships.

1.2 Introduction

Low-frequency noise (5-400 Hz) in the ocean is dominated by commercial shipping (Hildebrand 2009; Wenz 1962). In regions exposed to ship noise, ambient sound levels have risen over the past several decades due to increases in the number, gross tonnage, and horsepower of commercial vessels (McDonald, Hildebrand, and Wiggins 2006; Ross 2005). In addition to these parameters, vessel underwater radiated noise levels and vessel speed are positively correlated, suggesting noise pollution may be mitigated by reducing vessel speed (Gassmann, Wiggins, and Hildebrand 2017; MacGillivray et al. 2019; Megan F. McKenna et al. 2012; Megan F. McKenna, Wiggins, and Hildebrand 2013).

In 2014, the Channel Islands National Marine Sanctuary (CINMS) partnered with the Santa Barbara County Air Pollution Control District, Ventura County Air Pollution Control District, National Marine Sanctuary Foundation, and the Environmental Defense Center to implement a voluntary, incentive-based vessel speed reduction (VSR) initiative known as the Protecting Blue Whales and Blue Skies Program (hereafter VSR program) (Birney 2015). Enrollment was made available to companies operating container ships or vehicle carriers within the VSR zone, which extends approximately from Point Conception southeast to the Long Beach Harbor. Enrolled vessels were requested to reduce their speeds to a target speed to receive a financial reward. Vessels that participated in the VSR program from 2014 through 2017 received financial incentives of up to $2,500 per one-way transit and positive public press (Birney 2015; Byrd, M. Flannigan 2017). In 2018, the financial rewards ranged approximately from $1000 to $35,000 per company based on level of cooperation(National Marine Sanctuary Foundation 2018). In addition to its original goals of reducing the risk of ship strikes on endangered whales and decreasing air pollution emissions, the VSR program also recognizes the opportunity to address underwater noise pollution in the Santa Barbara Channel (SBC). For example, acute and chronic noise pollution generated from commercial shipping has been documented to impact marine mammals, fish, and invertebrates in the form of acoustic communication masking, behavioral alterations, increased physiological stress, and reduced reproductive success (Erbe et al. 2019; Weilgart 2018; Mckenna et al. 2009). Because of this, the potential for reducing noise pollution from commercial shipping by reducing vessel speed may allow the VSR program to address an even more comprehensive conservation initiative than originally anticipated.

The SBC is an ideal region for the study of underwater noise pollution due to its position as a basin shielded from deep ocean noise by the presence of the Channel Islands and its

proximity to the San Pedro Bay Port Complex (i.e., the ports of Los Angeles and Long Beach), which results in an abundance of low-frequency ambient noise that is directly correlated with commercial vessel traffic (Figure 1.1) (Mckenna et al. 2009). The Port of Los Angeles, in particular, is the busiest seaport in the United States, in terms of vessel traffic flow, and plays an essential role in the economic stability of California (Zhang et al. 2019). In addition to the economic importance of the SBC, measured by transported commerce, it is also a highly productive region that has led to a diversity and richness in zooplankton, fish, squid, and marine mammals (Checkley and Barth 2009; Star and Mullin 1981). The SBC is also an important summer foraging area for endangered baleen whale populations, as they aggregate in cold upwelling regions to feed primarily on krill (Barlow, 1995; Croll et al., 1998; Fiedler et al., 1998). Because of the ecologically important habitats in the SBC, noise pollution from commercial vessel traffic is a continuing management concern.

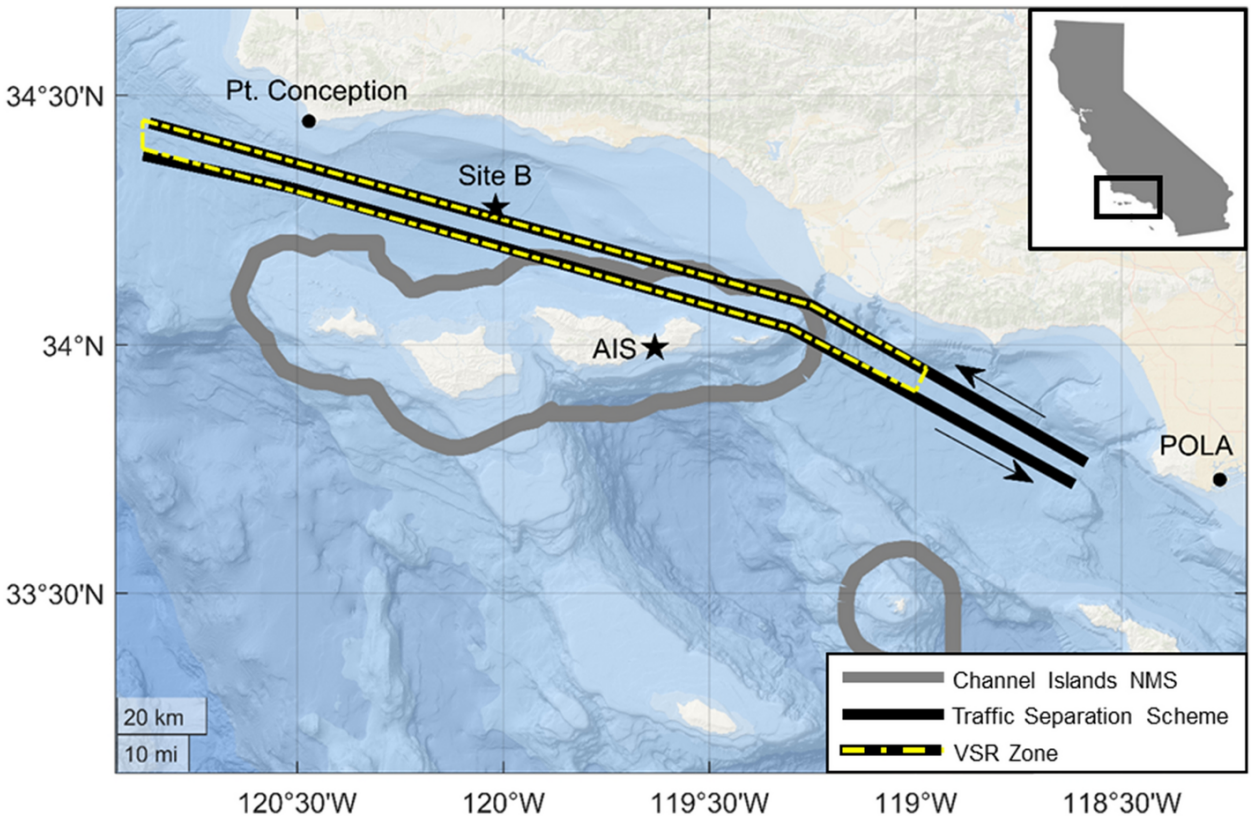

Figure 1. 1: Map of the Santa Barbara Channel. The boundary of the Channel Islands National Marine Sanctuary (NMS) is shown as gray lines, the Traffic Separation Scheme is shown as black lines, and the Vessel Speed Reduction zone is shown as a yellow dashed line. Arrows denote the northbound and southbound shipping lanes. Stars show the acoustic recorder location at Site B and the Automatic Identification System (AIS) antenna location on Santa Cruz Island. Map tiles are courtesy of arcgisonline.com.

In this study, we evaluated the efficacy of a VSR program in the SBC for reducing underwater radiated noise of participating vessels. By using long-term acoustic records from the SBC, we compared ship source levels (SLs) and sound exposure levels (SELs) in relation to Automatic Identification System (AIS) speed over ground (SOG) values measured at the closest point of approach to the recording site. SLs are estimated with a surface-reflection compensated spherical spreading propagation model and compared between VSR participants at different SOGs and levels of cooperation. The analysis allows for a comprehensive acoustic analysis of two variations of the incentive-based VSR program (transit-by-transit and fleet-based). Both of the approaches showed a reduction in SL and SEL estimates for participating vessels compared to non-compliant vessels when fleets slowed at least 25% of their transits in the VSR zone

1.3 Methods

1.3.1 Ship Passages

Locations of all ships, including ships that were not participating in the VSR program, transiting in the SBC were tracked by an AIS receiver located on Santa Ynez Peak that is maintained by the Santa Barbara Wireless Foundation (Figure 1.1). AIS messages were logged continuously by an on-site computer and decoded with the ShipPlotter program (ver. 12.4.6.5 COAA) for further analysis. To isolate ship transits on the northbound shipping lane, the monitoring area included transits within a 6 km radius of the acoustic recorder described below. Transits on the southbound shipping lane were excluded in order to minimize the ranges from the ships to the recording device. The ship name, IMO identification, type, speed over ground (SOG), draft, and position (latitude and longitude) were decoded from the AIS messages. The effect of surface currents on SOG was estimated to be less than 0.1 m s^{-1}, from a moored Acoustic Doppler Current Profiler (ADCP) in the Santa Barbara Channel34. Additional

information, such as ship length, was obtained from Lloyd's Register of Ships35. The detailed vessel type was identified with the Marine Traffic online database36. Ship types were categorized into three groups: container ships (including reefers), bulkers (including bulk carriers, general cargo, wood chip carriers, timber carriers, and other cargo types), and vehicle carriers (including roll-on roll-offs). Tankers were not targeted for speed reduction in the SBC in the Protecting Blue Whales and Blue Skies incentive program from 2014 through 2018, and therefore were not included in this study.

Vessels transits were eliminated if another vessel transit occurred within the monitoring area within 1 h to ensure that each ship transit was acoustically isolated8. To assess the ANSI/ASA (2009) environmental condition requirements for underwater measurements of ship sounds, wind speed from the National Oceanic and Atmospheric Administration (NOAA) buoy (station 46053) near the acoustic recorder were checked and any transits that were associated with wind speeds greater than 10.28 m s^{-1} were discarded, as higher wind speed can increase ambient noise levels37,38.

1.3.2 Acoustic Recordings

High-frequency Acoustic Recording Packages (HARPs) have been maintained at a long-term acoustic monitoring station (Site B) in the SBC (34° 16.2′ N, 120° 1.8′ W) at ~ 580 m depth, 3 km off of the northbound shipping lane from 2007 to present (Wiggins & Hildebrand, 2007) (Figure 1.1). HARP hydrophone electronics were calibrated at Scripps Institution of Oceanography and select full systems were calibrated at the U.S. Navy's Transducer Evaluation Center facility in San Diego, California. Acoustic recordings were collected at a sampling rate of 200 kHz over 1508 days between January 2014 and December 2018. To reduce computational requirements, the recordings were decimated by a factor of 20 resulting in a sampling rate of 10

kHz. The data were lowpass filtered with an 8th order Chebyshev Type I IIR filter to prevent aliasing during decimation. The acoustic recordings were scanned for data quality, and transits that were contaminated with low-frequency hydrophone cable strumming were excluded.

The underwater radiated source level (SL) from an individual vessel was estimated from the received sound pressure level (RL) by accounting for the frequency-dependent transmission loss (TL) at the distance from the source to the receiver at the closest point of approach (CPA),

$$SL = RL + TL$$

1.3.3 Received Level (RL)

Received levels for each vessel transit were averaged over the data window period that equaled the time it took the ship to travel its length, as defined in ANSI/ASA (2009) (Eq. 1). Received levels were calculated for each ship passage by dividing the sound pressure time series into 1 s non-overlapping segments. For each 1 s interval, a fast Fourier transform (FFT) and Hanning window with FFT length of 10,000 samples and no overlap provided the power spectral density (PSD) in 1 Hz bins. Ten times the base-10 logarithm of the PSD in 1 Hz bins was used to convert to sound pressure received levels in decibels (dB) referenced to a unit pressure density (1 μPa^2). The frequency-dependent hydrophone calibration was then applied to the PSDs to achieve RL in dB re 1 μPa^2. To compute broadband RL values, hydrophone calibration-corrected RL levels in 1 Hz bins were converted to linear sound power spectra densities and summed across the 5–1000 Hz band, which is the approximate band for which ships are the principal source of noise within the SBC. The broadband RL values were then re-converted into dB re 1 μPa^2.

1.3.4 Transmission Loss (TL)

To account for surface reflection interference (Lloyd's mirror) that may reduce sound measurements at recording sites at much greater horizontal distances than the water depth, such

as at Site B, we used a modified Lloyd's mirror TL model, which was demonstrated to reproduce the sound levels received from ships transiting near their CPA in the northbound shipping lane (Gassmann, Wiggins, and Hildebrand 2017; Carey 2009). A combination of the Lloyd's mirror model and a spherical spreading model was used to account for the surface induced, source depth-dependent increase in TL seen with decreases in frequency (Urick 1975). The modified Lloyd's mirror model utilizes the Lloyd's mirror model from 5 Hz up to the frequency at which the Lloyd's mirror TL and the spherical spreading model intersect. From the frequency of intersection to 1000 Hz, a spherical spreading model is used (Gassmann, Wiggins, and Hildebrand 2017). The intersection point between models depended on the source depth (see Effective Source Depth section) during a specific ship transit and ranged from 46 to 701 Hz.

Harmonic mean sound speed required for the TL model was calculated with data from the California Cooperative Oceanic Fisheries Investigations (CalCOFI) and California Underwater Glider Network (Rudnick 2016). Harmonic mean sound speed was calculated by dividing the total depth by the sum of the time it takes the sound to pass through each layer of constant sound speed. Depth, temperature, and salinity were measured near Site B (34° 15.150′ N, 119° 51.200′ W) on CalCOFI line 81.8 and station 46.9 four times per year and multiple times per year by the California Underwater Glider Network on line 80 (Mackenzie 1981). Between these two data sources, 30 sound speed profiles were measured from 2014 through 2018. Of the 49 months with paired acoustic and AIS data in this study, there were 30 months with corresponding sound speed profiles. For months that did not have a sound speed profile measurement, the sound speed profile measurement with the closest date was used.

1.3.5 Effective Source Depth

Propeller diameter and draft are directly related to acoustic source depth, as cavitation occurs near the tip of the rotating propellers (Gray & Greeley, 1980). Constructive and destructive interference from surface reflections depends on the depth and frequency of the acoustic source, requiring that propeller dimensions and draft be determined for use with the modified Lloyd's mirror model.

Propeller diameters were modeled from a subset of 35 propeller measurements from the 2020 World's Merchant Fleet utilizing the relationship between the propeller diameter and the ship length (Figure 1.6). The depth of the acoustic source was assumed to be equal to 85% of the propeller diameter subtracted from the AIS reported ship draft44. Source depths ranged from 0.3 to 11.1 m with an average of 3.7 m ± 1.4 m.

1.3.6 Source level (SL)

Source levels were estimated by adding the modified Lloyd's mirror TL to the RL over the data window period. Broadband SLs were measured by summing across the 5–1000 Hz frequency band. Source level spectra were measured from 5 to 1000 Hz, and displayed in 1 Hz bins and 1/3 octave bands in compliance with ANSI/ASA (2009) ("AMERICAN NATIONAL STANDARD Quantities and Procedures for Description and Measurement of Underwater Sound from Ships-Part 1: General Requirements" 2014).

The relationship of SL versus vessel speed was determined by calculating the slope (regression coefficient) of the least-squares linear-fit, minimizing the sum of the squares of the deviations of the data from the model. The relationship was measured for each ship type.

1.3.7 Sound Exposure Level (SEL)

The sound exposure level (SEL) was estimated as if each ship were transiting directly over the HARP by subtracting the frequency dependent TL from SL to estimate RL (in units of μPa2) at various ranges of interest (ROI), and integrating over the duration of the transit:

$$SEL = 10log10\int 0T\sum fmaxfmin10\text{^}\left(\frac{\left(SL(f) - TL(f,t)\right)}{10}\right)dt$$

where T is the total transit duration in seconds. To keep the SEL measurements consistent with past ship noise studies in the SBC, T was defined as the time that the RL during the transit was 15 dB above background sound levels in the SBC, as ambient noise levels are elevated by approximately 15 dB when a ship is nearby14. ROIs for each transit ranged from the depth of the hydrophone to the distance the ship travelled over the duration T, before and after CPA. Estimated RLs were calculated for each 1 min interval over the duration of the passage.

1.3.8 Vessel Speed Reduction Approaches

The VSR program requested that enrolled vessels reduce speeds to a target of 6.17 m s^{-1} (12 knots) or less in 2014 and 2016 and 5.14 m s^{-1} (10 knots) or less in 2017 to present when transiting through the designated VSR zone. The target speeds were chosen because they have been shown to maximize reduction in ship strike risk, along with the added benefit of reduced air emissions (Conn and Silber 2013; Lindstad, Asbjørnslett, and Strømman 2011). The VSR program was active during the summer and fall (July 1 through November 15). During the winter and spring (November 16 through June 30) the VSR program was inactive, which served as control months to measure baseline noise measurements from the participating vessels.

In 2014, 2016, and 2017 the VSR program utilized a transit-by-transit approach for vessel enrollment. With this approach, enrolled companies signed up individual vessels and selected

transits at the beginning of the program season to receive financial rewards and positive public relations for traveling at the reduced target speeds in the VSR zone.

In 2018, the VSR program changed to a fleet-based approach to incentivize slow speeds across all transits taking place in the VSR zone. In the fleet approach, container ship and vehicle carrier companies that cooperated in the program were rewarded based on the percentage of nautical miles that all vessels in their fleets traveled at 10 knots or less during the 2018 program season in the VSR zone. Companies with fleets that demonstrated higher percentages of cooperating transit miles were awarded with financial rewards and positive press. The award scale adopted by the VSR program in these years was based on percentage of cooperation (sapphire tier = 100–75%, gold = 50–74%, silver = 25–49%, bronze = 10–24%, and non-compliant = 0–9%).

Across all years of the program, historical AIS data was obtained from the United States Coast Guard, processed by the National Marine Fisheries Service, and provided to the VSR program administrators to monitor enrolled vessel speeds. In years that utilized a transit-by-transit approach, historical AIS data were analyzed to ensure the transits enrolled in the VSR program had an average speed of 6.17 m s^{-1} or higher prior to program enrollment. By doing this, the transit-by-transit VSR program was able to ensure that it was incentivizing companies that were voluntarily slowing transit speeds from previous years. The fleet-based VSR approach did not require a minimum historical average SOG qualifier for vessel enrollment in order to enroll all transits of involved fleets under operation by the participating companies. A total of 18.7% of the transits extracted with paired AIS and acoustic data, that met all required criteria for analysis, were associated with ships that participated in the VSR programs.

1.3.8 Noise Reduction Statistical Analysis

1. Rewarded (transit-by-transit approach)
2. Control (transit-by-transit approach)
3. Program active (fleet-based approach)
4. Program inactive (fleet-based approach)

The effects of the incentive-based VSR program were calculated for the transit-by-transit approach and the fleet-based approach separately. The effect of the transit-by-transit approach was calculated by comparing the rewarded group to the control group. A t-test was used to determine if the SL measurements of the two groups were equal or not equal. The null hypothesis for the t-test is that the SL measurements of the control group and the rewarded group were equal.

A Kruskal–Wallis test was conducted to determine the effect of the fleet-based approach by comparing the fleet award tiers to one another, and comparing each fleet award tier to itself while the program was active versus inactive. The null hypothesis of the Kruskal–Wallis test is that mean ranks of the SLs between award tiers and within award tiers while the program was active versus inactive are the same. A Dunn's test of multiple comparisons was conducted to establish any significant differences within and between specific tiers. p-values were adjusted with the Benjamini and Hochberg (1995) method to control for false discoveries with multiple comparisons (Benjamini, Yoav. Hochberg 1995).

1.4 Results

From 2014 through 2018, paired AIS and acoustic recordings were extracted for 9,297 vessel transits, including all types of vessels travelling through the SBC. The three vessel types under investigation in this study constituted 6,738 of the extracted transits (72.5% of the AIS tracked vessels). Of these, 3,778 vessel transits from 1,299 unique vessels passed the 1 h

isolation, no hydrophone cable strumming, and environmental conditions requirements for analysis inclusion. The transits were made up of 2,677 container ships, 485 vehicle carriers, and 616 bulkers.

1.4.1 Vessel Speed

Across all ship types studied, the average SOG measured at the closest point of approach (CPA) was 7.3 ± 1.9 m s^{-1} (14.2 ± 3.6 knots, Table 1.1). The fastest ship type was container ships (7.6 ± 2.0 m s^{-1}, 14.7 ± 3.8 knots, Table 1.1), while the slowest ship type was bulkers (6.1 ± 0.8 m s^{-1}, 11.9 ± 1.6 knots, Table 1.1).

Table 1. 1: Sound level metrics for container ships, vehicle carriers, and bulkers. Number of transits, mean (± standard deviation) speed over ground (SOG), broadband (5–1000 Hz) received level (RL), source level (SL), and sound exposure level (SEL) for container ships, bulkers, and vehicles carriers. The slope (regression coefficient) of the least-squares regression is shown for SOG vs. SL and SOG vs. SEL (SOG vs. SL|SOG vs. SEL) and the coefficient of determination (r2, SOG vs. SL|SOG vs. SEL) is displayed for three vessel types and their total.

Type	**# of Transits**	**SOG** ($m\ s^{-1}$)	**RL** (dB re 1 μPa^2)	**SL** (dB re 1 μPa^2 @ 1 m)	**SEL** (dB re 1 μPa^2 s)	**Slope** (dB s m^{-1})	**r^2**
All	3,778	7.3 ± 1.9	110.0 ± 6.5	194.2 ± 6.6	158.1 ± 6.0	2.0 | 1.7	0.32 | 0.27
Container	2,677	7.6 ± 2.0	110.3 ± 6.6	194.7 ± 6.8	158.4 ± 6.2	2.1 | 1.8	0.37 | 0.34
Vehicle Carrier	485	7.3 ± 1.6	108.5 ± 6.2	193.1 ± 5.7	156.8 ± 5.2	1.7 | 1.5	0.21 | 0.19
Bulker	616	6.1 ± 0.8	110.0 ± 6.2	193.0 ± 6.4	157.8 ± 6.0	2.6 | 2.2	0.11 | 0.09

1.4.2 Broadband levels

Broadband (5-1000 Hz) RL (received level), SL, and SEL estimates from 3,778 recorded transits of the three ship types studied are shown in Table 1.1. The distances that the broadband levels were measured at ranged from 600 to 4,999 m. Including all ship types, average RL was 110.0 ± 6.5 dB re 1 μPa^2 and average SL was 194.2 ± 6.6 dB re 1 μPa^2 @ 1 m. SL estimates were highest for the container ships and lowest for the bulkers.

Broadband SEL allows for an estimate of total acoustic energy radiated into a region taking into account the transit duration. Including all ship types, the average broadband SEL was 158.1 ± 6.0 dB re 1 μPa^{2}s. Average duration of 15 dB above background sound levels for all ship types transiting at different speeds was 727 s. Duration was specific to each ship transit and was dependent on speed and CPA. The average duration of transits with speeds less than 5.1 m s^{-1} (10 knots) was 676.2 s, while the average duration of transits with speeds greater than 9.3 m s^{-1} (18 knots) was 791.4 s. The duration of the faster transits was longer than the slower transits because of increased RL with increased speed, causing the RL to remain above the threshold for longer.

1.4.3 SOG versus SL and SEL Relationships

The relationship between SOG versus broadband SL and SEL was determined by a linear regression model (Figure 1.2). Including all three ship types, the slope of the linear least-squares fit between SOG and SL was 2.0 dB s m^{-1} (1.0 dB/knot, $r^2 = 0.32$). Bulkers had the highest slope between SOG and SL (2.6 dB s m^{-1}, $r^2 = 0.11$), while vehicle carriers had the lowest slope (1.7 dB s m^{-1}, $r^2 = 0.21$) (Table 1.1). The slope of the linear least-squares fit between SOG and SEL for all vessel types was 1.7 dB s m^{-1} (0.9 dB/knot, $r^2 = 0.27$), which was smaller than the slope of SOG and SL. Bulkers had the highest slope between SOG and SEL, although it was smaller than

the SOG versus SL relationship (Table 1.1). The smallest slope reported was found between the SOG and SEL of the vehicle carrier transits (Table 1.1).

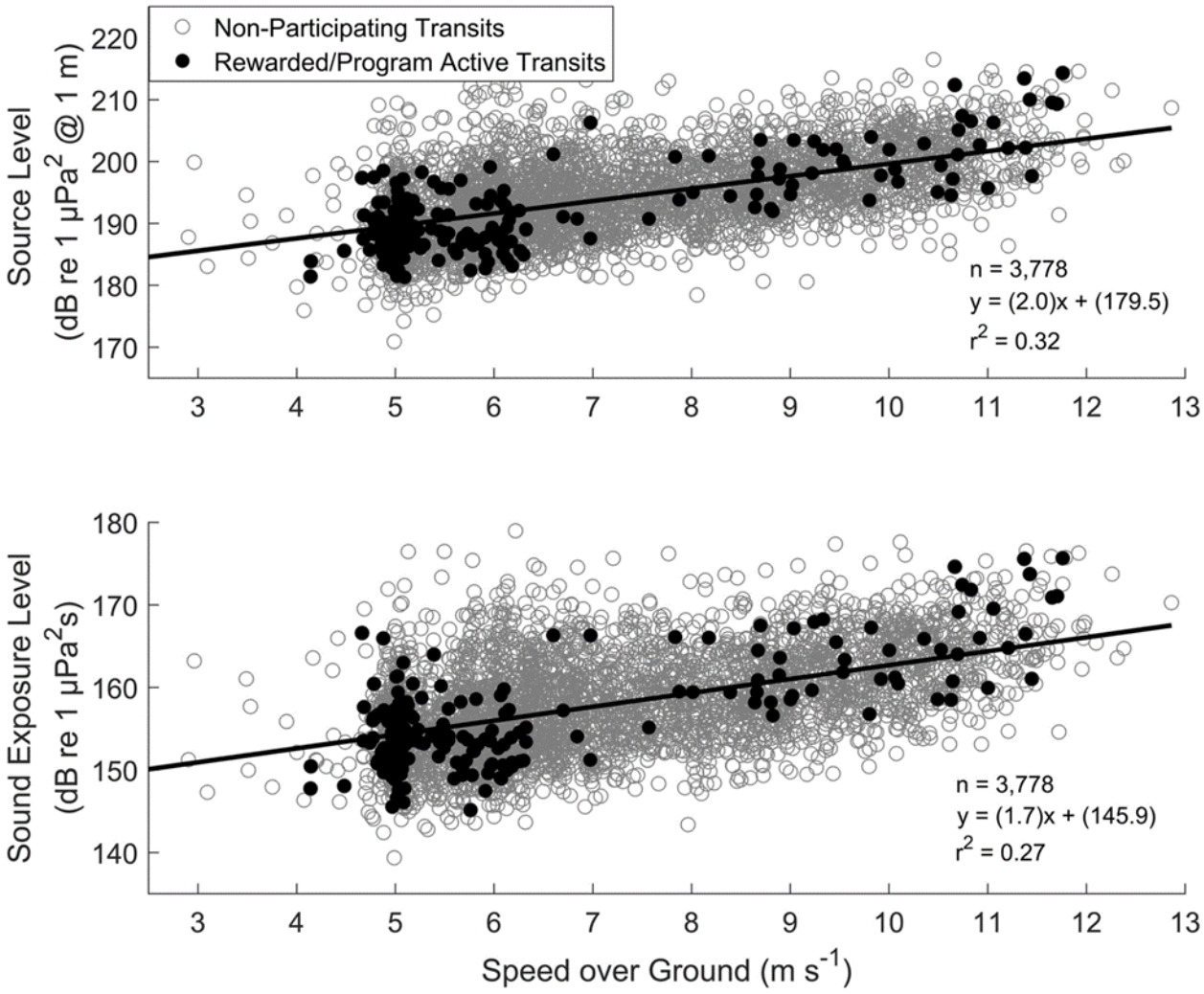

Figure 1. 2: Relationship of Sound Levels and Speed Over Ground. Broadband (5-1000 Hz) source level (dB re 1 μPa^2 @ 1 m) and sound exposure level (dB re 1 μPa^2s) in relation to speed over ground (m s^{-1}) for 3778 cargo ship (container, bulker, and vehicle carriers) transits recorded between 2014 and 2018. Sound exposure level versus speed over ground shows a smaller positive slope than source level versus speed over ground. Rewarded transits from the transit-by-transit vessel speed reduction approach (2014-2017) and program active transits (all award tiers) from the fleet-based vessel speed reduction approach (2018) are shown in black.

1.4.4 Transit-by-transit Vessel Speed Reduction Approach

Of the 2,609 transits with paired acoustic and AIS data from 2014 through 2017, 152 transits (5.9% of transits) were associated with ships that participated in the transit-by-transit VSR program. The association was determined by matching the VSR program-supplied transit time and International Maritime Organization (IMO) identification number of the rewarded transits with the transits in the AIS and acoustic data. The 152 transits represented 47 unique vessels. The rewarded group consisted of 43 transits and the remaining 109 transits were recorded from the control group. Container ships represented 98.0% of the participating vessel transits, and vehicle carriers represented 2.0% of the participating vessel transits. Container ships represented 42 out of the 43 transits in the rewarded group, while 1 transit was a vehicle carrier. The control group consisted of 107 container ship transits and 2 vehicle carrier transits from 1 unique vehicle carrier.

The average speed over ground of the control group was 2.5 m s^{-1} faster than the average speed over ground of the rewarded group. The average SL of the control group was 5.2 dB higher than the average SL of the rewarded group (Table 1.1, Figure 1.3). There was a less than 0.2 m difference in the effective source depth between the control and rewarded group. The reduction in frequency-dependent SL ranged from 0 to 10 dB depending on the frequency. The largest reduction (~ 5–10 dB) occurred at frequencies below 100 Hz (Figure 1.4). There were lesser reductions above 100 Hz (~ 0–5 dB). The average speed over ground, broadband RL, SL, and SEL for the two groups are shown in Table 1.2. The histograms for SOG and SL (1 m s^{-1} and 1 dB bin, respectively) are shown in Figure 1.3. The mean source level spectra for the rewarded and control groups are shown in Figure 1.4.

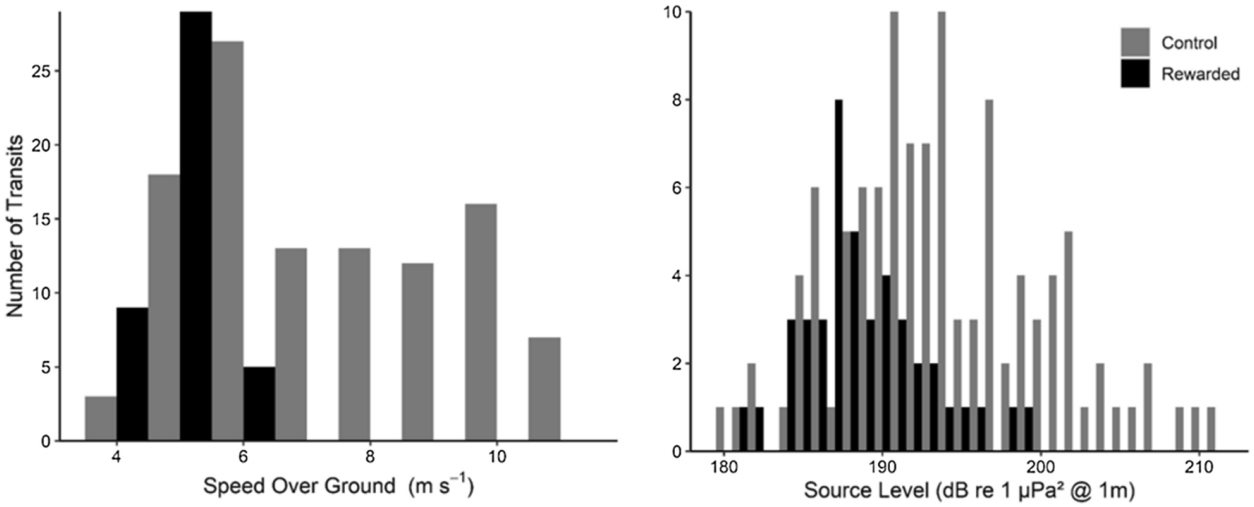

Figure 1. 3: Sound levels and Speed Over Ground for control and rewarded groups. Histogram of speed over ground (m s^{-1}, left panel) and broadband (5-1000 Hz) source level (dB re 1 μPa^2 @ 1 m, right panel) for the control group and the rewarded group from the transit-by-transit vessel speed reduction approach (2014–2017).

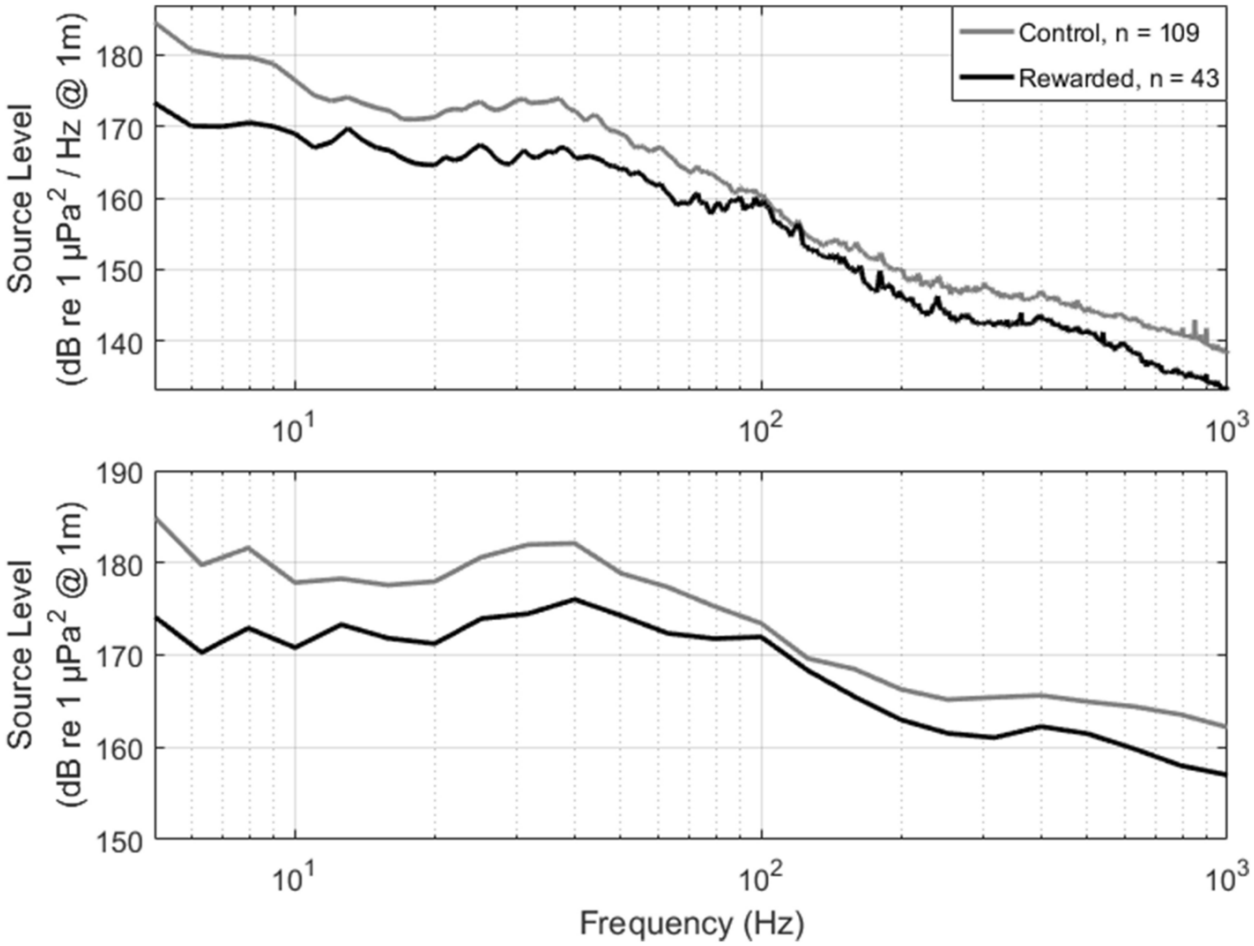

Figure 1. 4: Source level spectra for control and rewarded groups. Mean source level spectra for control and rewarded groups during the transit-by-transit vessel speed reduction program in 1 Hz bins (top panel) and 1/3 octave bands (bottom panel).

Table 1. 2: Speed Over Ground and sound levels for Control and Rewarded groups. Number of transits, mean (± standard deviation) speed over ground (SOG), broadband (5–1000 Hz) received level (RL), source level (SL), and sound exposure level (SEL) for the transit-by-transit vessel speed reduction approach from 2014 to 2017.

Group	**# of Transits**	**SOG** ($m\ s^{-1}$)	**Source Depth** (m)	**RL** (dB re 1 μPa^2)	**SL** (dB re 1 μPa^2 @ 1 m)	**SEL** (dB re 1 μPa^2 s)
Control	109	7.9 ± 2.0	3.8 ± 1.0	109.6 ± 5.8	194.4 ± 6.5	157.1 ± 5.7
Rewarded	43	5.4 ± 0.4	3.6 ± 0.6	101.0 ± 3.7	189.2 ± 3.9	152.4± 3.4

1.4.5 Fleet-based Vessel Speed Reduction Approach

In 2018, of the 1,169 vessel transits that were recorded with paired acoustic and AIS data, 555 were from vessels participating in the fleet-based VSR program, of which 254 occurred when the program was active and 301 occurred when the program was inactive. Fleets were binned in award tiers based on percentage of cooperation. The participating vessel transits consisted of 50 recorded from fleets in the sapphire award tier, 113 from the gold award tier, 180 from the silver award tier, 177 from the bronze award tier, and 35 from the non-compliant tier (Table 1.3). Container ships made up 88.8% of the ship types in the transits recorded from the fleet-based program. The average SOG, broadband RL, SL, and SEL for each award tier are shown in Table 1.3. The distributions of SOG and broadband SL for transits in each award tier are shown in Figure 1.5.

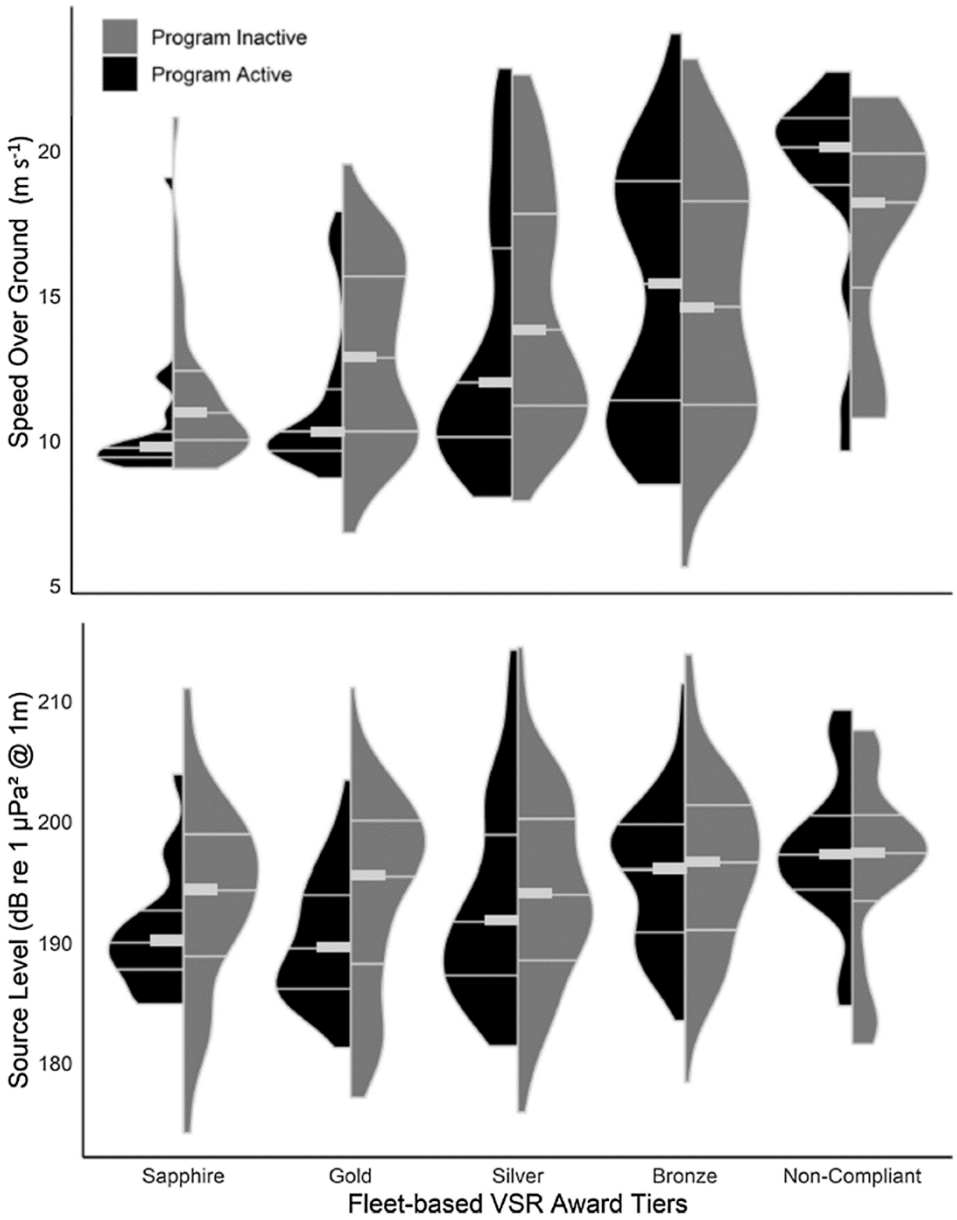

Figure 1. 5: Sound levels and Speed Over Ground during fleet-based program. The distribution of speed over ground (m s^{-1}, top panel) and broadband (5–1000 Hz) source level (dB re 1µPa^2 @ 1 m, bottom panel) for each award tier while the fleet-based vessel speed reduction program (2018) was active and inactive. Quantiles (0.25, 0.5 and 0.75) are displayed on the distributions. The median is marked with a bolded line. Distributions were trimmed to the range of the data. All distributions were scaled to have the same maximum width.

Table 1. 3: Percent cooperation during fleet-based program. Award tiers and percent cooperation for the fleet-based vessel speed reduction program in 2018. Number of transits, average speed over ground (SOG) measured at the closest point of approach, broadband (5–1000 Hz) received level (RL), source level (SL), and sound exposure level (SEL) are shown for groups program active and program inactive.

	PROGRAM ACTIVE					PROGRAM INACTIVE				
Award Tiers (% Cooperation)	**# of transits**	**SOG** ($m\ s^{-1}$)	**RL** (dB re 1 μPa^2)	**SL** (dB re 1 μPa^2 @1m)	**SEL** (dB re 1 μPa^2 s)	**# of transits**	**SOG** ($m\ s^{-1}$)	**RL** (dB re 1μPa^2)	**SL** (dB re 1 μPa^2 @1m)	**SEL** (dB re 1 μPa^2 s)
Sapphire (75-100%)	18	5.4 ± 1.2	109.9 ± 3.6	190.6 ± 5.0	156.1 ± 4.9	32	5.9 ± 1.3	114.9 ± 6.9	193.6 ± 7.9	159.6 ± 6.5
Gold (50-74%)	49	5.8 ± 1.4	108.3 ± 4.4	190.2 ± 5.1	155.7 ± 4.7	64	6.7 ± 1.6	114.5 ± 7.7	193.9 ±7.9	159.8 ± 6.8
Silver (25-49%)	80	6.8 ± 2.3	110.6 ± 6.5	193.2 ± 8.1	157.5 ± 7.5	100	7.5 ± 2.1	116.7 ± 7.3	194.2 ± 7.9	159.5 ± 7.2
Bronze (10-24%)	89	7.8 ± 2.3	113.1 ± 6.1	195.6 ± 5.8	160.1 ± 5.7	88	7.7 ± 2.2	117.8 ± 7.7	196.4 ±7.1	161.8 ± 6.2
Non-Compliant (0-9%)	18	9.9 ± 1.8	115.7 ± 6.1	197.7 ± 6.3	161.4 ± 6.1	17	8.8 ± 2.1	118.6 ± 5.3	196.2 ± 7.6	161.1 ± 7.1

1.4.6 Statistical Analysis

In the transit-by-transit VSR program, there was a significant difference ($p < 0.001$) between the control and rewarded groups for SOG, broadband SL, and SEL. The average reduction in SOG, SL, and SEL between control and rewarded groups was 2.5 m s^{-1} (4.8 knots), 5.2 dB, and 4.7 dB, respectively.

While the fleet-based VSR program was active, broadband SL and SEL estimates from the sapphire, gold, and silver award tiers were significantly different from the non-compliant tier (Table 1.4). The greatest difference in broadband SL and SEL was between the gold award tier and non-compliant tier (7.4 dB and 5.7 dB, respectively). SOGs from the sapphire, gold, silver, and bronze award tiers were significantly different from the non-compliant tier while the program was active. The greatest difference in SOG while the program was active was between the sapphire award tier and non-compliant tier (4.5 m s^{-1}).

While the program was inactive, there were no statistical differences in broadband SLs between any of the award and non-compliant tiers. SOGs from the sapphire and gold award tiers were significantly different from the non-compliant tier. The greatest difference in SOG while the program was inactive was between the sapphire award tier and non-compliant tier (2.9 m s^{-1}).

There was a statistical difference in SOG, SL, and SEL within the gold award tier (-0.9 m s^{-1}, -3.7 dB, -4.2), and a statistical difference in SOG and SEL within the silver award tier (-0.7 m s^{-1}, -2.0 dB) while the program was active versus inactive. The SOG, SL, and SEL within the sapphire and bronze award tiers, and non-compliant tier were not significantly different while the program was active versus inactive.

All of the statistical results for the 2018 fleet-based approach are shown in the matrix in Table 4. The differences in means as well as the degree of significance ($p < 0.05$ = *, $p < 0.01$ = **, $p < 0.001$ = ***) within award tiers and between award tiers while the program was active versus inactive are displayed.

Table 1. 4: Statistical analysis for fleet-based program. Matrix showing the difference in speed over ground, broadband (5–1000 Hz) source level, and sound exposure level (SOG (m s−1)|SL (dB re 1 µPa2 @1 m)|SEL (dB re 1 µPa2s)). Asterisks show degree of significance ($p < 0.05$ = *, $p < 0.01$ = **, $p < 0.001$ = ***). Light grey cells show the difference in means between award tiers while the fleet-based vessel speed reduction program was active. Dark grey cells show the difference in means between award tiers while the fleet-based vessel speed reduction program was inactive. White cells show the difference in means within an award tier while the fleet-based vessel speed reduction program was active v. inactive.

	Sapphire	Gold	Silver	Bronze	Non-compliant
Sapphire	-0.6 | -3.1 | -3.5	0.4 | -0.4 | -0.5	1.5 | 2.6 | 1.4	2.4*** | 5.0*| 4.0*	4.5*** | 7.1*| 5.3*
Gold	0.7 | 0.3 | 0.2	-0.9* | -3.7** | -4.2**	1.0 | 3.0* | 1.8	1.9*** | 5.4***| 4.4***	4.0*** | 7.4** | 5.7**
Silver	1.6*** | 0.6 | -0.1	0.9* | 0.3 | -0.3	-0.7** | -1.0 | -2.0*	0.9** | 2.4* | 2.6*	3.0*** | 4.5* | 3.9*
Bronze	1.7*** | 2.7 | 2.2	1.0* | 2.4 | 2.0	0.1 | 2.1 | 2.3*	0.1 | -0.8 | -1.7	2.1** | 2.1 | 1.3
Non-Compliant	2.9*** | 2.5 | 1.5	2.1** | 2.3 | 1.3	1.3 | 1.9 | 1.6	1.2* | -0.2 | -0.7	1.0 | 1.5 | 0.2

1.5 Discussion

The broadband (5–1000 Hz) SL estimates in this study are consistent with the broadband SL estimate in Gassmann et al. (2017). The average SL for a ship transiting at 10.5 m s^{-1} (20.4 knots) in this study was 201.2 dB re 1 uPa^2 @ 1 m, which is within 1 dB of the SL estimate for a ship transiting at the same speed at Site B in Gassmann et al. (2017). Our SL estimates are higher than SLs from other vessel noise studies at Site B because our SL estimates included a TL model which corrected for surface reflections that occur at sites with low inclination angles (Lloyd's mirror) between ship near-surface sources and the seafloor-mounted acoustic recorder (Megan F. McKenna et al. 2012; Megan F. McKenna, Wiggins, and Hildebrand 2013; Veirs, Veirs, and Wood 2016). An approximate compensation to compare broadband source levels from 10 to 1000 Hz at Site B in McKenna et al. (2012) to Lloyd's mirror corrected broadband levels from 5 to 1000 Hz can be derived by adding 20 to 27 dB. Adding 20 dB to the average broadband SL estimates of containerships in McKenna et al. (2012) traveling on average at 10.85 m s^{-1} is 205.5 dB re 1 uPa^2 @ 1 m, which is within 2–3 dB of the SL estimates of container ships traveling at the same speed in this study. When comparing overlapping frequencies, surface-reflection corrected mean SL spectra from vessels transiting on average at 5.4 m s^{-1} in this study were within 0-8 dB of the mean SL spectra calculated from a full-wave propagation loss model from vessels transiting at 5.8 m s^{-1} in Haro Strait, British Columbia6. Our SL spectra across frequencies was on average 3 dB higher than the SL estimates from Haro Strait, which may be due in part to the difference in depth at which the recording device was deployed (MacGillivray et al. 2019). The SL spectra from container and cargo ships estimated in St. Lawrence Seaway with a full-wave propagation loss model were within 5-9 dB of the SL spectra of container ships travelling at similar speeds in this study (Simard et al. 2016), with our SL spectra across

frequencies approximately 6 dB lower. Our surface-reflection corrected SL estimates from vessels transiting at 18 knots were within 0–10 dB from SL estimates from a single vessel transiting at 18 knots computed via Bayesian marginalization techniques (Tollefsen and Dosso 2020). Differences may be due to the high SL levels at prominent frequency tonals for the single ship spectra compared to our SL spectra averaged over multiple transits. The discrepancies between SL estimates measured at different locations, depths, and with varying propagation loss models is an ongoing issue and should continue to be investigated, in order to establish a method that enables comparison across sites and effective management plans for mitigating SLs. Because the transits in this study were recorded from the same site and the SL estimates were computed using the same transmission loss model, the measured change during the program active months is a reliable reduction.

Our results show a positive relationship between SOG and SL, similar to past studies (Ross 2005; MacGillivray et al. 2019; Megan F. McKenna, Wiggins, and Hildebrand 2013; Veirs, Veirs, and Wood 2016; Simard et al. 2016; Chion, Lagrois, and Dupras 2019). Across all vessels, our relationship of 2.0 dB s m^{-1} (1.0 dB/knot) is within 0.2 dB s m^{-1} from the relationship found in Viers et al. (2016) and within 0.1 dB/knot from the relationship found in ships greater than 250 m in length in Simard et al. (2016). The relationship between SOG and SL for containerships in McKenna et al. (2013) was 1.1 dB/knot, which is within 0.1 dB/knot of the relationship for containerships in this study. The relationship between SOG and SEL in this study had a smaller positive slope than the relationship between SOG and SL. As noted in McKenna et al. (2013), this is likely due to differences in the duration a vessel is transiting in the region. Although the SEL slope is slightly less than the SL slope, we found that slower transits decreased the duration of time that the RL was above the 15 dB background sound level

threshold in the majority of the vessel transits under investigation. The increased SL with increased speed may allow for some vessel sounds to travel farther distances and therefore be received above the threshold for longer durations.

Seasonal differences in radiated noise may also be contributing to differences in SL values. McKenna et al. (2013) identified that "month" was an important covariate in predicting SL estimates. While our study incorporates a specific harmonic mean sound speed value in the transmission loss model for every month, there may be additional variability in underwater propagation that changes with season. For instance, there may be a decrease in radiated noise during the fall due to warm surface waters, creating downward refraction. In spring, the sound speed profile is closer to homogeneous, because of increases in storms creating a deeper mixed layer allowing the modified-Lloyd's mirror model to be a better fit for spring environments, as sound travels in a straighter path than during the fall.

The Protecting Blue Whale and Blue Skies incentive-based VSR program was put into effect in the SBC in an effort to principally reduce air pollution impacts on local human populations and mitigate ship strikes on endangered whale species. At the inception of the program, reducing underwater noise from commercial shipping was regarded as a potential third conservation benefit of slowing large vessels. The added benefit of reducing underwater noise pollution from commercial shipping is quantified in this study. The transit-by-transit VSR approach (2014–2017) decreased SL estimates by over 5 dB and SEL estimates by over 4 dB for rewarded transits. The fleet-based approach (2018) allowed for significant reduction in SL and SEL estimates for ships that slowed 25% or more of their transits in the VSR zone (sapphire, gold, silver award tiers), when compared to non-compliant vessel transits. However, there was no statistical difference in SL or SEL between the bronze award tier and non-compliant tier,

highlighting the limited reduction in noise levels for fleets not slowing down compared to the higher cooperating fleets. There was no significant difference between SOG or SL between the sapphire and gold award tiers, which may be due to the small sample size of the sapphire award tier. Additionally, the SOG of the sapphire and gold award tiers were significantly slower than the lesser cooperating fleets while the program was inactive, and there was no significant reduction in SOG within the sapphire award tier while the program was active versus inactive. This suggests that there may be fundamental differences between tiers that were not related to the Protecting Blue Whales and Blue Skies program. Additional voluntary speed reduction efforts exist in the Santa Barbara Channel seasonally and year-round, including voluntary VSR requests from NOAA—which run from May through November each year, the year-round Green Flag incentive program established by the Port of Long Beach, and the Vessel Speed Reduction Program established by the Port of Los Angeles (Freedman et al. 2017; Linder 2018; Ahl, Frey, and Steimetz 2017). Slow speeds observed from the fleets in the sapphire award tier while the Protecting Blue Whales and Blue Skies program was inactive may be due to fleets' involvement in these additional speed reduction programs throughout the year.

A vessel speed reduction program initiated in British Columbia also identified slowing vessel speed as an effective method to reduce source levels of commercial vessels (MacGillivray et al. 2019). The Enhancing Cetacean Habitat and Observation (ECHO) program's average control speed was faster (9.7 m s^{-1}, 18.9 knots) on average than the control speed in this study (7.9 m s^{-1}, 15.4 knots). This allowed for an SOG reduction of 4.0 m s^{-1} (7.7 knots) during the ECHO program, compared to the Protecting Blue Whale and Blue Sky VSR program SOG reduction of 2.5 m s^{-1}. Because of this, the ECHO program had a larger reduction in SL (11.17 dB for container ships) between the control and participating groups compared to the SL

reduction found in this study. Similarly to this study, the ECHO program found the largest reduction in noise below 100 Hz, and the smallest reductions in the intermediate frequency range6. This is most likely attributed to the reduction in noise brought about by cavitation, which is most prominent in frequencies below 100 Hz.

An additional single ship transit in the Santa Barbara Channel can increase ambient noise levels averaged over a day by 1 dB (Mckenna et al. 2009). Taking into account the average duration of approximately 12 min that a ship transit was 15 dB above background sound levels in this study, there would need to be at least 10 ships slowing down to half of their speed to result in a 0.7 dB reduction in daily average ambient noise levels. In order to maximize the reduction in daily average ambient noise levels, regulating the speed of vessels in the VSR zone, or fleets as a whole, may be necessary given the low cooperation with the incentive-based VSR program.

There are likely many reasons why certain fleets showed lower cooperation rates or would be less inclined to slow their speeds during the VSR program months; for example, scheduling, cost, competition, mechanics, weather and other issues along their overall routes. The incentive-based VSR program includes public recognition, which shows promise for the importance of positive public relations and its role in commercial shipping fleets' willingness to participate in VSR programs (Linder 2018). Employing regulations for mandatory speed restrictions of 10 knots, as is done in the Seasonal Management Areas along the U.S. East Coast, would ensure that efforts to reduce the threat of lethal ship strikes, air pollution, and ocean noise are undertaken by all fleets in the region. Third-party certification and labeling programs such as Organic, Fair Trade, Rainforest Alliance, and Green Marine have promoted social and environmental sustainability, with appropriate private and public recognition (Raynolds 2006; Walker 2016). Involving the VSR program and more commercial shipping fleets into

certification programs like Green Marine may be an effective approach to further reduce speeds and improve voluntary cooperation or enhance government regulations. Additionally, the International Maritime Organization has identified quieting technologies, such as specific propeller and hull designs, as a potential method to reduce underwater noise. Retrofitting vessels in the commercial shipping industry may allow for a method to reduce noise on an international scale (Chou et al. 2021; Organization International Maritime 2014).

Mitigating underwater noise generated from commercial shipping has the potential to reduce acoustic, physiological, and behavioral impacts that have been identified in marine mammals, fish, and invertebrates, allowing for an ecosystem-based approach to management. Effort into the investigation of biological responses to decreases in noise levels brought about by VSR programs is vital to ensure that measured SL and SEL reductions are adequate in reducing ship noise impacts on endangered whales and other marine organisms. Because the commercial shipping industry is a complex, intermodal system that operates under suites of constraints and externalities, an investigation into the various processes and stakeholders affected by the VSR program, including consumers, may aid in discovering how to permanently build conservation into commercial shipping.

1.6 Acknowledgements

We thank NOAA's Channel Islands National Marine Sanctuary and the National Marine Sanctuary Foundation for important conversations and data sharing. Special thanks to the lab members of the Scripps Whale Acoustics Lab for maintaining the HARP at Site B over the past 12 years. Thank you to Bruce Thayre, John Hurwitz, and Ryan Griswold for their help in HARP deployment and recovery. We also thank the crew of R/V Shearwater for use of the vessel to deploy and recover the acoustic instruments. We express our gratitude to Erin O'Neill, who

helped in processing acoustic data. We greatly benefited from the AIS data acquired by Brian Milburn of the Santa Barbara Wireless Foundation. The authors acknowledge support by the Office of Naval Research and Task Force Ocean (Robert Headrick). This research was also supported by the Channel Islands National Marine Sanctuary, the Dr. Nancy Foster Scholarship, the Wyer Family Fund, the Archie Arnold Foundation, as well as the National Aeronautics and Space Administration Biodiversity and Ecological Forecasting program (NASA Grant No. NNX14AR62A), the Bureau of Ocean and Energy Management Ecosystem Studies program (BOEM award No. MC15AC00006), and NOAA in support of the Santa Barbara Channel Marine Biodiversity Observation Network. We thank Robert Miller and other members of the SBC MBON Project.

Chapter 1, in full, is a reprint of the material as it appears in Scientific Reports, ZoBell, Vanessa M., Kaitlin E. Frasier, Jessica A. Morten, Sean P. Hastings, Lindsey E. Peavey Reeves, Sean M. Wiggins, and John A. Hildebrand. "Underwater noise mitigation in the Santa Barbara Channel through incentive-based vessel speed reduction." The dissertation author was the primary investigator and author of this paper.

Chapter 2: Retrofit-induced changes in the radiated noise and monopole source levels of container ships

2.1 Abstract

The container shipping line Maersk undertook a Radical Retrofit to improve the energy efficiency of twelve sister container ships. Noise reduction, identified as a potential added benefit of the retrofitting effort, was investigated in this study. A passive acoustic recording dataset from the Santa Barbara Channel off Southern California was used to compile over 100 opportunistic vessel transits of the twelve G-Class container ships, pre- and post-retrofit. Post-retrofit, the G-Class vessels' capacity was increased from ~9,000 twenty-foot equivalent units (TEUs) to ~11,000 TEUs, which required a draft increase of the vessel by 1.5 m on average. The increased vessel draft resulted in higher radiated noise levels (<2 dB) in the mid- and high-frequency bands. Accounting for the Lloyd's mirror (dipole source) effect, the monopole source levels of the post-retrofit ships were found to be significantly lower (>5 dB) than the pre-retrofit ships in the low-frequency band and the reduction was greatest at low speed. Although multiple design changes occurred during retrofitting, the reduction in the low-frequency band most likely results from a reduction in cavitation due to changes in propeller and bow design.

2.2 Introduction

Ambient noise levels in the ocean have risen over the past five decades due, in part, to a tripling in the number of vessels in the world's merchant fleet (Hildebrand 2009; McDonald, Hildebrand, and Wiggins 2006; Frisk, n.d.; Ross 2005). With the goal of mitigating noise impacts on marine organisms, a number of source-centric efforts to reduce underwater noise emitted from commercial ships have been implemented on regional scales through vessel speed reduction programs near ports (MacGillivray et al. 2019; ZoBell et al. 2021), as vessel speed and

noise levels are positively correlated (Megan F. McKenna, Wiggins, and Hildebrand 2013; Simard et al. 2016; Veirs, Veirs, and Wood 2016). To reduce underwater noise generated by anthropogenic sources on a larger spatial scale and across national boundaries, the potential for individual vessel noise reductions are being discussed by the International Maritime Organization (IMO), International Whaling Commission (IWC), and the International Union for Conservation of Nature (IUCN) (Chou et al. 2021). Retrofitting commercial ships with specific propeller and hull design modifications has been identified by the IMO as a potential method to reduce underwater noise from commercial ships on an international scale(Organization International Maritime 2014).

Maersk is the world's largest container ship operator in both fleet size and cargo capacity ("Maersk," n.d.; Sornn-Friese 2019). Maersk has grown to a fleet of over 700 container ships, serving 59,000 customers around the world, with access to 343 port terminals ("Maersk," n.d.; Sornn-Friese 2019). Maersk has completed a $1 billion, 5-year "Radical Retrofit" initiative focused on improving energy efficiency and fuel consumption to reduce emissions. During this effort, twelve G-Class sister ships, designed for transport of containers, were retrofitted from 2015 through 2018. The Radical Retrofit program included redesigning the bulbous bow to reduce drag and derating the engine to improve vessel efficiency at slower speeds. Additionally, the propeller blade number was reduced from 6 to 4, engine rpm was increased by 10%, propeller diameter increased from 9 to 9.3 m, area and thickness of the propeller blades was reduced, and propeller boss cap fins were installed to reduce cavitation. Each vessel's container capacity was increased from ~9,000 twenty-foot equivalent units (TEUs) to ~11,000 TEUs, which also increased the vessel draft (Figure 2.1).

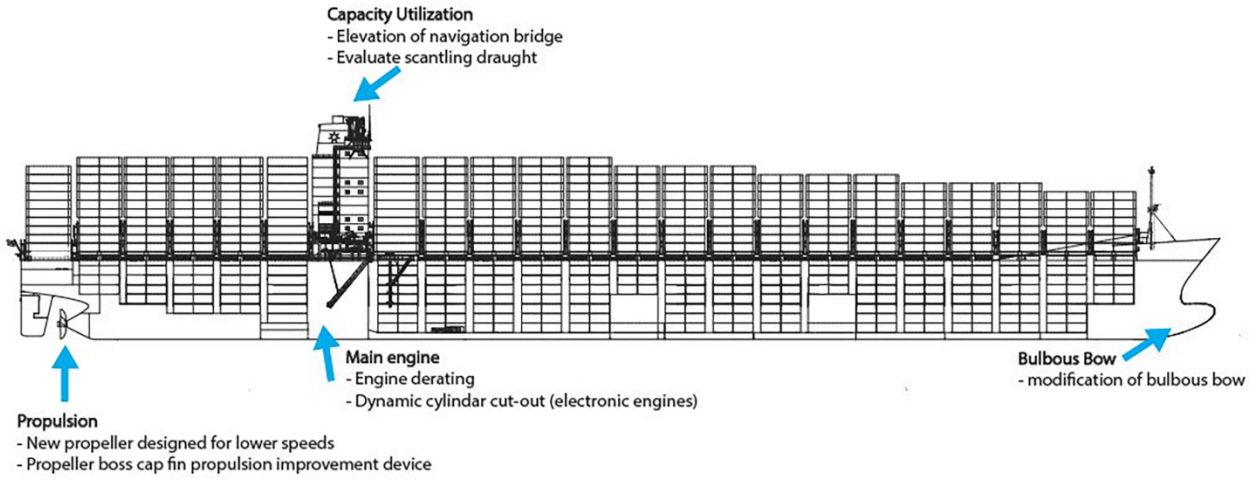

Figure 2. 1: G-Class vessel post-retrofit, modified from the original blueprint provided by Maersk. Changes from pre- to post-retrofitting are identified with arrows.

Reduction of underwater noise was identified as a potential added benefit of emission reductions following the Radical Retrofit program (Gassmann, Wiggins, and Hildebrand 2017). To compare the underwater noise of these container ships pre- and post-retrofit, long-term acoustic recording datasets in heavily trafficked shipping lanes were used. Over the past ten years, the Scripps Institution of Oceanography opportunistically recorded over 100 transits of the twelve G-Class Maersk vessels pre- and post-retrofitting as they transit through the Santa Barbara Channel (SBC) to and from the Ports of Los Angeles and Long Beach. In this study, the changes in radiated noise levels and monopole source levels after retrofitting are investigated.

2.3 Methods

2.3.1 Ship Passages

Automatic identification system (AIS) receiver stations were operated in the Santa Barbara Channel to determine ship locations in this study (Table 2.1). The IMO number of each G-class vessel was used to search these AIS databases for passages that were within 5 km of an acoustic recording device used in this study. When a passage from one of the twelve G-Class vessels was identified, corresponding information such as Speed Over Ground (SOG), Course Over Ground, and position (longitude and latitude) were decoded from the AIS messages. Speed Over Ground was converted to Speed Through Water (STW) by accounting for speed and direction of surface currents from High-Frequency (HF) Radar data from the Southern California Coastal Ocean Observing System ("Southern California Coastal Ocean Observing System," n.d.).

Table 2. 1: Automatic identification system data sources.

AIS Station	Latitude	Longitude	Date Range
UC Santa Barbara	34.408° N	119.878° W	June 2007 - May 2013
Santa Cruz Island	33.994° N	119.632° W	March 10 - October 2017
Coal Oil Point	34.411° N	119.877° W	September 2013 - June 2018
Santa Ynez Peak	34.029° N	119.784° W	August 2016 - present

2.3.2 Acoustic recordings

A High-frequency Acoustic Recording Package (HARP) was maintained in the Santa Barbara Channel (Site B; 34.270° N, 120.030° W) at ~580 m depth, ~3 km north of the northbound shipping lane from February 2008 to November 2018 (Figure 2.1) (Wiggins & Hildebrand, 2007). The HARP was equipped with a single, omni-directional hydrophone that was suspended 10 m above the seafloor. HARP hydrophone electronics were calibrated at Scripps Institution of Oceanography and representative hydrophones were calibrated at the U.S. Navy's Transducer Evaluation Center facility in San Diego, California. Recordings were collected at a sampling rate of 200 kHz. Acoustic data were decimated by a factor of 20 to reduce computational requirements. The data were low-pass filtered with an 8th order Chebyshev Type I IIR filter during decimation to prevent aliasing and then resampled at 10 kHz. Identified G-Class vessel transits from the AIS data were paired with corresponding acoustic recordings and extracted for manual review by a trained analyst (VMZ). Transits contaminated with low-frequency hydrophone cable strumming, electronic noise from the instrument, marine mammal vocalizations, or ship noise from another vessel were discarded. Frequencies associated with electronic noise were excluded from the spectra and broadband calculations.

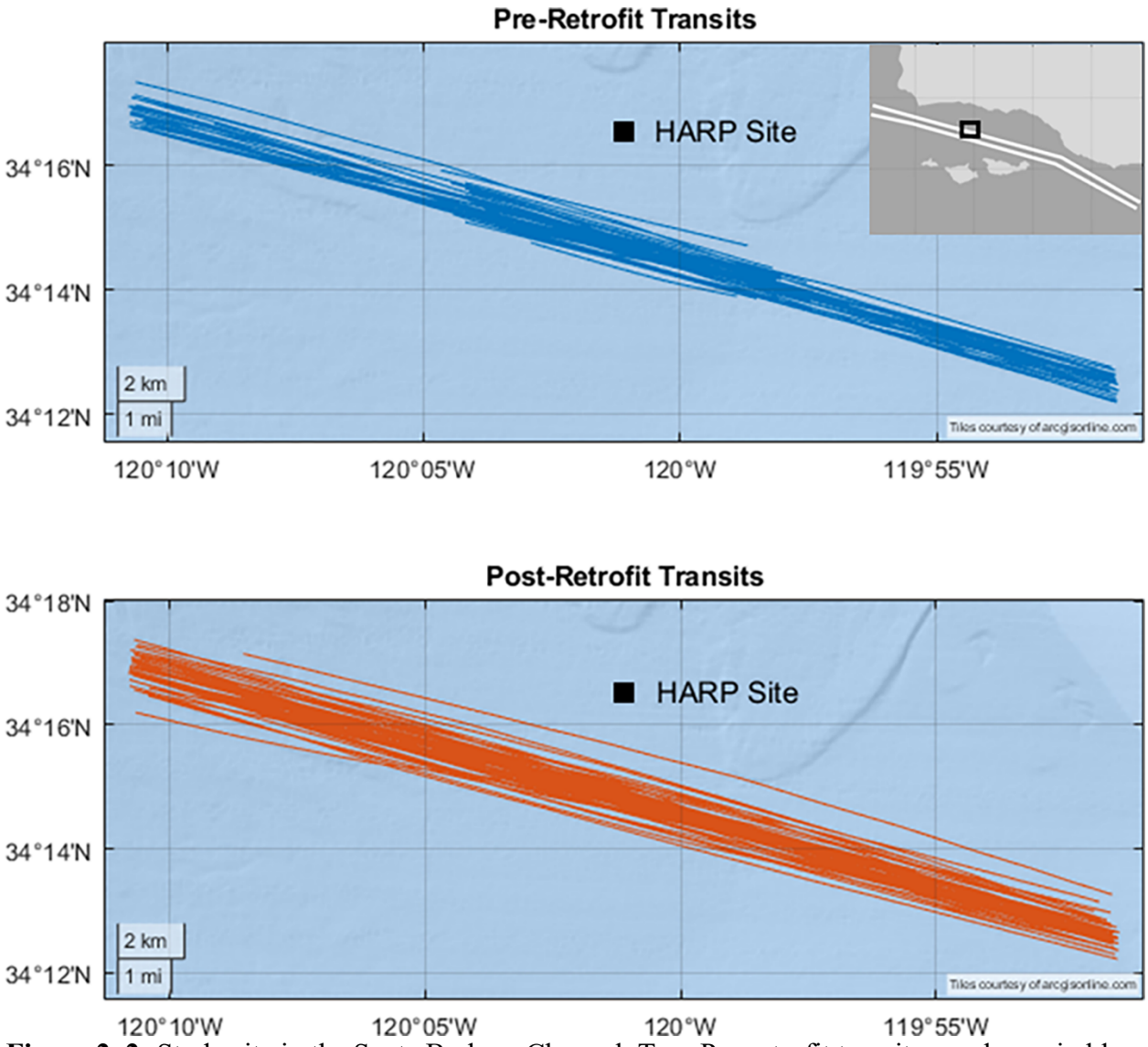

Figure 2. 2: Study site in the Santa Barbara Channel. Top: Pre-retrofit transits are shown in blue. Bottom: Post-retrofit transits are shown in red. The location of the High-frequency Acoustic Recording Package (HARP) is labeled with a square. The inset map in the upper right corner shows the north-south Traffic Separation Scheme as white lines.

2.3.3 Vessel noise metrics

At speeds corresponding to commercial operation of the ships (e.g., 5–10 m/s), the most energetic source of vessel noise is propeller cavitation (Ross 2005), that is, the creation of a water cavity by reduction in local pressure due to motions of the propeller. Because cavitation involves a water volume change, it is a monopole sound source, but since propellers are operated near the surface of the ocean (at least for surface vessels) reflections from the sea surface result in an image sound source with reversed polarity, called the Lloyd's mirror effect, effectively creating a dipole sound source. At low-frequency (i.e. when the distance between the monopole and sea surface is small by comparison to the acoustic wavelength), a dipole sound source has directionality and the strength of radiated energy varies with angle as cos(theta) where theta is the normal angle with respect to the sea surface. Vessel radiated noise levels (L_{RN}) are calculated in a manner that does not take into account the source depth, nor the dipole nature of the source. Instead, an explicit account of the dipole source is calculated by the monopole source level, which is a better metric for the energy due to cavitation or other near-surface sources estimated 1 meter away from the source (Gassmann, Wiggins, and Hildebrand 2017).

Radiated noise levels (L_{RN}) were calculated and monopole source levels (L_S) obtained by correcting for the effect of Lloyd's mirror using the approach of Gassmann et al. (2017) (Gassmann, Wiggins, and Hildebrand 2017). ASA/ANSI (2009) and ISO (2019) standard measurement methods were adhered to, with the exception of observation angles, which were not controlled for during these opportunistic recordings ("AMERICAN NATIONAL STANDARD Quantities and Procedures for Description and Measurement of Underwater Sound from Ships-Part 1: General Requirements" 2014). Measurements of the twelve sister ships were conducted at ranges varying from 1.7–4.9 km; therefore, the vertical and horizontal observation angles

deviated from the ASA/ANSI (2009) requirements ("AMERICAN NATIONAL STANDARD Quantities and Procedures for Description and Measurement of Underwater Sound from Ships-Part 1: General Requirements" 2014). To estimate monopole source levels at 1 m range, frequency-dependent sound pressure levels (L_P) were measured at and near the closest point of approach (d_{CPA}), and a frequency-dependent propagation loss model (N_{PL}) with a unique source depth (d_S) was applied with the following equation:

$$Ls = Lp + Npl$$

2.3.4 Sound Pressure Level (Lp)

Each G-Class vessel recording was divided into non-overlapping segments with a duration of 1 s, and a 10,000-point Fast Fourier Transform (FFT) applied to each 1 s segment to provide a frequency bin spacing of 1 Hz. Over the duration of the transit, the mean sound pressure level was averaged over 5 s segments every 3 s to smooth the time-frequency distribution. The resulting sound pressure levels (L_P) were reported in decibels (dB) with a reference pressure of 1 μPa^2. Ambient noise levels in the absence of ships were calculated for each deployment as the 10^{th} percentile of daily ambient noise over the course of each deployment and were compared to L_P values to compute signal to noise ratios for each transit.

$$Lp = 10log10(\frac{P^2}{p0}) \qquad \text{dB}$$

2.3.5 Propagation Loss

A variety of propagation loss models have been applied to vessels transiting in the Santa Barbara Channel (ZoBell et al. 2021; Megan F. McKenna, Wiggins, and Hildebrand 2013; Gassmann, Wiggins, and Hildebrand 2017; Megan F. McKenna et al. 2012). To estimate L_{RN}, a spherical spreading propagation loss model (N_{SS}) was calculated with the following equation:

$$Nss = 20log10(\frac{R}{r0}) \qquad \text{dB}$$

where R is the distance from the dipole source to the receiver and r_0 is the reference distance (1 m).

Additionally, a propagation loss model that corrects for the Lloyd's mirror effect (N_{PL}) was applied to account for sea surface image source interference, in compliance with ISO (2019) ("Underwater Acoustics-Quantities and Procedures for Description and Measurement of Underwater Sound from Ships-Part 1: Requirements for Precision Measurements in Deep Water Used for Comparison Purposes Acoustique Sous-Marine-Grandeurs et Modes de Description et de COPYRIGHT PROTECTED DOCUMENT Copyright International Organization for Standardization Provided by IHS under License with ISO" 2016). The N_{PL} model ignores sound refraction in the water column and reflections from the seafloor and solely accounts for reflections from the sea surface (Gassmann, Wiggins, and Hildebrand 2017). The propagation loss of a sound source near the surface in deep water considering the Lloyd's mirror effect is given by:

$$Npl = -20log10(r0\left|\frac{e-jk1}{r1} - \frac{e^{-jkr2}}{r2}\right|) \quad \text{dB}$$

where r_1 is the distance from the source to the receiver, r_2 is the distance from the image source to the receiver, and k is the wave number in rad/m. Harmonic mean sound speeds were calculated from depth, temperature, and salinity data obtained from the California Cooperative Oceanic Fisheries Investigations (line 81.8, station 46.9) and California Underwater Glider Network using the nine term equation from Mackenzie (1981) (Mackenzie 1981; "California Cooperative Oceanic Fisheries Investigations," n.d.; Rudnick 2016).

A modification of the Lloyd's mirror model was applied to remove mismatched interference lobes identified with ship noise measurements in compliance with ANSI/ASA (2009) and ISO (2019) (Gassmann, Wiggins, and Hildebrand 2017; "AMERICAN NATIONAL

STANDARD Quantities and Procedures for Description and Measurement of Underwater Sound from Ships-Part 1: General Requirements" 2014; Organization International Maritime 2014). The modification involves using the Lloyd's mirror model from 5 Hz up to the lowest frequency at which the Lloyd's mirror model (Equation 4) and the spherical spreading model (Equation 3) intersect, while at the higher frequencies, the spherical spreading model was used (Gassmann, Wiggins, and Hildebrand 2017).

2.3.6 Source Depth (ds)

The spherical spreading propagation loss model used to compute radiated noise level does not require a source depth (d_S). Multiple types of cavitation can occur at various locations around the propeller, including tip, blade, and hub vortex, making any method of source depth calculation subject to some error. To correct for changes in d_S when calculating monopole source level, ISO (2019) recommends a d_S equal to 70% of the vessel draft ("Underwater Acoustics-Quantities and Procedures for Description and Measurement of Underwater Sound from Ships-Part 1: Requirements for Precision Measurements in Deep Water Used for Comparison Purposes Acoustique Sous-Marine-Grandeurs et Modes de Description et de COPYRIGHT PROTECTED DOCUMENT Copyright International Organization for Standardization Provided by IHS under License with ISO" 2016). Approximating the source depth by a percentage of the vessel draft does not take into account the propeller diameter, an important factor in d_S, since cavitation is most prominent at the propeller tip at the top of its rotation (Gray and Greeley, n.d.). Propeller diameter measurements are challenging to obtain, and are not reported in Lloyd's Register of Ships, or any publicly available datasets. By communicating with the vessel designers, we obtained the propeller diameters of each G-Class vessel pre- and post- retrofitting (9 m and 9.3 m, respectively); therefore, we used a d_S equal to 85% of the propeller diameter subtracted from

the ship draft (Gray and Greeley, n.d.). Draft measurements were obtained from the Chief Engineers (CEs) of each ship and compared to those reported in the AIS data. The AIS reported draft measurements were up to 3 m different from the draft measurements obtained from the CEs of the ships; therefore, the CEs' measurements were used as these were considered more reliable. The draft measurements from the CEs for each transit are shown in Figure 2.3.

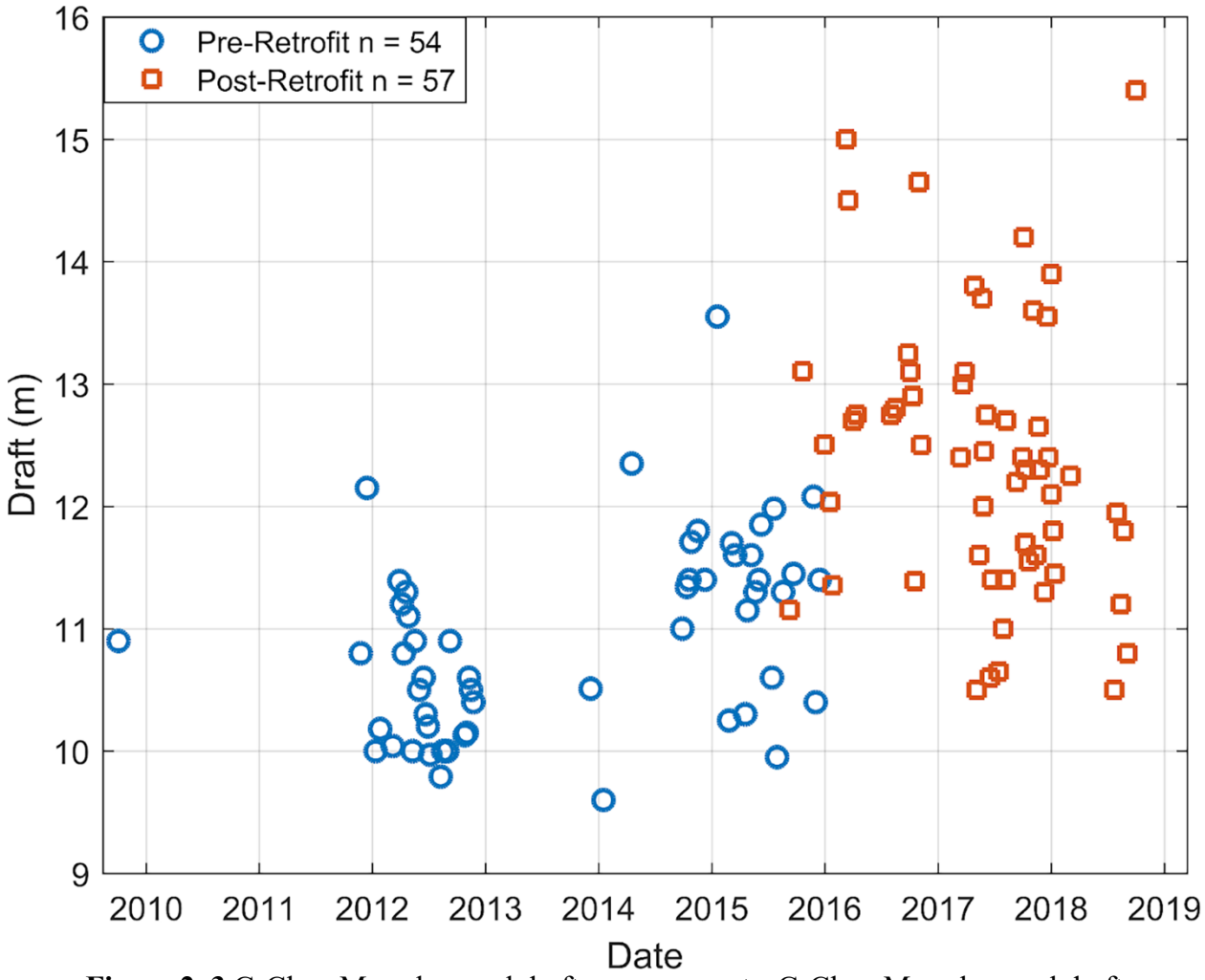

Figure 2. 3 G-Class Maersk vessel draft measurements. G-Class Maersk vessel draft measurements pre-retrofit (blue circles) and post-retrofit (red squares), provided by vessel Chief Engineers. Pre-retrofit draft measurements were shallower on average than post-retrofit draft measurements.

2.3.7 Radiated Noise Level (Lrn) and Source Level (Ls)

Sound pressure levels (L_P) for each G-Class vessel transit were obtained by averaging over the time it took the ship to travel +/- 30 degrees with respect to the d_{CPA}, adhering to ANSI/ASA, 2009. Radiated noise level (L_{RN}) was determined by applying spherical spreading loss (N_{SS}) to L_P, and monopole source level (L_S) was determined with the addition of the Lloyd's mirror effect by applying the modified N_{PL} to L_P. L_{RN} and L_S were expressed in 1 Hz bins to provide enough frequency resolution to allow the blade lines, the frequency at which blades pass the top of the rotation, to be identified. The G-Class vessels typically transit with propeller shaft speeds of 60–70 revolutions per minute (rpm) (Cooper et al. 2017), allowing for a fundamental blade rate pre-retrofitting of approximately 6–7 Hz. Because of the decrease in the number of propeller blades and the increase in rpm during the Radical Retrofit, the fundamental blade rate was reduced to approximately 4.5–6 Hz. Ocean waves become the dominant source of energy below ~5 Hz (Webb 1998), and the fundamental blade rate post-retrofitting was not able to be resolved in some transits. A lower limit of 8 Hz was selected in order to ensure that the fundamental blade rate was excluded from both pre- and post-retrofitted transits. Broadband levels were computed in the frequency range of 8 Hz to 4000 Hz, by dividing into low- (8–40 Hz), mid- (40–200 Hz), high- (200–1000 Hz), and very high- (1000–4000 Hz) frequency bands. These four bands distinguish changes due to noise generated (Ross 2005) by the propeller (low-frequencies), ship machinery, such as diesel engines, compressors, and pumps (high- and very high-frequencies), and the combination of these noise sources (mid-frequencies). Broadband levels were computed by summing across each of the low-, mid-, high-, and very high-frequency bands in the linear domain. Broadband levels in relation to CPA were investigated to determine if propagation loss models were over or underestimating values with distance from the HARP.

First-order polynomials were fitted to each of the sound levels in the low-, mid-, high-, and very high-frequency bands as a function of Speed Through Water using linear least-squares regression. First-order polynomials were fitted to the pre-retrofit distributions to establish baselines for L_P, L_{RN}, and L_S. Differences between the post-retrofit sound levels and the pre-retrofit baseline levels were computed in the low-, mid-, high-, and very high-frequency bands.

2.3.8 Statistical Analysis

Since the G-Class vessels are sister ships with identical measurements, the twelve vessels were pooled for statistical analysis, and each transit was treated as an independent observation. An analysis of covariance was used to test for significant differences and effect size (generalized eta squared η_g^2), in the three reported sound levels metrics (L_P, L_{RN}, L_S) for low-, mid-, high-, and very high-frequency bands between pre- and post-retrofit groups controlling for STW. Significant interactions between retrofit and STW were investigated to identify the influence of retrofit on sound levels for various STW.

Estimated marginal means (EMMs) controlling for STW, were computed for radiated noise and monopole source levels in 1 Hz bins and low-, mid-, high-, and very high-frequency bands. The differences between the EMMs pre- and post- retrofitting were calculated.

2.4 Results

Opportunistic recordings of G-Class Maersk vessels were obtained for 177 transits over ten years of data collection in the SBC. Of the 177 transits, 66 transits were excluded because of the presence of singing whales, acoustic interference from other vessels, and hydrophone cable strumming, leaving 111 transits for the analysis. Acoustic recordings from all twelve of the G-Class Maersk vessels were obtained. Transits that occurred pre-retrofit and post-retrofit made up 48.7% and 51.4% of the dataset, respectively.

Some parameters of the vessels changed during the Radical Retrofit. The vessel draft increased by 1.5 m on average between pre- and post-retrofit (Figure 2.3) owing to the expanded container capacity. Draft measurements pre-retrofit ranged from 9.6 to 13.6 m (average of 10.9 ± 0.8 m) and post-retrofit ranged from 10.5 to 15.4 m (average of 12.4 ± 1.1 m). The secondary harmonic was reduced post-retrofit from 12 Hz to 10 Hz due to the reduction in the number of propeller blades from 6 to 4 during the Radical Retrofit (Figure 2.4) along with a corresponding 10% increase in propeller rpm. The range (d_{CPA}) of the vessel closest point of approach to the seafloor sensor decreased between pre- and post-retrofit, 4,059 ± 578 m and 3,527 ± 561 m, respectively. Spectra from two transits of the vessel Gerda Maersk at similar speed and draft pre- and post-retrofit are shown in Figure 2.4.

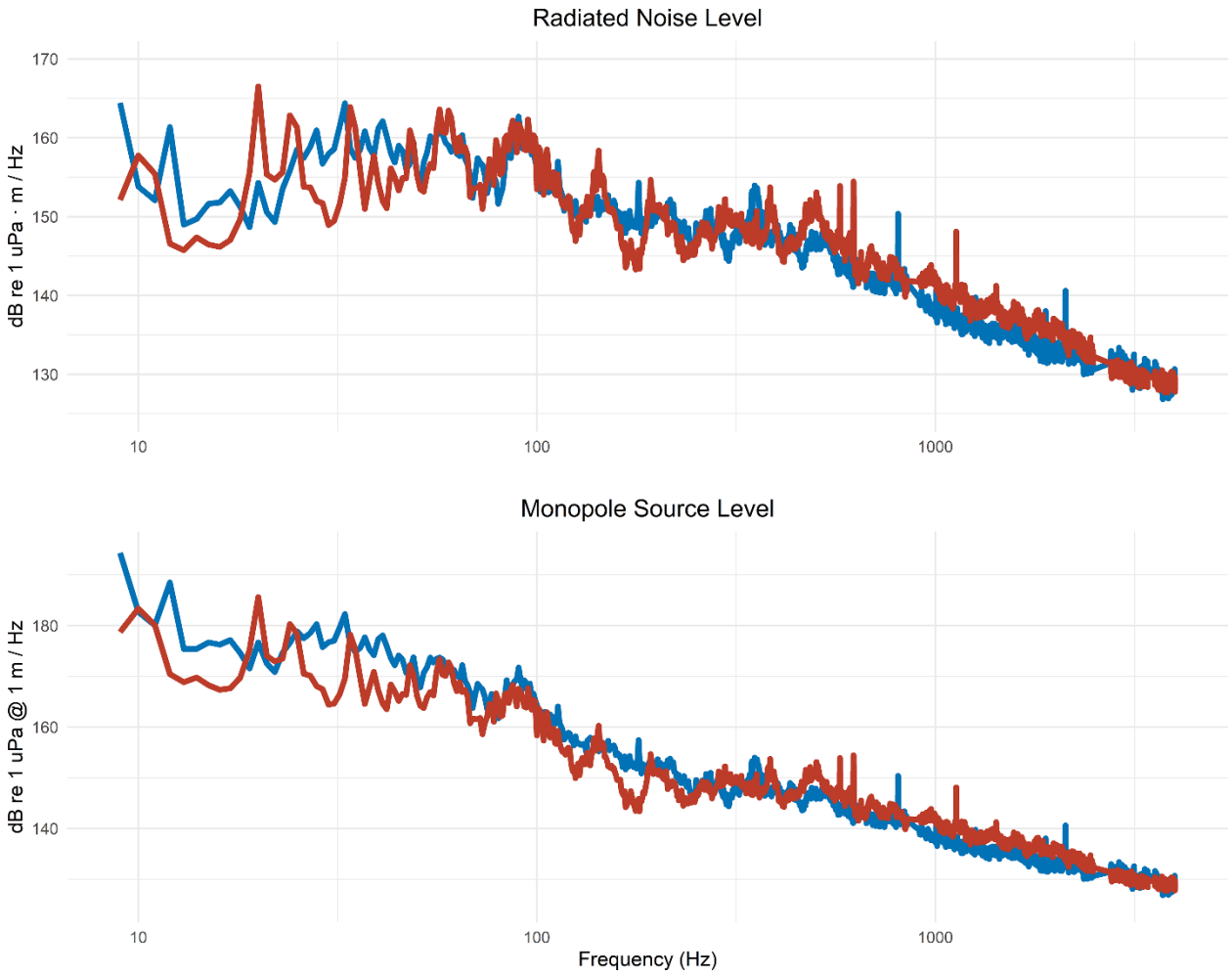

Figure 2. 4: Gerda Maersk noise levels pre- and post-retrofit. Radiated noise level (top) and monopole source level (bottom) from two transits of Gerda Maersk pre-retrofit (blue) and post-retrofit (red). The pre-and post-retrofit speed through water was 6.0 and 6.1 m/s, respectively. The pre- and post-retrofit draft was 11.2 and 12.2 m, respectively.

2.4.1 Broadband levels

At low-frequencies (8–40 Hz) the radiated noise levels pre- and post-retrofit were found to decrease by 1 dB (Figure 2.5, Figure 2.6). In contrast, the monopole source levels were 5.2 dB lower post-retrofit (Table 2.2). The discrepancy between radiated noise levels (small decrease) and monopole source levels (large decrease) is owed to the increased vessel draft. An increase in draft reduces the Lloyd's mirror effect on the radiated noise, creating higher radiated noise levels post-retrofit, whereas correcting for the Lloyd's mirror effect resulted in lower monopole source levels post-retrofit.

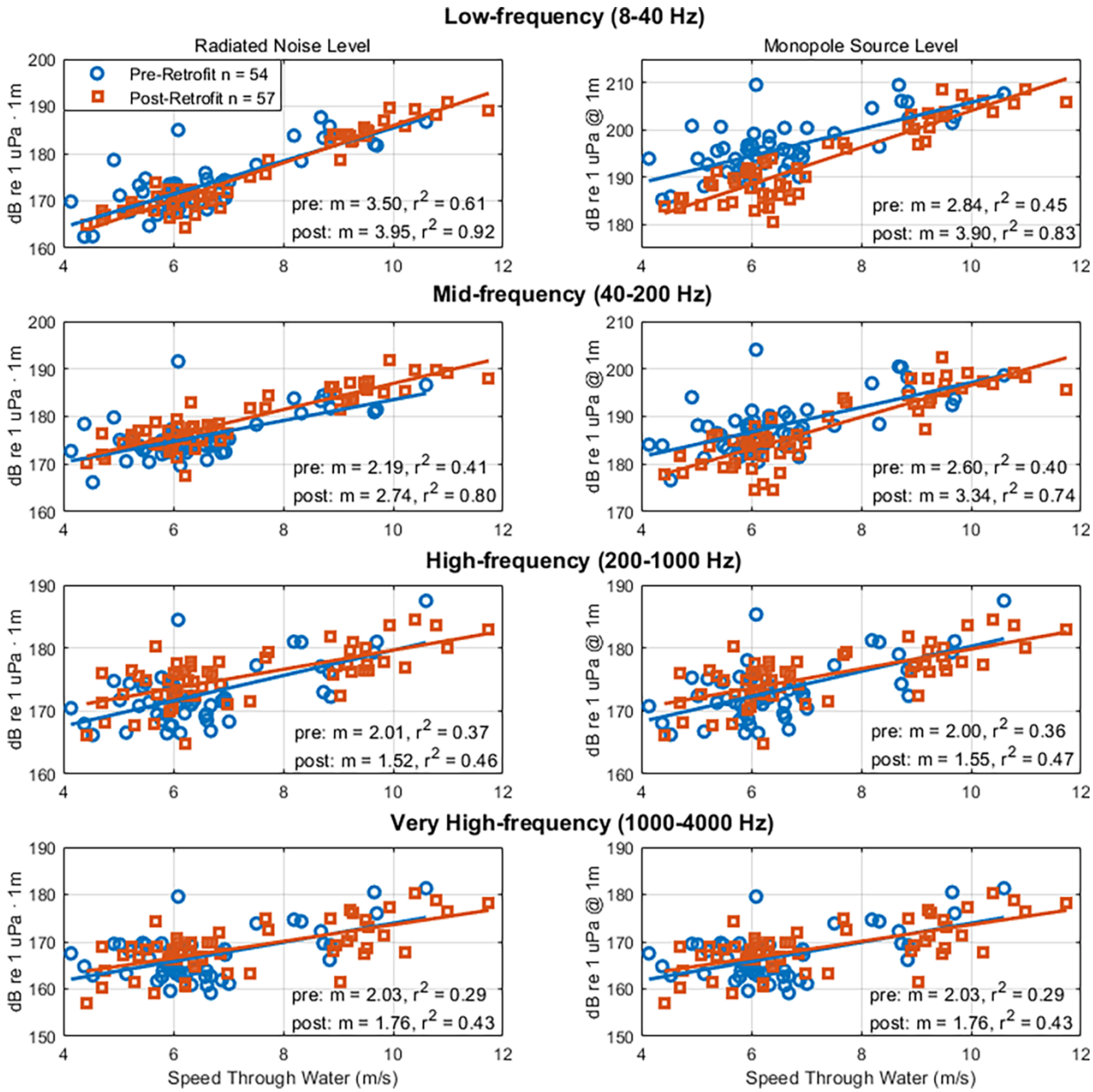

Figure 2. 5: G-Class Maersk vessel noise levels in relation to speed through water. Broadband radiated noise level (left) and monopole source level (right) in relation to Speed Through Water for 111 G-Class Maersk transits pre-retrofit (blue circles) and post-retrofit (red squares) for low-, mid-, high-, and very high-frequency bands.

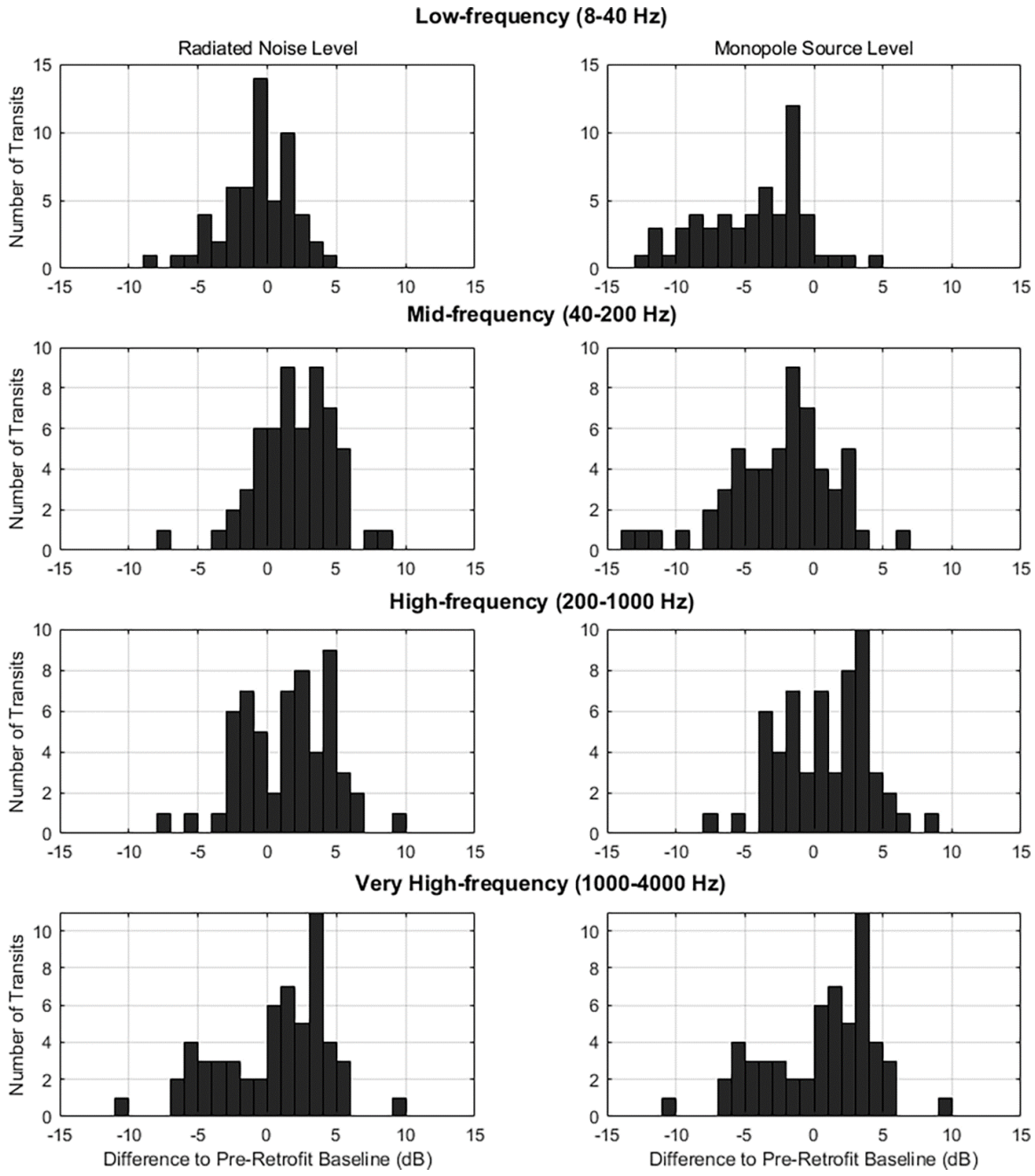

Figure 2. 6: Differences in dB pre- and post- retrofit. Differences in dB between the pre- and post-retrofit radiated noise level (left), and monopole source level (right) for low-, mid-, high-, and very high-frequency bands.

Table 2. 2: Radiated noise levels and monopole source levels pre- and post-retrofitting.

	Low-Frequency (8–40 Hz)		Mid-Frequency (40–200 Hz)		High-Frequency (200–1000 Hz)		Very High-Frequency (1000–4000 Hz)	
Retrofit	**Radiated Noise Level**	**Monopole Source Level**	**Radiated Noise Level**	**Monopole Source Level**	**Radiated Noise Level**	**Monopole Source Level**	**Radiated Noise Level**	**Monopole Source Level**
	L_{RN}	L_S	L_{RN}	L_S	L_{RN}	L_S	L_{RN}	L_S
Pre	174.7	197.3	176.9	189.3	173.3	174.0	167.6	167.6
Post	173.7	192.1	178.5	186.3	174.9	175.0	168.1	168.1
Δ	-1.0	-5.2	+1.6	-3.0	+1.6	+1	+0.5	+0.5
p	0.12	8.49e-10*	0.01*	3.03e-4*	0.02*	0.14	0.51	0.51
η_g^2	0.02	0.31	0.06	.12	0.05	0.02	0.00	0.00

At mid-frequencies (40–200 Hz) the radiated noise levels post-retrofit increased by 1.6 dB, while the monopole source levels decreased by 3.0 dB. At high-frequencies (200–1000 Hz) and very high-frequencies (1000–4000 Hz) the radiated noise levels post-retrofit increased over those pre-retrofit (1.6 dB and 0.5 dB, respectively); whereas, the monopole source levels increased by 1 dB and 0.5 dB, respectively (Table 2.2), again subject to the changes in vessel draft.

The broadband radiated noise levels decreased in relation to CPA with varying slopes. The broadband monopole source levels in the low- and mid-frequencies bands did not change in relation to CPA (m = 0.001 and m = 0.000, respectively). Because of the modification of the Lloyd's mirror model switching to N_{ss} in the higher frequencies, the high- and very high-frequency broadband monopole source levels decreased in relation to CPA.

Pre-retrofit baselines are subtracted from post-retrofit levels to provide the difference, such that a positive value is an increase and a negative value is a reduction (Figure 2.6). From the perspective of the vessel monopole source level, the retrofit resulted in a decreased level at low- and mid-frequencies; whereas, at high- and very high-frequencies the pre- and post-retrofit monopole source levels are comparable, suggesting that the retrofit had different effects on different noise generating mechanisms.

2.4.2 Statistical Analysis

When controlling for STW, the difference in the EMMs varied between pre- and post-retrofitting for radiated noise levels and monopole source level. The highest reduction was 7.5 dB at 39 Hz in the monopole source level. The highest increase was in the radiated noise level with 4.7 dB at 92 Hz (Figure 2.7, 2.8). Retrofit had a significant effect on monopole source level in the low- and mid-frequency bands and radiated noise level in the mid- and high-frequency

bands (Table 2.2). The explained variance (η_g^2) of the retrofit was the highest for the low-frequency monopole source level, with a value of 30%. However, for the monopole source level in the low-frequency band, the interaction between retrofit and STW was significant ($p = 0.04$). The interaction between retrofit and STW was investigated further to determine the contribution of the retrofit to sound levels for various STWs (Figure 2.9). The effect of retrofitting on the low-frequency monopole source level ranges from -7 dB at 4 m/s (7.8 knots) to 0 dB at 12 m/s (23.3 knots), suggesting that the primary impact of the retrofit was to reduce source levels when the vessel is operated at low speed. The 95% confidence intervals of the coefficients are wider for the high speeds, mostly likely because there were fewer transits at speeds > 10 m/s contributing to the model.

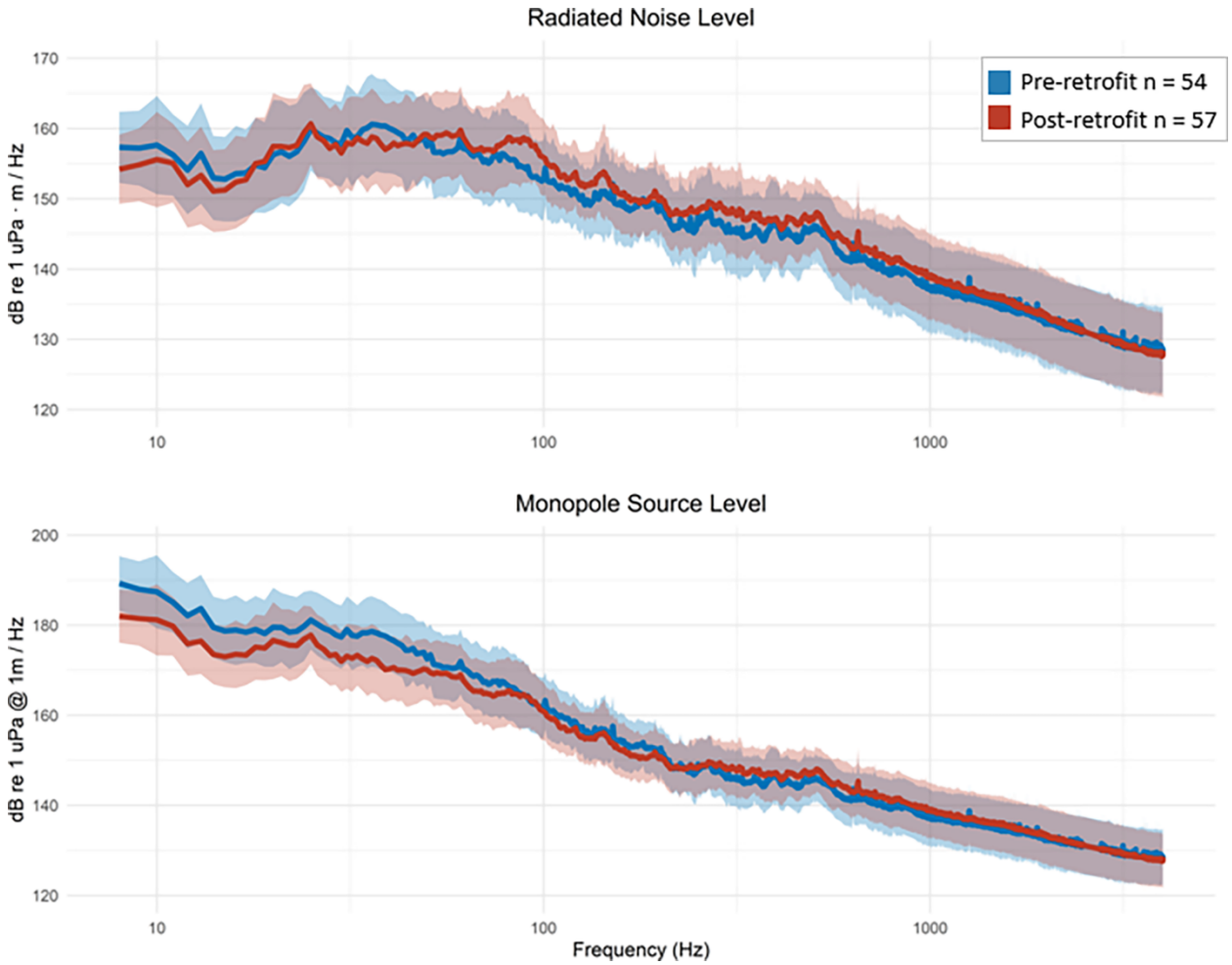

Figure 2. 7: Estimated marginal means for noise levels pre- and post-retrofitting. Estimated marginal means (EMMs) ± standard deviation of radiated noise level (L_{RN}) and monopole source level (L_S) pre- and post-retrofitting.

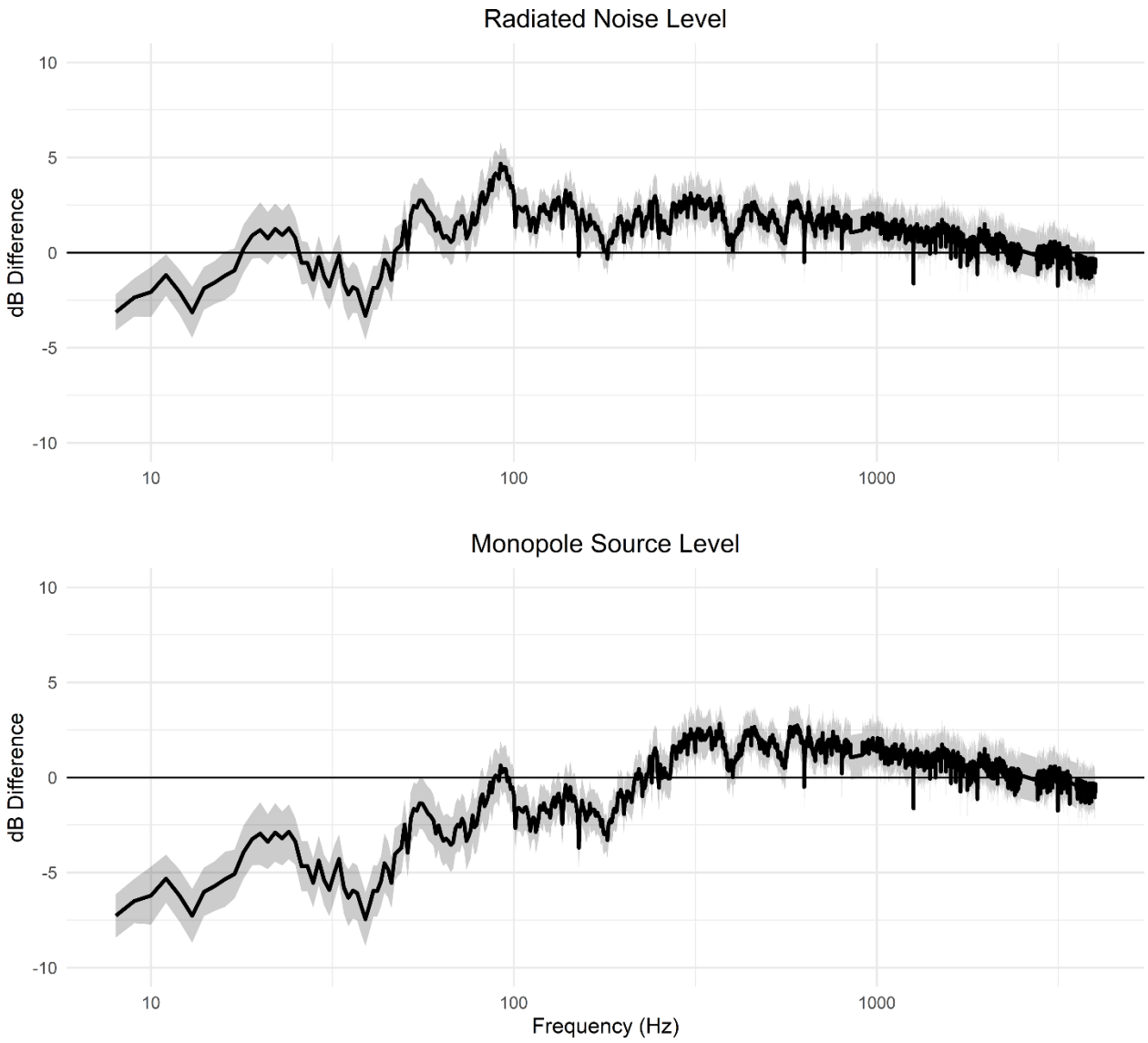

Figure 2. 8: Difference in estimated marginal means for noise levels pre- and post-retrofitting. Difference +/- standard error of estimated marginal means pre- and post-retrofitting for radiated noise levels and monopole source levels.

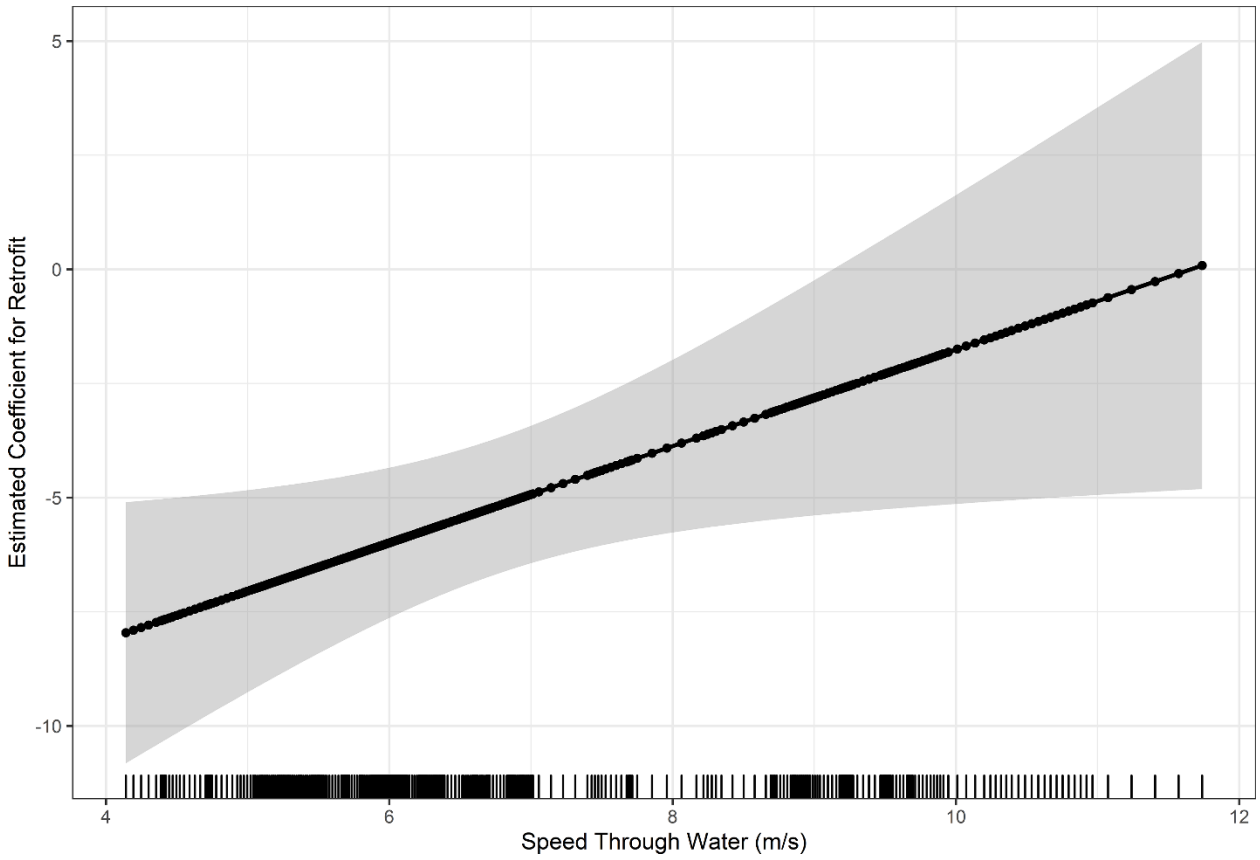

Figure 2. 9: Investigation into monopole source level interaction with speed through water. Noise reduction of retrofit (dB) with Speed Through Water for low-frequency (8–40 Hz) monopole source level. Estimated coefficients and 95% confidence intervals are displayed.

2.5 Discussion

Retrofitting efforts undertaken by Maersk were investigated for the potential of vessel noise reduction. A long-term passive acoustic dataset spanning over ten years in the SBC was used to estimate radiated noise levels and monopole source levels for more than 100 transits of Maersk G-Class vessels pre- and post-retrofit. With multiple changes to the design of the sister ships undertaken during the Radical Retrofit, there were several possible sources for the changes to sound levels highlighted in this study. An increased demand in cargo led to an increase in maximum draft during the Radical Retrofit, which led to increased cargo capacity. From one perspective, the increased cargo capacity will lead to fewer trips and thereby reduce ocean noise, however, this will only be true if global demand stays constant. From the perspective of the radiated noise level of individual vessels, a deeper draft increases the noise output, owing to a decrease in Lloyd's mirror effect at low-frequencies. The radiated noise levels are higher post-retrofit because they are not corrected for the depth of the acoustic source. Additionally, the CPA pre-retrofit was approximately 500 m farther from the sensor, which may have underestimated total levels by 2 dB in the high- and very high-frequency bands, making the difference between pre- and post-levels -1.5 to 0 dB (Figure 2.10). The low-frequency monopole source level is reduced because it accounts for the Lloyd's mirror effect, making it possible to better understand the contribution of components of the retrofit, other than the draft, to noise-generation by the vessel. Without the correction for source depth and image source interference, this study would not have resolved the monopole source level reduction in the low- and mid-frequency bands. Without an increase in TEU capacity post-retrofit and subsequent increases in draft, there might have been a reduction in radiated noise in addition to monopole source level; additional

experiments studying this effect should be conducted. Overall, the actual sound power radiated by the ships is affected by Lloyd's mirror, making the draft a key parameter for vessel noise measurements.

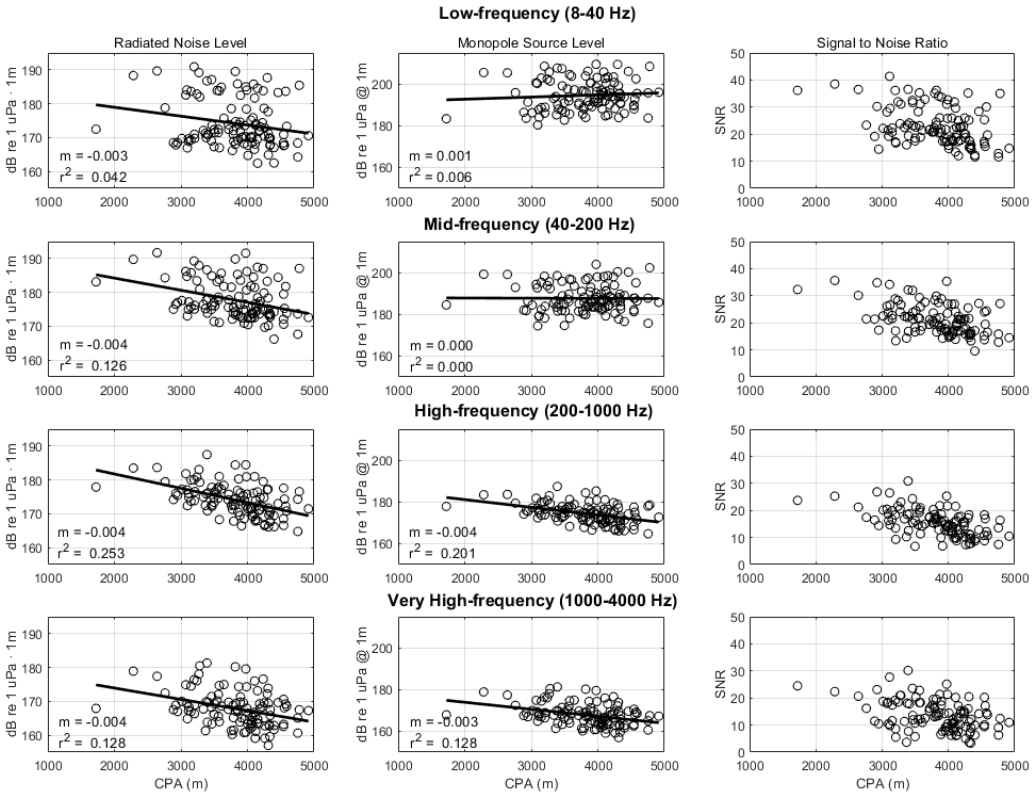

Figure 2. 10: Supplemental analysis of broadband noise levels**.** Radiated noise levels and monopole source levels in relation to Closest Point of Approach (CPA) in low-, mid-, high-, and very high-frequency bands. Signal to noise ratio for each transit in relation to CPA.

2.5.1 Retrofit Interaction with Speed

The interaction between retrofitting and STW was significant for the low-frequency monopole source level, highlighting that the retrofit-induced quieting is speed dependent. The propeller design post-retrofitting was developed for higher efficiency at slower speeds, which may be the cause of the reduction of source level due to retrofitting. Additionally, the 95% confidence intervals of the interaction were wider at high speeds because of the low number of transits obtained traveling at speeds faster than 10 m/s (19.4 knots). There were five post-retrofit transits faster than 10 m/s, but only one pre-retrofit transit faster than 10 m/s. As more shipping lines retrofit their vessels, this interaction should be investigated and verified.

2.5.2 Source of Noise Reduction

There were multiple changes during the Radical Retrofit effort undertaken by Maersk, including changes to the bow, propellers, and engine. To disentangle the effects of those changes, this study highlighted four frequency bands. Since the monopole source level noise reduction is limited to the low- and mid-frequency bands and is greatest at low speed, the noise improvement is probably related to reduction in propeller cavitation at low speed. Based on a 9 m diameter propeller turning at 60 rpm, the blade tip speed pre-retrofit would be 28.3 m/s. This is less than the post-retrofit speed of 32.1 m/s obtained from a 9.3 m diameter propeller turning at 66 rpm. Higher propeller tip speed should result in increased cavitation, so other factors must have played a decisive role in reducing the net cavitation. The addition of propeller boss cap fins most likely minimized hub vortex cavitation and subsequent vibrations in the rudder and shaft. The reduction in propeller blades and area may have reduced the number of cavitation inception points. Modifications to the bulbous bow may be another factor since this could reduce vessel resistance allowing the propeller to operate at a lower rpm, reducing propeller cavitation. Further

studies and modeling would be required to estimate the degree to which each of these factors contributed to the monopole source level reduction.

2.6 Conclusion

A reduction of monopole source level in the low-frequency band following a Radical Retrofit effort undertaken by Maersk is identified in this study. Although there were many alterations to the ship design during retrofitting, the reduction in the low-frequency band suggests that noise reduction was due to the changes in the propeller and bow design. The interaction between retrofit and speed in this study was significant, highlighting that the effect of retrofitting on monopole source level was greatest at slower speeds. As more shipping lines are implementing design changes for lower carbon shipping, source level reductions due to modifications should be investigated to reveal which alterations lead to the greatest reductions. Additionally, the interaction between retrofitting and speed found in this study should be tested in future analyses.

Ship design specifications and technologies for the reduction of noise generated by commercial ships have been identified by the International Maritime Organization with the intention to reduce ship noise on an international level. However, the specific goals of noise reduction need to be further developed. For instance, this study has demonstrated that ~2,000 more TEU can be moved with only a 0–2 dB increase in radiated noise level per transit, resulting in a reduction in noise per TEU, and a potential 20% reduction in transits. This study also demonstrated that the retrofit design efforts could reduce radiated noise levels per transit if not for the requirement to increase TEU capacity. Therefore, the IMO, IWC, and additional parties considering noise reduction will need to refine the goal of noise reduction, whether that be reducing transits, reducing noise per TEU, or reducing noise per transit. Future studies should

focus on testing the reductions found in this study with larger sample sizes, different ship types, and different design approaches to identify the most efficient methods for reducing underwater noise on an international level.

2.7 Acknowledgements

We thank Leila Hatch, Michael Jasny, Patrick Ramage, Caroline Coogan and Mark Spaulding for their support. We also thank Bruce Thayre, John Hurwitz, Ryan Griswold, and Erin O'Neill from the Scripps Whale Acoustics Lab and the crew of the R/V Shearwater for their help with data collection and processing. We also thank the Masters and Chief Engineers of the G-Class Maersk vessels for sharing draft measurements, and Maarten Nijlandn from Maersk's Naval Architecture department for detailed information on changes to the ship design during the Radical Retrofit initiative. We thank Dr. John Ahlquist for thoughtful conversations regarding policy.

Chapter 2, in full, is a reprint of the material as it appears in PLOS One. ZoBell, Vanessa M., Martin Gassmann, Lee B. Kindberg, Sean M. Wiggins, John A. Hildebrand, and Kaitlin E. Frasier. "Retrofit-induced changes in the radiated noise and monopole source levels of container ships." The dissertation author was the primary investigator and author of this paper.

Chapter 3: Effective Management Calls for Accurate Measurements: Ship Source Levels for Marine Spatial Planning

3.1 Abstract

Marine spatial planning is necessary in determining how to spatially situate human-use in the ocean in a way that best protects marine organisms and critical habitats. Commercial shipping is a human activity that extends across states, countries, and ocean basins. In order to understand the spatial extent of ship noise in the ocean and create shipping lanes that will allow for the coexistence of marine wildlife and shipping, an accurate ship source level model is needed. The most up-to-date model was trained from a composition of ships in Canada, which may not be appropriate for mapping ship noise in other areas of the world that have different ships traveling in a variety of operating conditions. In this study, we created a ship source level model using a neural network framework for ships within the Santa Barbara Channel. The model was able to predict monopole source levels with an average absolute error of 4-5 dB depending on the frequency. Future studies should continue discovering which predictor variables are the most important and influential in monopole source level estimations.

3.2 Introduction

Underwater recording devices allow for point source measurements of sound which, depending on the sound source level, frequency, and sensor location, may only be receiving sounds located 1 to 10s of kilometers away from the sensor (CITE). In order to understand the spatial extent of human-made noise in the ocean, mapping is used as a marine spatial planning tool to identify areas in which human-made noise is prominent, areas that have remained relatively pristine, and areas where there is high overlap between animals and noise which may

be targeted for management efforts ((Erbe, MacGillivray, and Williams 2012; Erbe et al. 2021; Farcas et al. 2020).

Generating maps of human-made noise relies on an understanding of the sound source. In terms of shipping, source levels of ships depend on the ship type, design, and operating conditions. Although a standard for estimating ship source levels in deep water exists, it involves cooperation of vessels under controlled test conditions which is rarely feasible in real-world commercial shipping operations (*Underwater Acoustics-Quantities and Procedures for Description and Measurement of Underwater Sound from Ships-Part 1: Requirements for Precision Measurements in Deep Water Used for Comparison Purposes Acoustique Sous-Marine-Grandeurs et Modes de Description et de COPYRIGHT PROTECTED DOCUMENT Copyright International Organization for Standardization Provided by IHS under License with ISO*, 2019). Because of this, quantifying ship source levels opportunistically has been the primary method for source level estimation (Simard et al. 2016; Megan F. McKenna, Wiggins, and Hildebrand 2013; Gassmann, Wiggins, and Hildebrand 2017; Veirs, Veirs, and Wood 2016; MacGillivray et al. 2019; ZoBell et al. 2021).

Opportunistic source level estimation has proven difficult, with different parties developing a wide variety of methodologies, including different sensor types, propagation loss models, and recording configurations (Wales and Heitmeyer 2002; MacGillivray et al. 2019; Megan F. McKenna et al. 2012; M. F. McKenna et al. 2012; Veirs, Veirs, and Wood 2016; Gassmann, Wiggins, and Hildebrand 2017; Chion, Lagrois, and Dupras 2019; Simard et al. 2016; ZoBell et al. 2021). The results of these studies have led to discrepancies of up to 30 dB for vessels within the same class in similar operating conditions (Chion, Lagrois, and Dupras 2019). The most up-to-date source level model was developed by MacGillivray & de Jong 2021 with

over 1,800 ship source measurements as a part of the Joint Monitoring Programme for Ambient Noise in the North Sea (JOMOPANS). The reference spectrum model provides a source level spectrum at one-third-octave center frequencies as a function of speed, length, and AIS ship type. The ship source measurements in this model were estimated from three different systems in the Salish Sea ranging in depth from 173 to 250 m. In order to validate and improve upon the JOMOPANS source level spectrum model, the model needs to be validated on ship source level data bases recorded from different sites and under different operating conditions. This study first compares ship source levels recorded in the Santa Barbara Channel to the JOMOPANS model to identify discrepancies. The ship source levels recorded in the SBC are then used to develop a source level model with machine learning algorithms.

3.3 Methods

Monopole source level estimation was conducted with the same methods used in ZoBell et al. (2021) and will be briefly described here. Monopole source level data was compared to model estimates from three different speeds from the JOMOPANs model to evaluate deviations between ship data collected from the SBC to the model JOMOPANs model output.

3.3.1 Ship Passage Data

An automatic identification system (AIS) receiver station situated on the top of Santa Cruz Island operated by the Santa Barbara Wireless Foundation was used to determine ship locations in this study. Each ship transit within a 4 km radius of the High-frequency Acoustic Recording Package was extracted with corresponding information such as Speed Over Ground (SOG), ship type, Course Over Ground (COG), draft, and position (longitude and latitude).

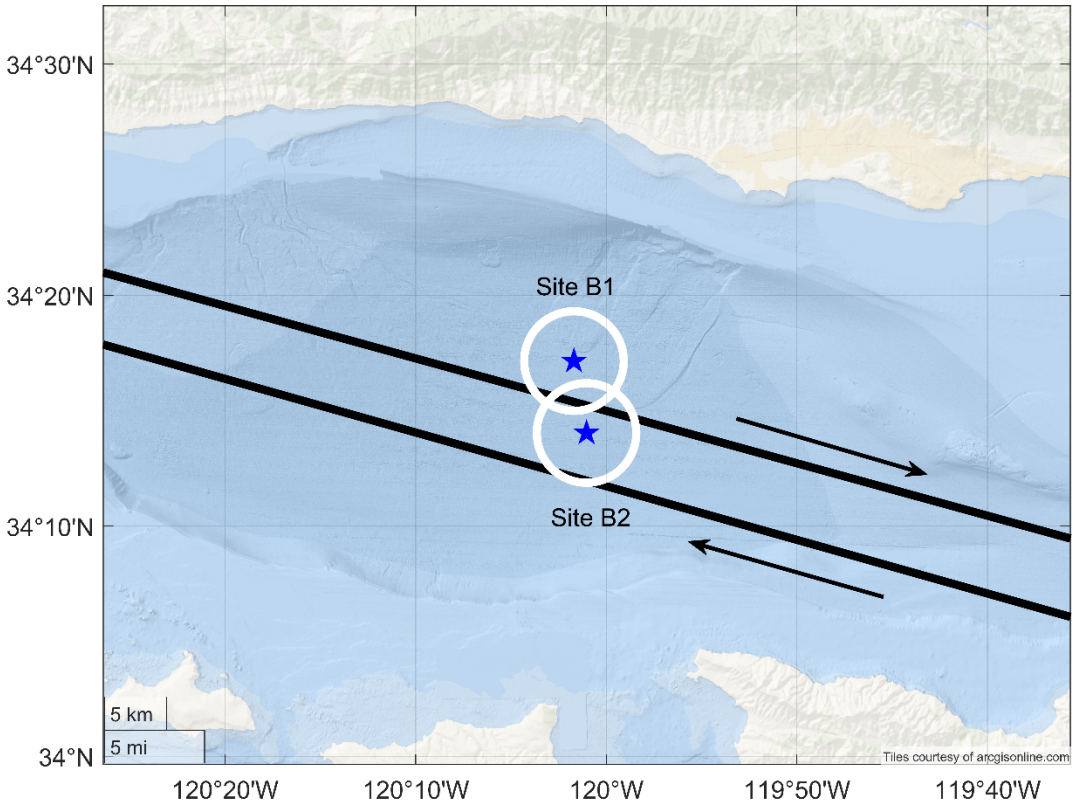

Figure 3. 1: Site Map of the two high-frequency acoustic recording packages in the Santa Barbara Channel that encompass Site B. Site B1 was in operation from 2008 to 2018. Site B2 was in operation from 2018 to present. The traffic separation scheme is shown as black lines. The arrows indicate the direction of traffic for each lane. The white circles delineate the 4 km threshold in which ships source levels were estimated.

3.3.2 Acoustic recordings

A High-frequency Acoustic Recording Package (HARP) was maintained in the Santa Barbara Channel (Site B, Figure 3.1) from February 2008 to November 2018 at 34.270°N, 120.030°W (Site B1, ~3 km north of the northbound shipping lane) and from February 2018 to present at 34.234°N 120.0173°W (Site B2, in the northbound shipping lane). Both locations are approximately ~580 m depth. The HARP was equipped with a single, omni-directional hydrophone that was suspended 10 m above the seafloor. HARP hydrophone electronics were calibrated at Scripps Institution of Oceanography and representative hydrophones were calibrated at the U.S. Navy's Transducer Evaluation Center facility in San Diego, California. Recordings were collected at a sampling rate of 200 kHz. Acoustic data were decimated by a factor of 20 to reduce computational requirements. The data were low-pass filtered with an 8th order Chebyshev Type I IIR filter during decimation to prevent aliasing and then resampled at 10 kHz. Transits contaminated with low-frequency hydrophone cable strumming, electronic noise from the instrument, marine mammal vocalizations, or ship noise from another vessel were discarded.

3.3.3 Vessel noise metrics

Radiated noise levels (L_{RN}) were calculated and monopole source levels (L_S) obtained by correcting for the effect of Lloyd's mirror using the approach of Gassmann et al. (2017) (Gassmann, Wiggins, and Hildebrand 2017). ASA/ANSI (2009) and ISO (2019) standard measurement methods were adhered to, with the exception of observation angles, which were not controlled for during these opportunistic recordings ("AMERICAN NATIONAL STANDARD Quantities and Procedures for Description and Measurement of Underwater Sound from Ships-Part 1: General Requirements" 2014; "Underwater Acoustics-Quantities and Procedures for

Description and Measurement of Underwater Sound from Ships-Part 1: Requirements for Precision Measurements in Deep Water Used for Comparison Purposes Acoustique Sous-Marine-Grandeurs et Modes de Description et de COPYRIGHT PROTECTED DOCUMENT Copyright International Organization for Standardization Provided by IHS under License with ISO" 2016). Measurements of the twelve sister ships were conducted at ranges varying from 580 m (directly above the HARP) to 4,000 m; therefore, the vertical and horizontal observation angles deviated from the ASA/ANSI (2009) requirements. To estimate monopole source levels at 1 m range, frequency-dependent sound pressure levels (L_P) were measured at and near the closest point of approach (d_{CPA}), and a frequency-dependent propagation loss model (N_{PL}) with a unique source depth (d_S) was applied with the following equation:

Source depth was set equal to 70% of the draft, as per the ISO 2019 standard. A modification of the Lloyd's mirror model, described in ZoBell et al (2021) was applied to remove mismatched interference lobes identified with ship noise measurements in compliance with ANSI/ASA (2009) and ISO (2019).

3.3.4 Model Framework

A neural network model was used as the MSL model framework. The response variables were monopole source level from 10 Hz to 2 kHz in 1 Hz bins, for a total of 1,990 response variables. The input variables were speed over ground (SOG), course over ground (COG), surface angle, ship length, draft, ship type, MMSI, and closest point of approach (CPA).

3.3.5 Model Implementation and Evaluation

Because the model had fewer input variables (8) than response variables (1,990) a principal component analysis was conducted to reduce the dimensionality of the output variables prior to training. First, the input variables and output variables were normalized by subtracting

the value by the mean and dividing by the standard deviation for each variable. A PCA was fit to each output variable with 99% explained variance, resulting in 1,000 principal components for the response variables. The predictor and response variables were then split into training (2 / 3) and testing (1 / 3) data sets and shuffled. The sequential neural network consisted of an eight node input layer, representing the eight predictor variables, four dense layers and four dropout layers, and the 1,000 principal components as the output layer. A leaky Relu activation with hyper-parameter alpha equal to 0.01 was used in all layers. Dropout layers used a dropout rate of 50%. The model was compiled with an SGD optimization with a learning rate of 0.1, and momentum of 0.5. Gradient norm scaling was achieved by setting a threshold of 1. If the norm for the gradient exceeded 1, then the vector was rescaled so that the norm of the vector equaled 1. The model was fit with a batch size of 30 and 200 epochs. Validation was performed on 10% of the training data. Predictions were computed from the test data and an inverse PCA was then conducted on the predictions to compute approximations. The approximations were de-normalized to achieve monopole source levels in 1 Hz bins. A schematic of the model implementation is shown in Figure 3.2. The model was evaluated by computing the root mean squared error and absolute error of the predictions.

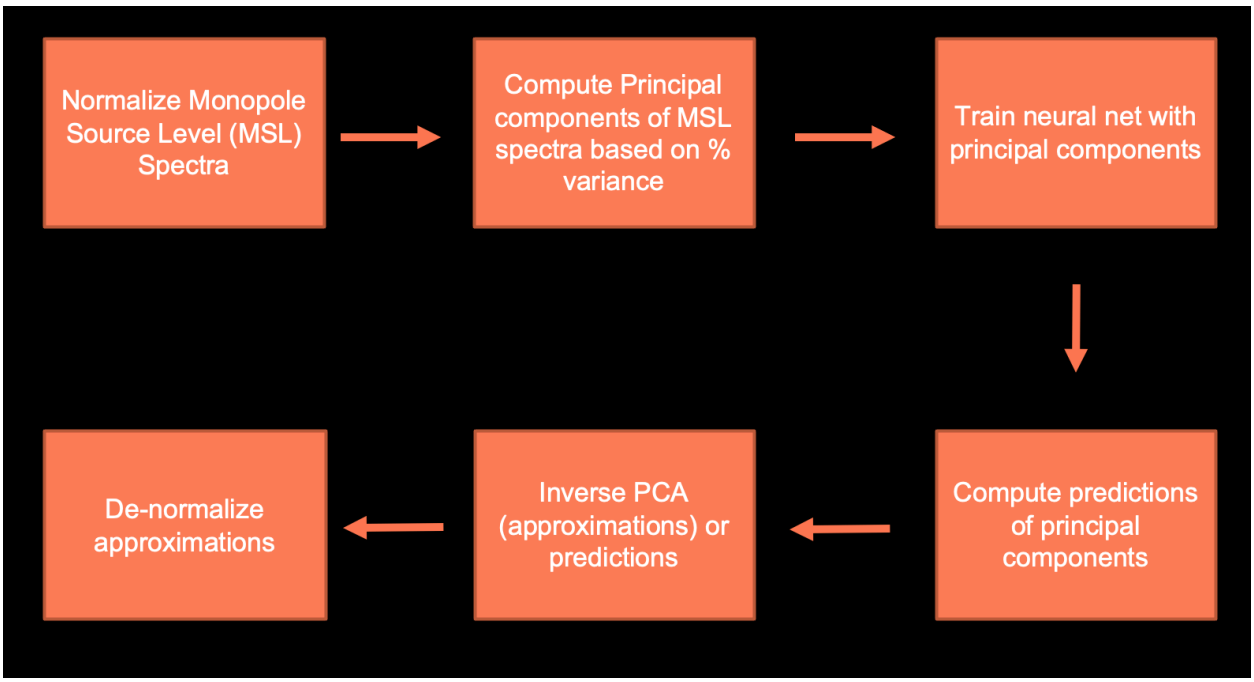

Figure 3. 2: Model Framework and Implementation Schematic.

3.4 Results

The purpose of this study was to first identify the deviations in the existing open-access model from the Joint Monitoring Programme for Ambient Noise in the North Sea (JOMOPANs) from the measurements obtained by the Scripps Whale Acoustics Lab (SWAL) in the Santa Barbara Channel (SBC).

3.4.1 Model Comparison

When comparing monopole source level estimates for container ship measurements transiting at 3 different speeds, the JOMOPANS model was approximately 0 to 22 dB different from the estimates obtained in the SBC (Figure 3.3). For monopole source levels obtained from ships transiting at 10 knots, the JOMOPANS model was approximately 10-22 dB lower than the SBC measurements, with the largest difference occurring at the lowest frequency of the model (10 Hz). When comparing the SBC measurements to the 15 knot model, there was a difference of 0 - 17 dB, with the largest difference occurring at 10 Hz. The 18 knot source level model was the closest to the SBC measurements with differences of 0 to 14 dB, with the largest difference at the lowest frequencies. Above 200 Hz, the 15 knot model is within 5 dB and the 18 knot model is within 3 dB, however, the 10 knot model at best is 10 dB different.

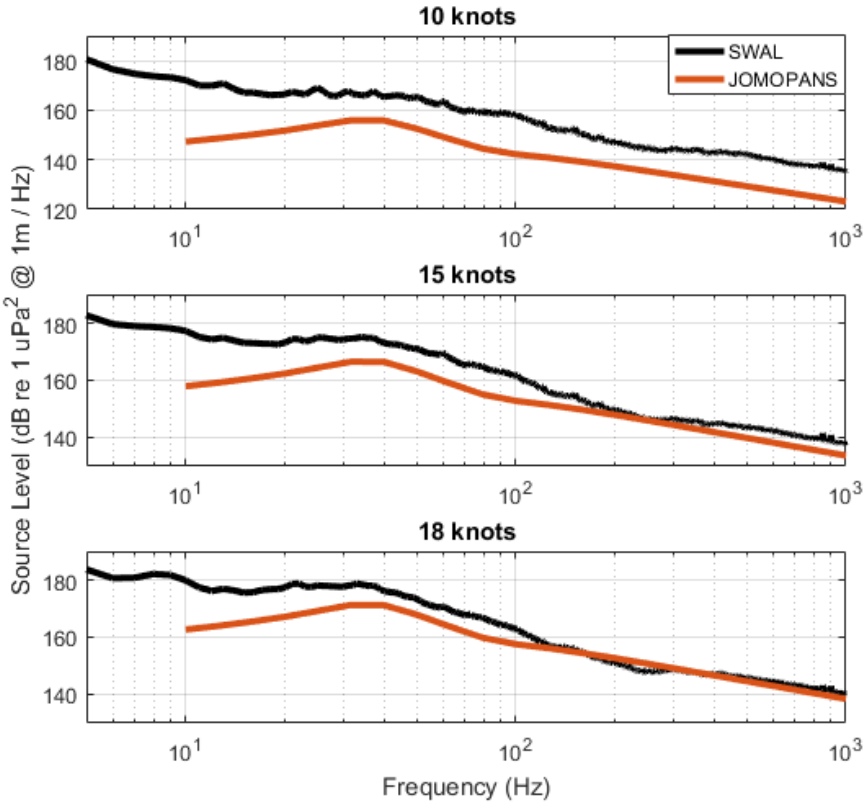

Figure 3. 3: Container ship measurements from the S compared to the JOMOPANS source level spectra model.

3.4.2 Neural Network Performance

Neural network performance was computed by calculating the RMSE and absolute error of the predictions from the original data. The min, max, and mean RMSE for the predictions of the model was 4.3, 7.8 and 5.27 dB, respectively. The RMSE was reduced with increasing epochs and leveled out at approximately 100 epochs (Figure 3.4). The min, max, and mean absolute error was 3.98, 34.88, and 4.13 dB, respectively. The mean absolute error was consistently around 5 dB, with slightly lower error from ~200 Hz to 900 Hz at approximately 4 dB (Figure 3.5). High absolute error points are due to subtraction of the model from the blade lines of the test data that were not resolved in the model (Figure 3.5). The test data is shown on the top subplot of Figure 3.6 and the predicted MSL for each transit from the model is shown on the bottom subplot. General patterns such as higher amplitude at lower frequencies are seen, however blade lines and some high amplitude transit were not resolved.

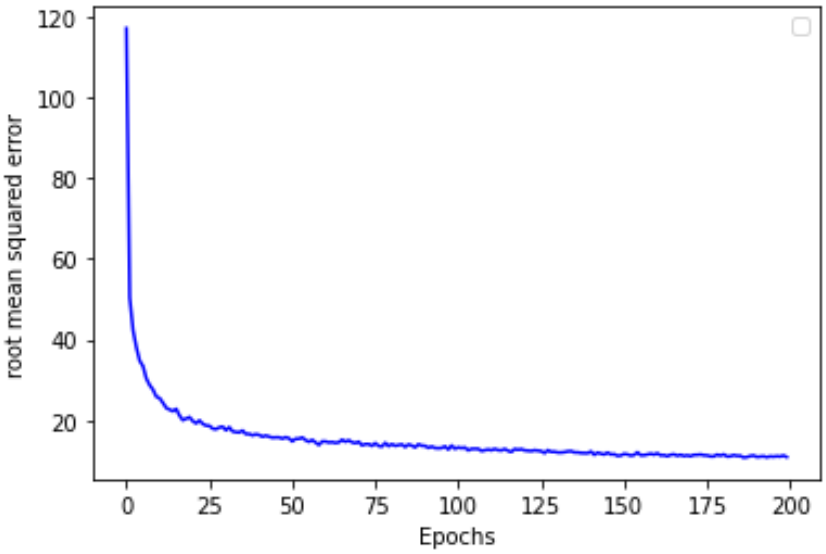

Figure 3. 4: Root mean squared error of training data over the 200 epochs.

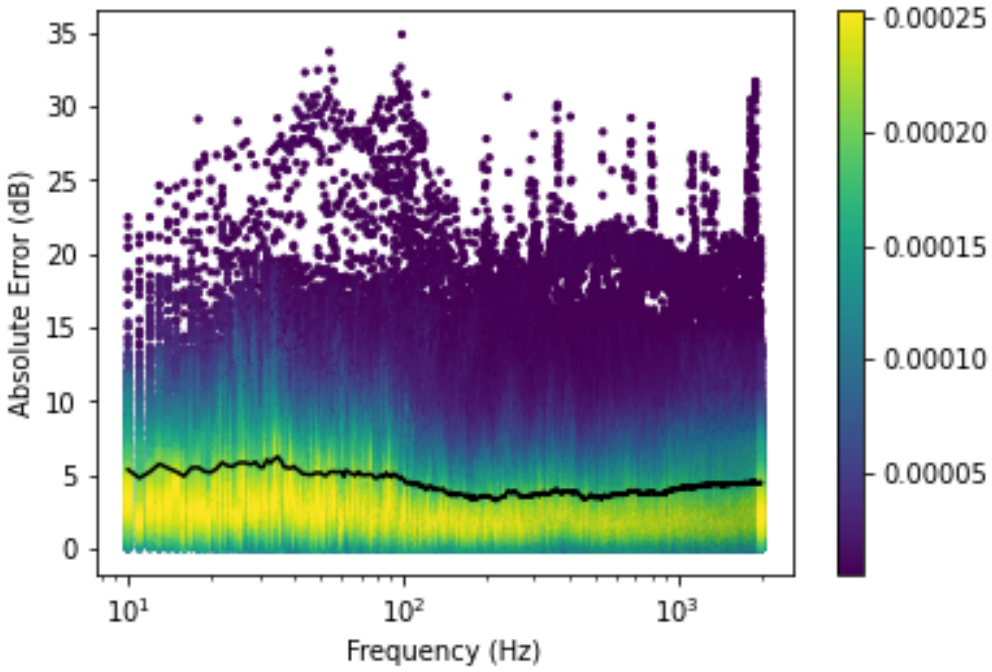

Figure 3. 5: Absolutely error for each frequency (response variable). The color bar shows the kernel density estimate.

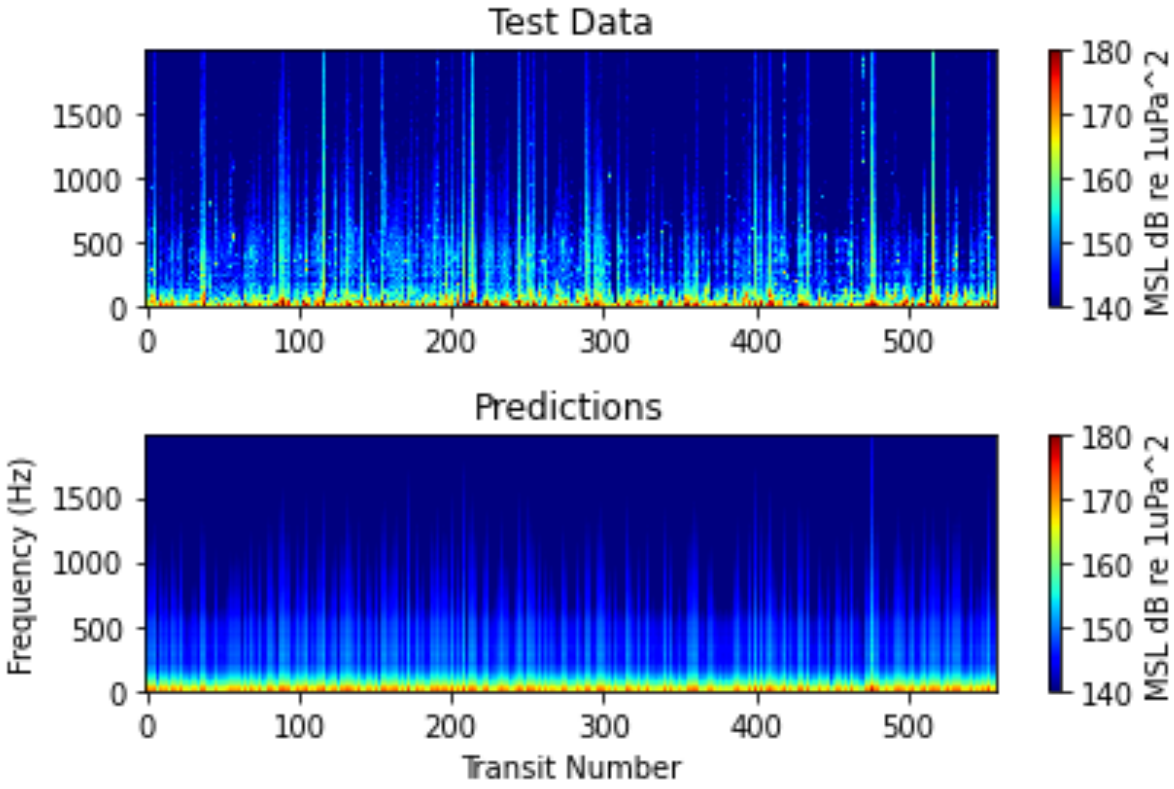

Figure 3. 6: Test data versus predictions for each transit modeled.

3.5 Discussion

Source level models are used in marine spatial planning to map noises from human-made noise sources, including commercial shipping. Accurate source level models with the composition of ships within the area being mapped are required. The most up-to-date model, JOMOPANS, was compared to ship MSLs from the SBC database and were seen to deviate, especially at frequencies < 100 Hz. In this study, a neural network approach was used to create a source level model for ships recorded within the SBC.

Eight AIS derived variables were used to compute monopole source level from 10 Hz to 2000 Hz. Principal component analysis was performed on the outputs to reduce the dimensionality from 1990 to 1000. The model was able to predict the output with mean RMSE of ~5 dB and mean absolute error of ~ 4 dB. This is comparable to the mean RMSE from the JOMOPANs model, but with predictions that are specific to the composition of ships seen in the SBC.

The model could be improved in the future by analyzing additional model frameworks, and including additional variables that are specific to the ships from the Lloyd's registry of shipping, as well as variables specific to the environment like wind, current, and wave height, although this would likely introduce complexities as well as make the model less user-friendly as some data is not open access.

Although the dimension of the output was reduced by 900 components with PCA, 1000 components is still much greater than the number of input variables. Future studies should analyze if the output could be reduced further, or try additional dimensionality reduction techniques such as autoencoders.

3.7 Acknowledgements

We thank Bruce Thayre, John Hurwitz, Ryan Griswold, and Erin O'Neill from the Scripps Whale Acoustics Lab and the crew of the R/V Shearwater for their help with data collection and processing. We also thank the Santa Barbara Wireless Foundation for their guidance on using and processing the Automatic Identification System data. This project was funded by the Dr. Nancy Foster Scholarship and the Office of National Marine Sanctuaries.

Chapter 3 contains unpublished material coauthored with ZoBell, Vanessa M., John A. Hildebrand, and Kaitlin E. Frasier. The dissertation author was the primary author of this chapter.

Chapter 4: Noise Modeling in the Santa Barbara Channel: Establishing baselines and Effective Noise Reduction Efforts for Critical Habitats

4.1 Abstract

Human-activities introduce high levels of noise into the ocean. Commercial shipping, in particular, has increased to the point that ships make a larger contribution to ocean noise than natural noise sources for most ocean locations and over a broad range of frequencies. Primeval ocean noise levels, those that would have been experienced before the advent of human-made noise in the ocean, are largely unknown. Ocean noise monitoring efforts began post-industrialization, leaving baseline sound levels under which marine organisms evolved unclear. This study modeled primeval (wind-driven) ocean noise levels and modern (wind noise plus ship noise) ocean noise levels in the Santa Barbara Channel off Southern California to establish baseline levels with and without shipping. The modern noise levels were validated with acoustic measurements from two sites equipped with High-frequency Acoustic Recording Packages. There was good agreement (~2-3 dB) between the modern noise level models when compared to measured levels for high frequencies (1 kHz), and at a site shielded by islands from long range sound propagation. There was poorer agreement (8-9 dB) for low-frequency (50 Hz) noise levels that were exposed to long-range shipping in the North Pacific. The lower frequency acoustic environment was more affected than the higher frequency noise levels, modeled at 1 kHz. Source-centric and space-centric noise reduction efforts were modeled to identify techniques with the greatest potential for conservation in critical habitats.

4.2 Introduction

Anthropogenic noise has been introduced into the ocean through numerous activities, including commercial shipping, resource extraction, and use of explosives (both civilian and

military), and has expanded at a rapid rate with the industrialization of the ocean (Wenz 1962; Hildebrand 2009). Commercial shipping is a global human-threat that crosses countries, continents, and ocean basins. Containerization was introduced in the 1950s, and has allowed for the improved efficiency of transported goods globally (Levesque 2012). According to the United Nations Conference on Trade and Development (UNCTAD), the volume of global containerized trade has more than tripled between 1990 and 2021 and is expected to continue to rise as consumer demand increases and global markets expand ("United Nations Conference on Trade and Development (UNCTAD): Navigating Stormy Waters" 2022).

Traditional methods of measuring ocean noise increases with growth in shipping have included passive acoustic monitoring, which allows for point source measurements of ambient noise from 1 - 10s of km away from the recording device based on the frequency and source level of the sound source (Andrew, Howe, and Mercer 2011; Mckenna et al. 2009; Hildebrand 2009; McDonald, Hildebrand, and Wiggins 2006). The majority of analyses have been conducted in the ocean post-industrial revolution; therefore, the ancient sound levels that marine invertebrates, fish, and mammals have evolved to thrive in are unknown, and management targets to strive for remain unclear. In order to understand primeval soundscapes that animals are adapted for across vast spatial regions, modeling is required (Sertlek et al. 2019; Erbe et al. 2021; Farcas et al. 2020). The establishments of baselines are needed in determining the levels to strive for during reduction efforts. In this study, we modeled primeval ocean noise by modeling wind-driven ocean noise and compared that to modern ocean noise by modeling noise generated by shipping.

Because noise levels have been increasing over the past several decades (McDonald, Hildebrand, and Wiggins 2006), federal and international bodies have recognized noise reduction

as a conservation need. A variety of techniques have been used to tackle noise reduction. Source-centric noise reduction has been established by speed reduction efforts as well as vessel design technologies (MacGillivray et al., 2019; ZoBell et al., 2021; ZoBell et al., 2023). Few regions have incorporated noise mitigation techniques, and the extent to which they are effective relies on vast participation from shipping companies to investigate how much participation is needed to have an effect on the acoustic environment. Space-centric noise reduction has also been identified as a method of noise mitigation through re-routing vessels to avoid noise in biologically important areas (J. V. Redfern et al. 2013). However, routing efforts can take decades to implement (US Coast Guard 2023). In addition, monitoring efforts only allow for analysis after the rerouting has been completed, which may not allow for modifications of the route that would allow for best conservation results.

In order to investigate ship noise extent and possible ship noise reduction solutions, we chose to study the Santa Barbara Channel (SBC). The SBC supports the transportation of cargo to and from the busiest shipping port in the United States, the Port of Los Angeles and the Port of Long Beach ("United Nations Conference on Trade and Development (UNCTAD): Navigating Stormy Waters" 2022). Commercial shipping in this region specifically has risen over the past several decades which has subsequently increased ocean noise levels in the Southern California Bight (Andrew, Howe, and Mercer 2011; McDonald, Hildebrand, and Wiggins 2006; Hildebrand 2009; Mckenna et al. 2009).

Temporal variability of underwater noise has been investigated in this region with point-source measurements from underwater moorings, however these recordings have not been able to extend back to the primeval ocean (Hildebrand 2009; McDonald, Hildebrand, and Wiggins 2006; Mckenna et al. 2009). Additionally, spatial variability of ship noise in Southern California

has been investigated by summing noise over the duration of one 3 month period (Jessica V. Redfern et al. 2017). However, spatiotemporal variability of ocean noise that takes into account biological relevant timescales and spatial scales are needed (Sertlek et al. 2019). No studies, to our knowledge, have been conducted in this region to understand the spatiotemporal variability of primeval ocean noise levels in comparison to the modern ocean noise levels. Having baseline noise levels will allow for an understanding of which areas have remained relatively pristine and which areas have become dominated with ship noise. Understanding the spatiotemporal variability of ship noise is required for creating focused and effective management and conservation efforts for marine mammals, fishes, and invertebrates, as species may utilize various regions of the Santa Barbara Channel during different times of the year.

Ship noise reduction has been identified as a goal by the International Maritime Organization and International Whaling Commission (Chou et al. 2021). Modeling which mechanism of noise reduction (vessel speed reduction, design) is the most effective may allow for managers to put more effort into certain techniques rather than others before changes are made. Re-routing has also been proposed in this region to identify risk to ship strikes (J. V. Redfern et al. 2013), however, the noise in which these changes would bring has not been studied. Simulating AIS data to discover how best to reduce risk to ship noise with re-routing, slow downs, and design changes will aid in streamlining changes to the most effective solutions.

The Santa Barbara Channel has been included in source-centric noise reduction efforts in ways of vessel speed reduction (ZoBell et al. 2021) and vessel design (ZoBellI et al. 2023), however, the analysis for these studies so far has been restricted to source level estimation and the spatial extent of noise reduction in unknown. In addition, the United States Coast Guard Pacific Area Command issued a Notice of Study (NOS) to determine whether new or modified

routing measures were needed to ensure safe navigation along the U.S. Pacific Coast, taking into account input from key stakeholders including National Oceanic and Atmospheric Administration and Channel Islands National Marine Sanctuaries (US Coast Guard 2023). The USCG proposed a new fairway to direct traffic from Port of Los Angeles and Port of Long Beach around the southern side of the Channel Islands National Marine Sanctuary, hereby called the "Point Mugu Fairway." To determine if the proposed fairway or modifications of the proposed fairway would reduce, increase, or keep ship noise similar to the current traffic separation scheme in the channel modeling is required. For the noise reduction analysis, we highlighted changes within three critical habitats: the Channel Islands National Marine Sanctuary, Humpback Whale Biologically Important Area, and Blue Whale Biologically Important area.

4.3 Methods

To compare with past ship noise mapping efforts in this region (Jessica V. Redfern et al. 2017), we modeled the primeval and modern ocean noise levels for the month of August, which is a rich habitat and important summer foraging month for the endangered northeastern pacific blue whale. This area also experiences high local acoustic impact from the traffic separation scheme that intersects with the blue whale and humpback whale biologically important feeding areas (BIA) and Channel Islands National Marine Sanctuary (CINMS, Figure 4.1). We looked into 4 different time resolutions, hourly, daily, weekly, and monthly, to compare differences in excess noise over different timescales and averaging methods. To validate the model with high-frequency acoustic recording packages, we first modeled primeval (wind-driven) noise and modern (wind-driven noise + ship noise) at 50 Hz and 1000 Hz in 2 x 2 km resolution within the bounds 33.80° to 34.70° and -121.22° to -118.83°, which captures the Santa Barbara Channel

and Channel Islands National Marine Sanctuary. We then validated the noise model with in situ recordings from two High-frequency Acoustic Recording Packages in the region (Figure 4.1).

For the noise reduction analysis, we modeled ship + wind noise at 50 Hz in a larger bounding box encompassing 33.26° to 35.23° and -121.22° to -118.83° to include the area with the Pt. Mugu Fairway.

4.3.1 Wind Data

To map the primeval ocean noise levels driven by wind, we used wind data that was exported from the Cross-Calibrated Multi-Platform (CCMP) wind vector analysis product and the National Oceanic and Atmospheric Administration (NOAA) buoy stations (46053 and 46054). The CCMP wind analysis is a gridded dataset of surface winds in 6-hour temporal and 0.25 degree spatial resolutions. The NOAA buoy data had a temporal resolution of 1 hour. Wind speeds varied between 0 and 18.1 m/s for the NOAA buoy data and 0 and 12.91 for the CCMP model. Wind speed from our datasets was matched with the wind speed interpolated to 0.1 m/s and the corresponding power spectral density from Hildebrand et al. 2021 in 50 Hz and 1000 Hz at the three depths under analysis. The sound pressure levels (SPLs) from wind were converted to cartesian coordinates for mapping.

4.3.2 Ship Data

Automatic identification system (AIS) data was collected from an antenna situated on the top of Santa Cruz Island serviced by the Santa Barbara Wireless Foundation (Figure 4.1, https://sbwireless.org/). Daily AIS logs were split into hourly logs in order to explore ship presence over a shorter temporal resolution. Ships were grouped into ship type based on the AIS ship type number, ship speed, and ship length, as described in MacGillivray et al. 2021 (Macgillivray and de Jong 2021). Dredgers were not found in our AIS data and were therefore

not included. Vehicle carriers cannot be distinguished from other types of cargo vessels and were therefore included within the bulker and containership types (Macgillivray and de Jong 2021). If a ship type was empty on the AIS log, the ship was labeled as “Other”. Ships with speeds equal to 0 knots were not included.

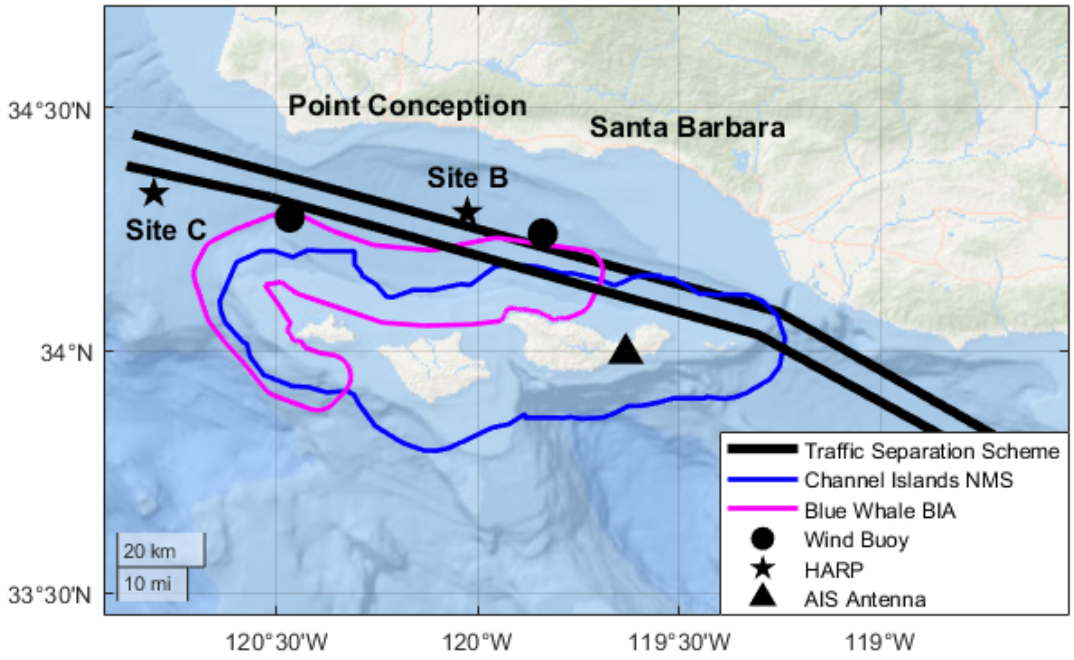

Figure 4. 1: Map of the Santa Barbara Channel with traffic separation scheme shown with black lines, high-frequency acoustic recording package sites (Site B and Site C) are labeled with pentagrams and the automatic identification system receiver site is labeled with a triangle.

Each ship track was linearly interpolated to 1 minute intervals. The cells in the 2 x 2 km grid were treated as source cells, in which the source cells activated by the presence of a ship within an hour were saved. The latitude and longitude of the source cells that were activated, the duration in minutes that the source cells were activated, and the type, speed, and length of the vessels activating the source cell were saved. All unique source cells that were activated for all ship types were also saved and used to batch run the propagation loss modeling.

4.3.3 Vessel Source Level Model

In order to model the noise generated from a ship at long ranges, the monopole source level (MSL) of the vessels are required. The MSL of a vessel is dependent on many variables including characteristics of the vessel as well as oceanographic variables (Megan F. McKenna, Wiggins, and Hildebrand 2013; Simard et al. 2016; Chion, Lagrois, and Dupras 2019; MacGillivray et al. 2019). Many source level models have been developed that use some of these characteristics to estimate source level of a ship under investigation, however, large uncertainties and variability remain (Wales and Heitmeyer 2002; Macgillivray and de Jong 2021). The most up-to-date reference spectrum model, created by the Joint Monitoring Program for Ambient Noise in the North Sea (JOMOPANS) uses data from the Enhancing Cetacean Habitat and Observation (ECHO) data set. The model uses ship speed, length, and ship class to estimate frequency-dependent MSL and was used for this study (Macgillivray and de Jong 2021). Because the composition of ships that were used to develop the model are different from the composition of ships in the Santa Barbara Channel, some adaptations were made, including the reference speeds for each ship and the total reference length for an average ship that is used in the model (Table 4.1). First, the model defines an “average ship” to have a length of 91.4 m. The average ship in our study was168.1 m, therefore the reference length was adapted to be more

specific to the vessels under investigation in our study. Additionally, the reference speeds per vessel class were adapted to equal the average speed for vessels in our study. Monopole source levels for each ship class from local AIS data and estimated from the JOMOPANS-ECHO model are shown in Figure 4.2.

Table 4. 1: Ship class categories from MacGillivray et al. 2021 with mean speed over ground (SOG, knots) and mean length over all (LOA, meters) from Santa Barbara Channel Automatic Identification System data.

Vessel Type	AIS Ship Type ID	Mean SOG (kn)	Mean LOA (m)
Fishing	30	7.5	35.0
Tug	31, 32, 52	7.3	128.9
Naval	35	12.8	45.2
Recreational	36, 37	12.5	43.9
Government/ Research	51, 53, 55	14.3	26.0
Cruise	60-69 (length l > 100 m)	10.5	152.0
Passenger	60-69 (length l ≤ 100 m)	14.3	21.6
Bulker	70, 75-79 (speed ≤ 16 kn)	11.9	240.4
Containership	71-74 (all speeds) 70, 75-79 (speed > 16 kn)	14.5	304.0
Tanker	80-89	12.4	213.6
Other	All other	11.5	73.2
Total		12.4	168.1

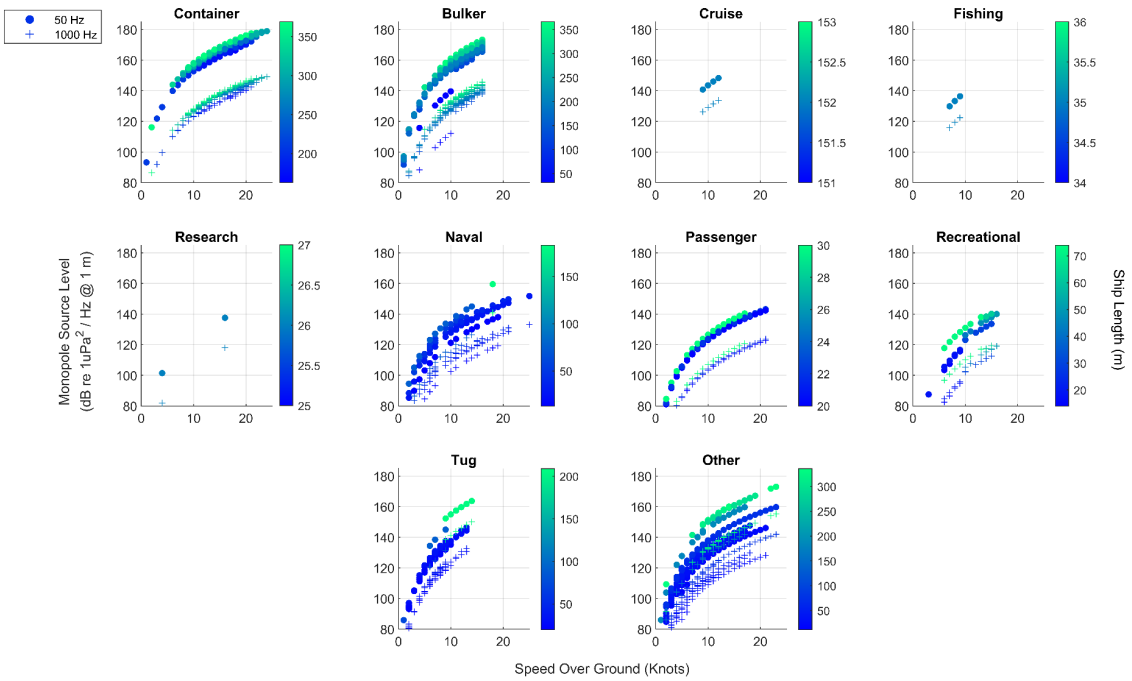

Figure 4. 2: Monopole source levels from ships within the study region in August 2017 modeled from the JOMOPANS-ECHO reference spectrum (MacGillivray et al. 2021). Monopole source levels vary with frequency, speed, length, and class.

4.3.4 Acoustic Properties of the Water Column and Sea Floor

Sound speed profiles from the California State Estimation (Short-term State Estimation) at Scripps (CASE-STSE) allowed for sound speed profiles in 1/16 degree spatial resolution of 72 depths between 0 and 2000 m at 1 day temporal resolution. The sound speed profiles were calculated with the nine-term equation for sound speed in the ocean (Mackenzie 1981).

Propagation loss modeling discussed below required information on the acoustic properties of the water column as well as the seafloor. Bathymetry data was collected from the General Bathymetry Chart of the Oceans ("General Bathymetric Chart of the Oceans (GEBCO) 2023 Grid," n.d.), which had a resolution of 15 arc-seconds. From the bathymetry data, the slope angle of the ocean floor was calculated as the arctangent of the magnitude of the gradient. Three acoustic floor types were identified from the bathymetry and slope angle: shelf, slope, and basin. Shelf was defined as regions where the bathymetry was less than 200 m and the slope angle was less than 0.75 degrees. Slope was defined as regions where slope angle was greater than 0.75 degrees. Basin was defined as regions where depth was greater than 200 m and slope angle was less than 0.75 degrees.

A sediment core was taken at each of the acoustic floor types. Compressional wave speed was measured by measuring the distance a sound wave travels through the sediment and the time taken to travel the distance. To achieve this, a sediment sample was taken from the cores. The sample was placed between two sending and receiving transducers with a dial micrometer attached to them so the travel distance was equal to the distance of the sample thickness (D). The time it took the signal to be received was recorded (T) and velocity in m/s was computed as D/T. Core locations are shown in Figure 4.3. Gravity cores were taken from the slope and basin sites and were sectioned, capped, and stored for compressional wave speed measurements in the

following weeks in the lab. A gravity core was attempted at the shelf site but was unsuccessful, as it was unable to penetrate the sediment. A multi-corer was successfully able to penetrate the sediment at the shelf site and compression wave speed measurements were taken onboard the ship directly after retrieving the sample. The compressional wave speed was 1485, 1500, and 1520 m/s for the basin, slope, and shelf site, respectively.

Surface sediment was mostly organic matter and clay (basin), silty clay (slope), and fine sand (shelf). Compressional wave speed and density at deeper sediment depths was gathered from the Ocean Discovery Program's drilling data (Site 893 Hole A) in the Santa Barbara Channel (Carson et al. 1992). The depth of the seismic basement was determined from the sediment thickness which was gathered from the Total Sediment Thickness of the World's Oceans and Marginal Seas Database (Straume et al. 2019).

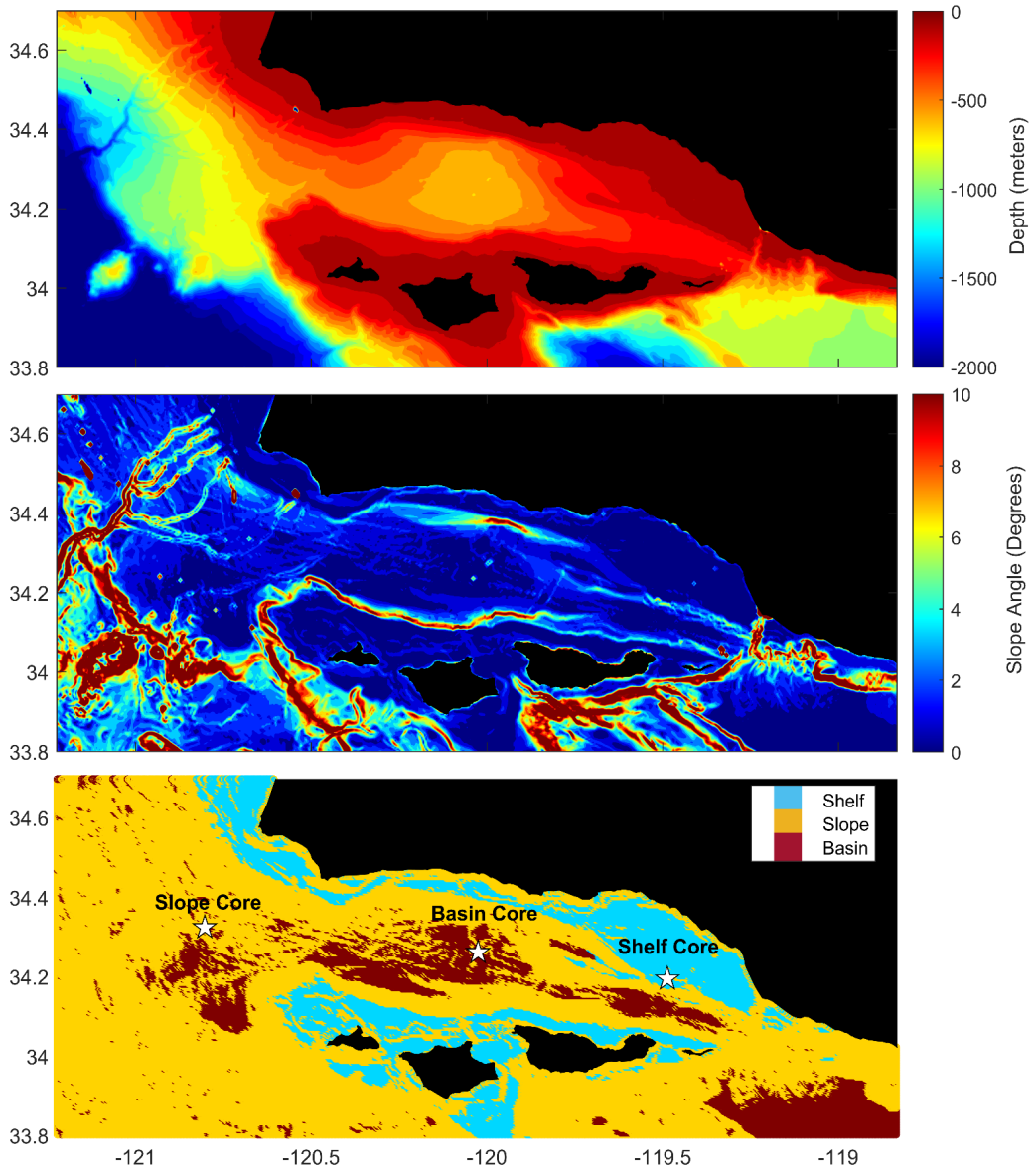

Figure 4. 3: Acoustic floor types in the Santa Barbara Channel identified by bathymetry (top) and slope angle (middle) data. The shelf zone is colored blue, slope zone is colored yellow, and the basin zone is colored red. Coring locations are labeled with a white pentagram.

4.3.5 Source-Receiver Transects

For each source cell activated by a ship transit, radials were cast in 10 degree intervals around the center latitude longitude point. The bathymetry was extracted along each radial in 500 m steps to a maximum range of 40 km. If a range step was on land, the radial stopped the point before. A range-dependent parabolic equation method, RAMGEO, was used to calculate range-depth sound propagation along each radial in a 10 m range and 5 m depth resolution. PL was then resampled at 1 m after modeling. Range-dependent sound speed profiles, sediment properties, and depth of the seismic basement were incorporated into the model. RAMGEO modeled sound propagation loss for two frequencies, 50 Hz and 1000 Hz, along each radial. The parabolic equation method is a far-field approximation. To correct for model distortions in the near-field, the minimum PL was extended from range 0 to the range of the minimum value for each depth. The two frequencies modeled allowed for an understanding of how the modern ocean may be different for low- and high-frequencies. The source depth for all ships was 5 m as that is the average depth of propellers in this region. An example of range depth propagation loss at 50 Hz and 1 kHz with the center point 34.29° and -120.14° and radial 250 degrees is shown in Figure 4.4. Bathymetry of the range depth slice is shown with a black line. Propagation loss for 50 Hz is lower beneath the sediment in comparison to 1 kHz. In the shallower depths (<50 m), constructive interference is seen for 1 kHz. In order to compare to sound levels in previous studies, PL at 30 meters was extracted from the full PL field, as this is the average depth of a swimming blue whale (Jessica V. Redfern et al. 2017). In order to validate the ship map from HARP data, the PL was also extracted at the depth of each sensor (Site B: 580 m, Site C: 750 m).

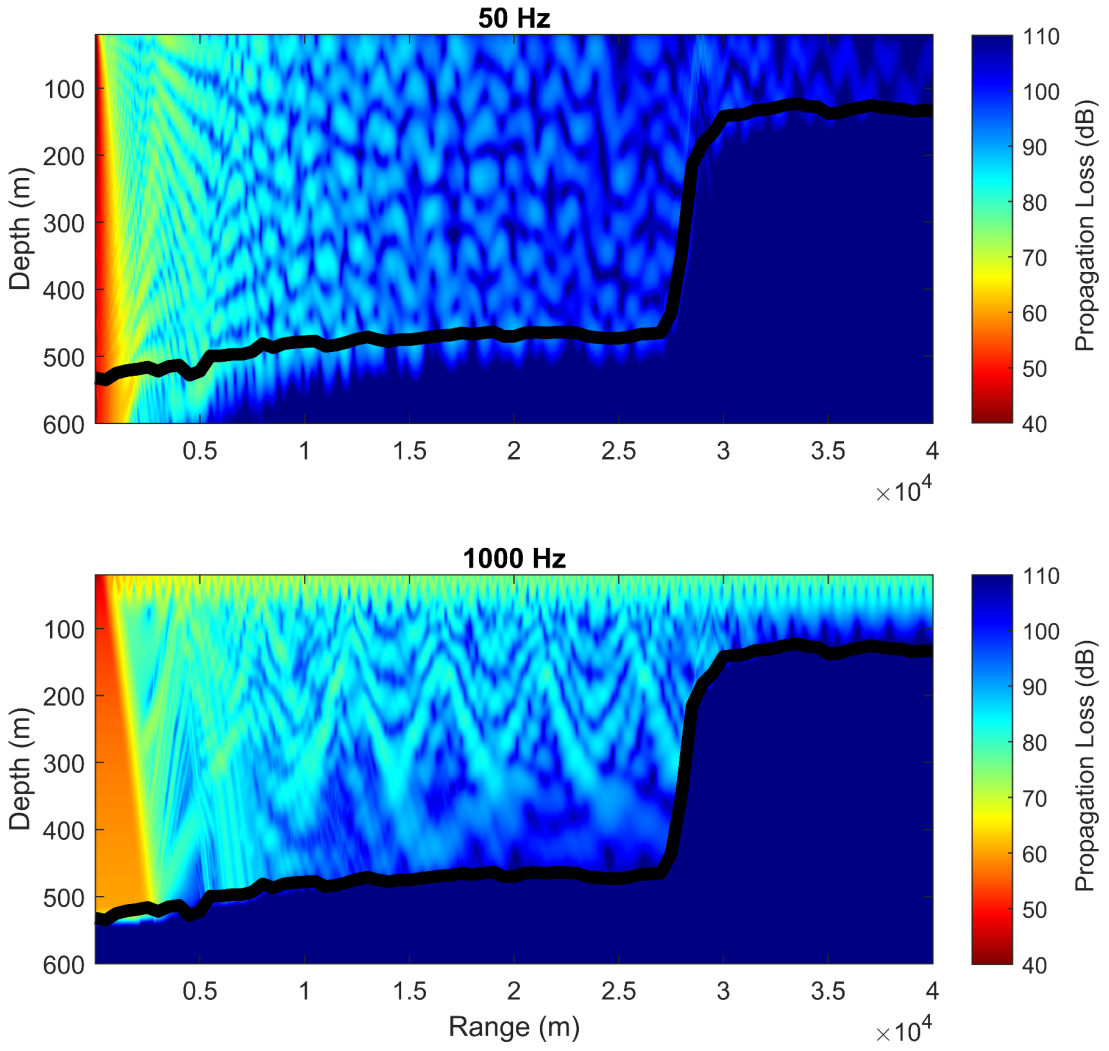

Figure 4. 4: Propagation loss at 50 Hz and 1000 Hz as a function of range and depth (meters). The dark red corresponds to lower propagation loss (40 dB) and the dark blue corresponds to high propagation loss (110 dB).

4.3.6 Sound Pressure Level (SPL) Calculation

For each hour, ships with unique source levels were treated one at a time. PL was subtracted from SL at each source center the ship activated for each depth under investigation. The duration (in seconds) that the ship with associated source level was in a source cell was added to determine sound exposure level (SEL). SPL was then calculated by subtracting 10*log10(seconds in an hour) (Equation 1). Source cells were assigned an SPL at 1.0 km (the mean distance between two random points inside the source cell) (Erbe et al. 2021).

$$SPL = SL + 10*\log10(T) - PL - 10*\log10(24*60*60) \qquad \textit{Equation 1}$$

The SPL was converted from polar coordinates to cartesian coordinates and SPL was interpolated to a 2 x 2 km grid for each of the depths. The cartesian matrix was cumulatively summed over each activated source cell and then summed across ship source level to get total SPL over the course of each hour for all ships within the region.

4.3.7 Validation

Hourly ambient noise levels were calculated from High-frequency Acoustic Recording Packages recordings. First, long-term Spectral Averages (LTSAs) were calculated by computing the spectra in 5 second bins (Wiggins and Hildebrand, n.d.). From here, 5 second time bins were averaged over an hour to result in average hourly SPLs in 1 Hz bins with values of dB re 1uPa^2/ Hz. SPLs at 50 Hz and 1 kHz were extracted and used for validation with the modern noise model. In order to use the most accurate data for validation, the modern noise model was computed with wind data from the NOAA buoy stations which allowed for hourly time

resolution. Modeled modern SPLs were compared to the measured SPLs by calculating the difference in SPL during each hour.

4.3.8 Modern versus Primeval Noise Levels

Primeval ocean noise was determined solely as the noise derived from wind speed. In order to allow for spatial differences in wind speed, the CCMP wind speed model was used for mapping wind noise. The total modern noise map was calculated by summing together wind noise and ship noise in linear space and converted to dB. Excess noise was defined as noise exceeding primeval noise, and was calculated as the difference between primeval noise and modern noise. Four temporal resolutions were investigated: hourly, daily, weekly, and monthly. The hourly map shows hourly SPL from August 1, 2017 00:00:00 to August 1, 2017 01:00:00. The daily map shows an average of hourly SPLs over the time range August 1, 2017, 00:00:00, to August 2, 2017, 00:00:00. The weekly map shows an average of hourly SPLs over the time range August 1, 2017 00:00:00 to August 8, 2017, 00:00:00. The monthly map shows an average of hourly SPLs over the entire month of August 2017.

4.3.9 Source-centric Noise Reduction

Noise reduction mechanisms were investigated to identify the greatest source of noise reduction within the three critical habitats: Channel Islands National Marine Sanctuary, Blue Whale Biologically Important Area (BIA), Humpback Whale Biologically Important Area.

Noise reduction was first modeled with a speed reduction approach. First, vessel speeds were reduced for any ship that was transiting faster than 10 knots to 10 knots. Any ship transiting at 10 knots or less was not changed. Source levels were recalculated for the ship type, length, and 10 knot speed. When ships slow down, they are in the area for a longer amount of time, thereby increasing the amount of noise injected into the environment. To account for this, the increase in

time the ship was in the source cell with the reduced speed was added to the source center. This was first modeled for all ship types and then for only container ships.

Another source-centric approach to reducing ship noise is certain ship designs. A retrofitting effort undertaken by Maersk was shown to reduce vessel source levels at 50 Hz by 2.9 dB. In order to investigate how this design and retrofitting efforts in general may affect the acoustic environment, the retrofit reduction was applied to all container ships in the month of study by subtracting 2.9 dB from the vessel's source level. Speeds were not modified in this approach.

To identify changes solely within the critical habitats, the pixels within each habitat boundary were extracted and the distribution of SPL was plotted. The pixels were extracted for the hourly, daily, weekly, and monthly time resolutions.

4.3.10 Space-centric Noise Reduction

An additional method for reducing noise is re-routing shipping traffic outside of critical habitats. To investigate the impacts of container ships transiting on different routes, five routes were analyzed: Santa Barbara Channel Traffic Separation Scheme (SBC TSS), the SBC TSS and the proposed Pt. Mugu Fairway (multi-route), the proposed Pt. Mugu Fairway, a modified Pt. Mugu Fairway, and the Pt. Mugu Fairway that allows for a 10 km buffer between the CINMS boundary and the closest lane (Figure 4.5). The average number of container ships per day within the bounds was 21, with an average speed of 13.4 knots, and an average length of 271.3 meters for the month of August 21. These metrics were used to evenly space 651 container ship transits on the four routes over the course of the month. The original AIS data was used to map ship noise contributions from vessels other than container ships.

To identify changes solely within the critical habitats, the pixels within each habitat boundary were extracted and the distribution of SPL was analyzed. The pixels were extracted for the hourly, daily, weekly, and monthly time resolutions.

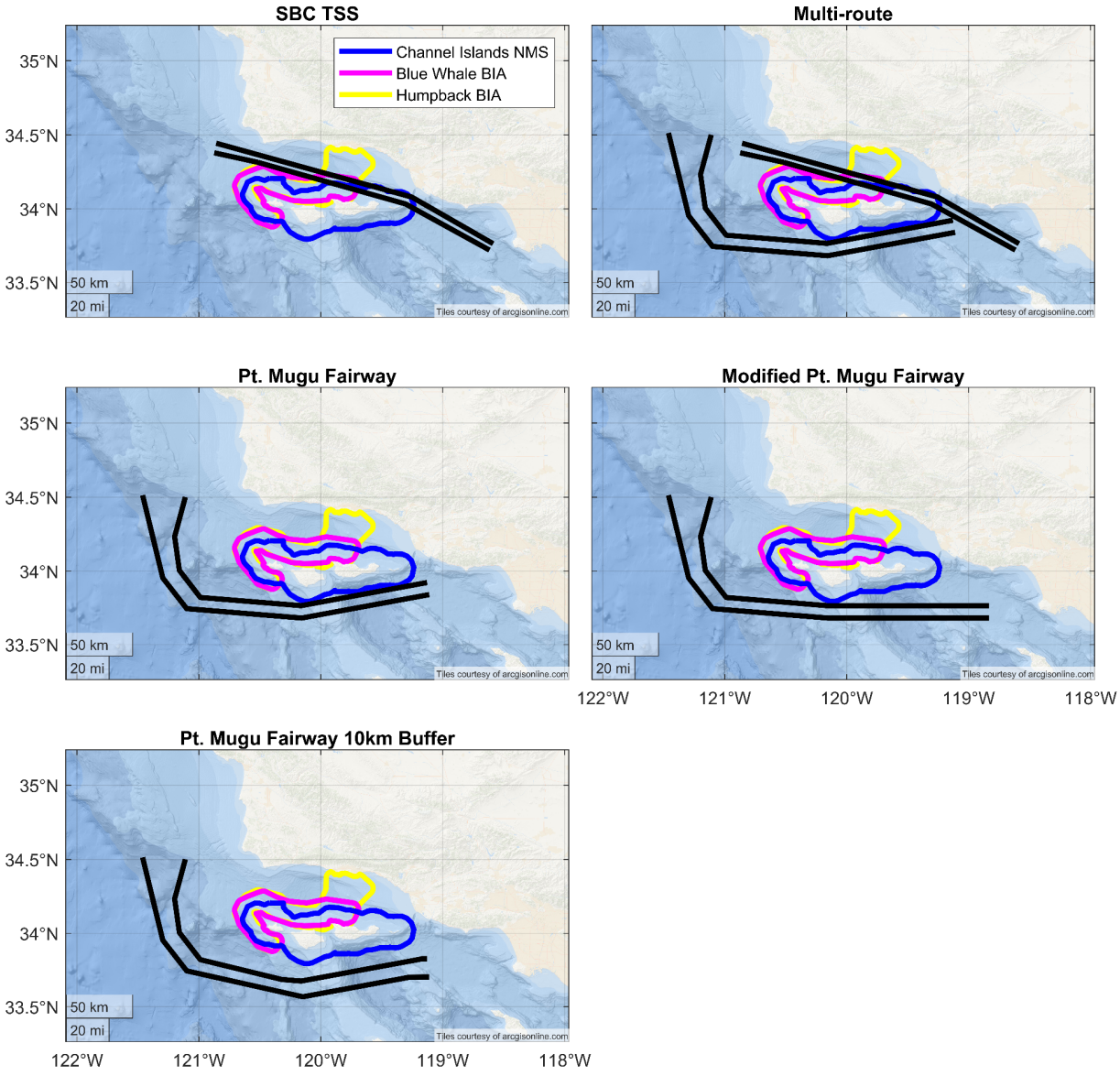

Figure 4. 5: Routes considered during space-centric noise reduction. Santa Barbara Channel Traffic Separation Scheme (SBC TSS) is the current route in the SBC. Pt Mugu Fairway has been proposed by the US Coast Guard to be put into place. Multi-route includes both the SBC TSS and the Pt. Mugu Fairway. The modified Pt. Mugu Fairway straightens the fairway away from the southeast side of the sanctuary boundary. Pt. Mugu Fairway 10 km buffer allows for the similar shape of the proposed fairway but with a spatial buffer.

4.4 Results

4.4.1 Validation

Site B 50 Hz measured SPLs (which include all noise sources) varied from 59.9 to 94.4 dB re 1uPa2/ Hz (Figure 4.6). The mean difference (modeled - measured) between the modeled SPLs and measured SPLs at Site B was 4.9 dB +/-4.0 dB, and was centered around zero. Site C 50 Hz measured SPLs varied from 72.4 to 95.0 dB re 1 uPa^2 / Hz. The difference between the modeled and measured SPLs was on average 9.8 +/- 4.9 dB, and was centered around -9 to -8 dB (Figure 4).

Site B 1 kHz measured SPLs varied from 48.1 to 68.2 dB (Figure 4.7). The mean difference was 2.9 dB +/- 2.3 dB, and was centered around 0 to -1 dB. The Site C 1 kHz measured SPLs varied from 50.3 to 69.7 dB. The mean difference of the measured data from the model was 2.5 +/- 2.0 dB and was centered around 2-3 dB.

Good agreement between the model and measurement noise levels were when ships were passing at close range, or when there were no ships present and wind noise dominated.
The model is lower at Site C than the measured data at Site C because of long range ship noise from the entire North Pacific that is able to reach the recording device that is not included in the model.

Disagreements between the measured and modeled data were investigated further by analyzing and listening to spectrograms. In times where the model was lower in SPL than the measured data, it was found that additional human operations such as winches operating on the ships were being conducted as well as marine mammal singing that was not included in the primeval model. In times where the model was higher than the measured data, it could be because the source levels used were overestimated and therefore creating an overestimated SPL.

Additionally, there may be some water column properties that are not being incorporated in the model, such as surface roughness.

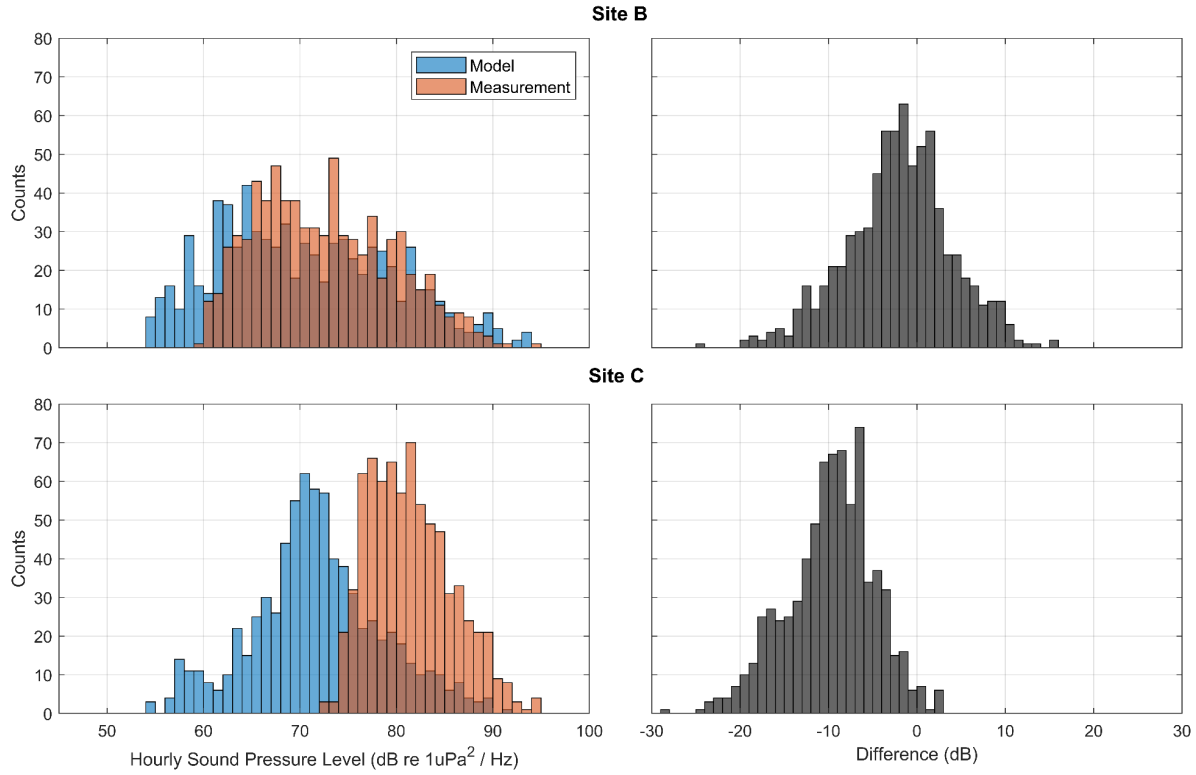

Figure 4. 6: Validation of 50 Hz hourly modeled modern sound pressure levels (SPLs) with measured SPLs from in situ High-Frequency Acoustic Recording Packages at Site B and Site C. Subplot A shows differences between 50 Hz SPLs and Subplot B shows differences between 1000 Hz.

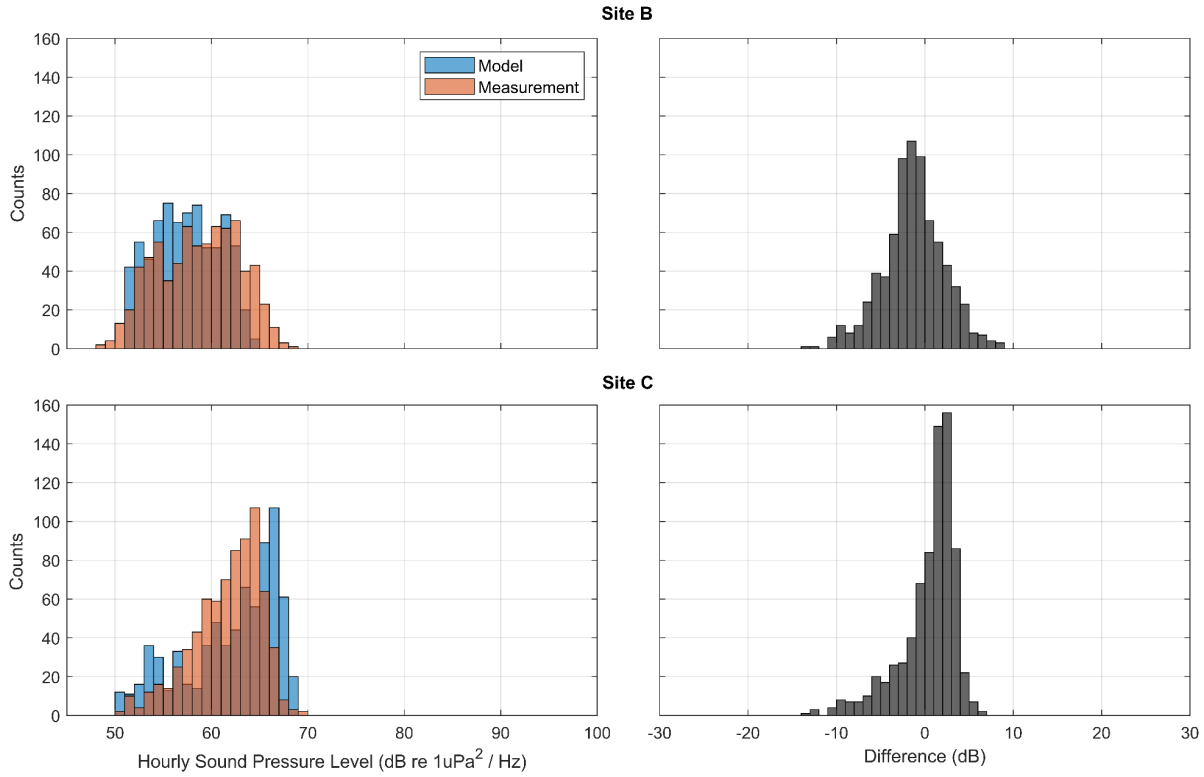

Figure 4. 7: Validation of 1000 Hz hourly modeled modern sound pressure levels (SPLs) with measured SPLs from in-situ High-Frequency Acoustic Recording Packages at Site B and Site C. Subplot A shows differences between 50 Hz SPLs and Subplot B shows differences between 1000 Hz.

4.4.2 Primeval versus Modern

Maps of SPLs for primeval, modern, and excess noise are shown in hourly, daily, weekly, and monthly averages in Figure 4.8 (50 Hz) and Figure 4.9 (1 kHz) over the month August 1 - August 31, 2017. Overall, the noise maps show the shipping lanes having majority of the noise, with smaller ships contributing to noise in the nearshore areas.

The 50 Hz noise map is higher in modern SPL and excess noise than the 1 kHz noise map for the majority of the region for all time resolutions. The 50 Hz hourly and daily primeval noise is higher than the weekly and daily noise maps in the southwest region due to high wind speeds during those specific hours that are being averaged out in the longer temporal resolutions. The weekly and monthly primeval noise maps show some gradient for wind noise but are more uniform across the region. The 50 Hz noise map had a maximum excess noise of 16.1 dB, 13.0 dB, 12.9 dB, and 13.4 dB for hourly, daily, weekly, and monthly temporal resolutions, respectively. The hourly modern and excess noise shows greater heterogeneity than the daily, weekly, and monthly modern and excess noise levels. There are two ships in the shipping lane contributing to higher modern noise levels due to higher source levels and smaller boats nearshore contributing less to modern noise levels due to likely lower source levels. The presence of small boats is seen in the hourly noise map north and west of Anacapa Island. The presence of small boats is not as well seen in the daily, weekly, and monthly noise maps, as these small boat instances are averaged out over longer temporal resolutions. The excess noise is mostly centered on the shipping lane, and extends farther in areas with deeper bathymetry, such as off of Point Conception and in the Santa Barbara Basin. There is also excess noise coming out of Santa Barbara and extending southwest.

The 1 kHz noise map had a maximum excess noise of 4.8 dB, 5.2 dB, 5.1 dB, and 5.3 dB for hourly, daily, weekly, and monthly temporal resolutions, respectively. Majority of the excess noise was concentrated in the shipping lane, with higher levels situated in the southwest corner of the shipping lane where traffic is congested between Anacapa Island and the mainland of California. The noise spreads wider distances outside of the Santa Barbara Channel off of Point Conception. As with the 50 Hz modern noise levels, heterogeneity of noise levels is captured in the shorter temporal resolution (hourly), and less so in the longer temporal resolutions.

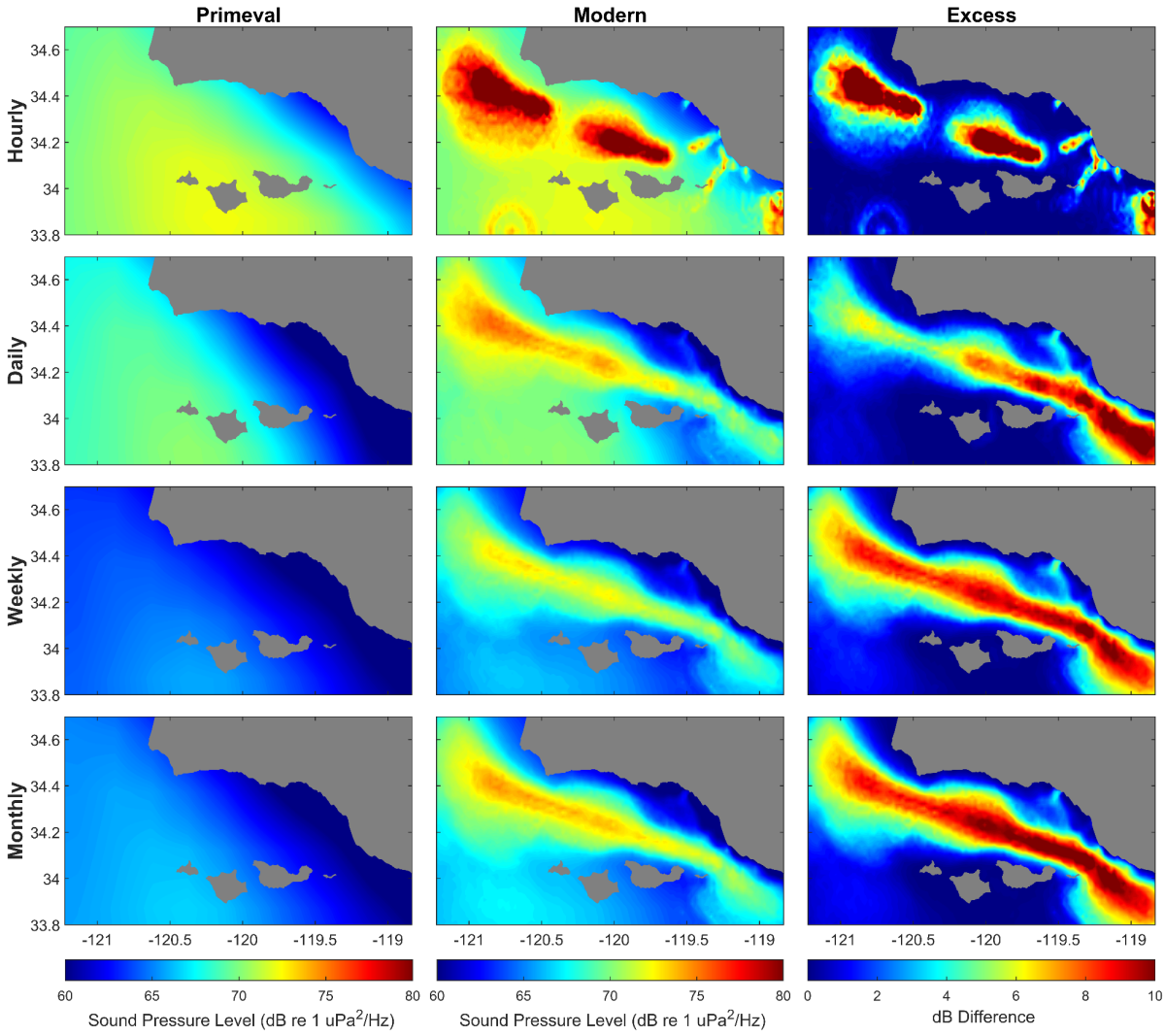

Figure 4. 8: Sound pressure levels for 50 Hz (modeled at 30 m) primeval and modern noise in hourly, daily, weekly, and monthly average time scales. Excess noise shows modern noise minus primeval noise. Note differences in color scale bars.

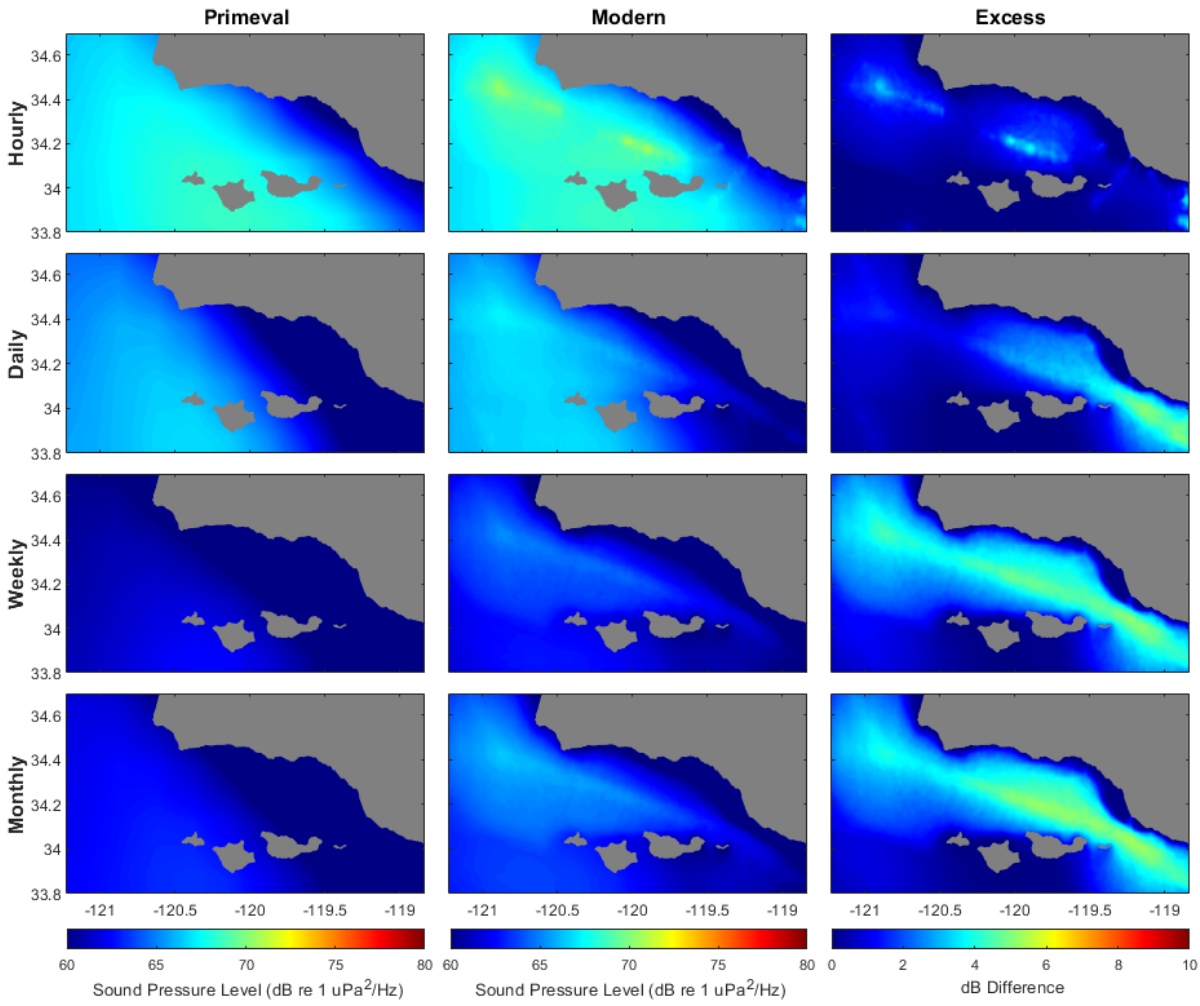

Figure 4. 9: Sound pressure levels for 1000 Hz primeval and modern noise in hourly, daily, weekly, and monthly average time scales. Excess noise shows modern noise minus primeval noise. Note differences in color scale bars.

4.4.3 Source-centric Noise Reduction

Reduction in noise through source-centric methods was investigated for speed reduction of all ships, speed reduction of container ships only, and retrofitting of container ships. The difference between the true noise levels (modern) and the simulated noise reduction techniques are shown in Figure 4.10. The speed reduction (all ship) technique had a maximum reduction of 6.80, 3.0, 3.34, 3.58 dB, respectively. The speed reduction (container ship) technique had a maximum reduction of 7.08, 2.05, 2.6, 3.22 dB, respectively. The container ship retrofit technique had a maximum reduction of 2.78, 1.25, 1.21, 1.45 dB, respectively.

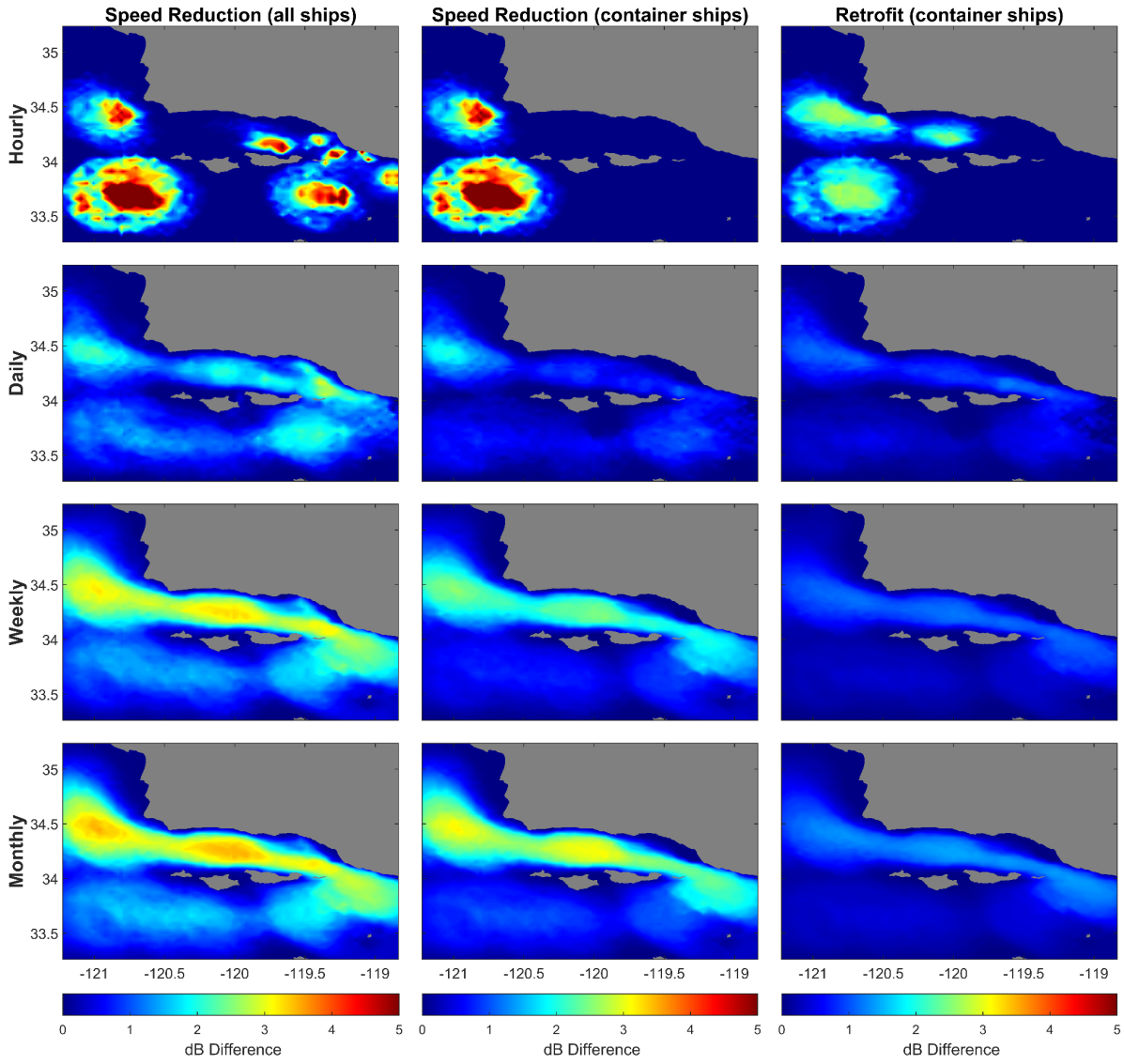

Figure 4. 10: Source-centric noise reduction approaches. Each map shows the difference from the modern noise levels calculated from the original AIS data.

When looking into the SPLs within the critical habitats, all of the speed reduction approaches reduced noise in comparison to the modern noise levels, but were not reduced enough to the primeval noise levels (Figure 4.11). The speed reduction (all ships) technique was the most effective scenario for reducing noise levels within the critical habitats. Reducing the speeds of container ships was more effective than retrofitting the container ships in all temporal resolutions under investigation. Retrofitting the container ships was the least effective scenario for reducing the noise levels in the critical habitats.

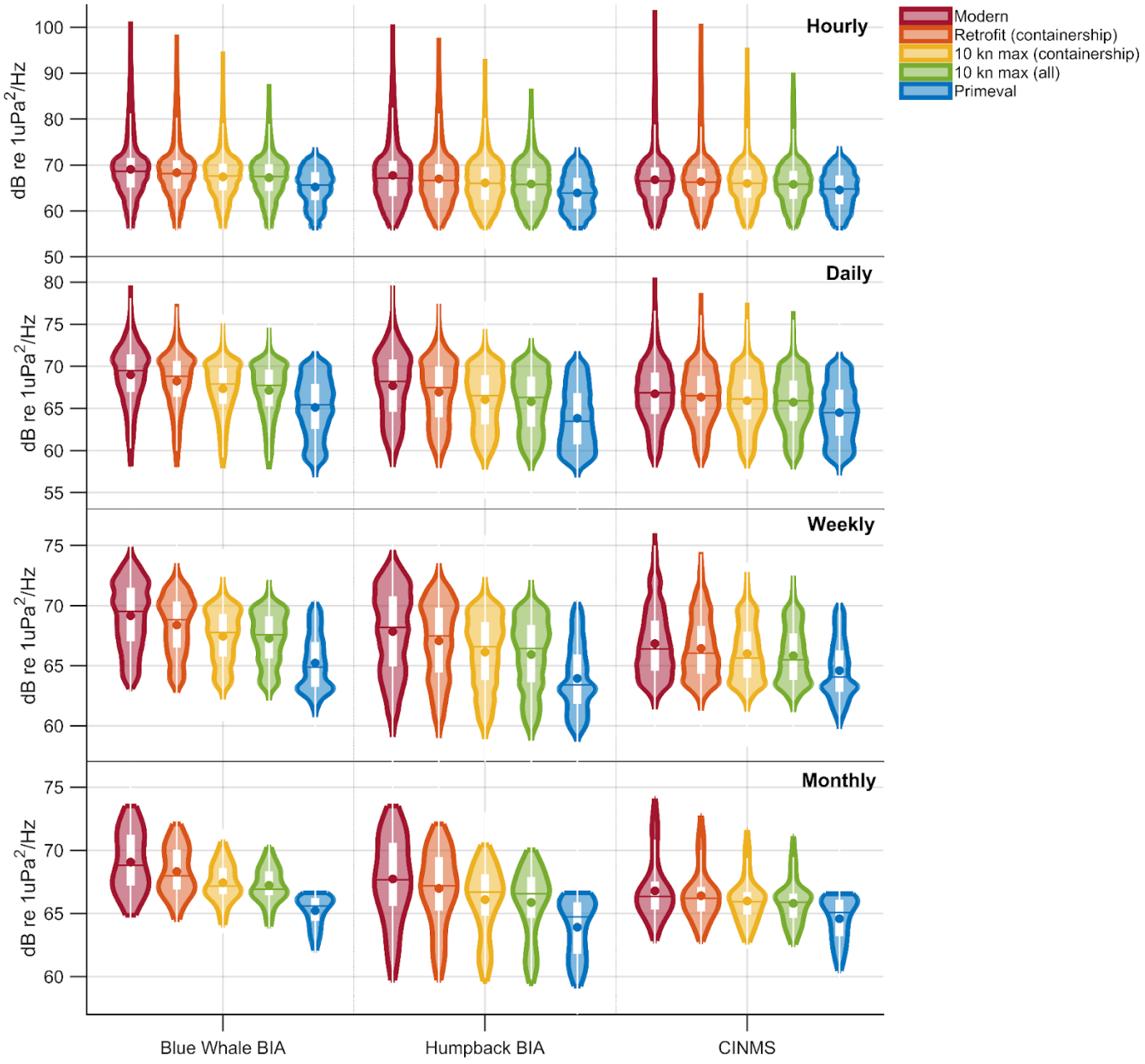

Figure 4. 11: Distribution of sound pressure levels within the blue whale BIA, humpback whale BIA, and Channel Islands National Marine Sanctuary (CINMS) for hourly, daily, weekly, and monthly temporal resolutions. Source-centric noise reduction simulations are shown with colors.

4.4.4 Space-centric Noise Reduction

The space-centric noise reduction was analyzed with 5 different routes. Because the original AIS data was modified both by averaging vessel metrics and by moving vessels, the maps were not compared to the original data. Instead, the route options were solely compared to each other (Figure 4.12). The SBC TSS route resulted in most of the energy restricted to the Santa Barbara channel. Because the bathymetry is shallower in the channel, the increase in amplitude does not spread as much as the Pt. Mugu Fairway. The Multi-route increased ship noise on the southern side of the island and reduced intensity of noise within the Santa Barbara Channel. The Pt. Mugu Fairway route decreased noise within the channel, and increased noise on the southern side of the channel. The intensity was highest where the fairway bends northeast on the south side of Santa Rosa Island. The Modified Pt. Mugu Fairway route moves noise away from the south side of Santa Cruz Island, but the intense levels on the south side of Santa Rosa Island remain. The Pt. Mugu Fairway 10 km Buffer route moves acute and chronic noise exposure away from Santa Rosa and Santa Cruz Island. Because the fairway is more offshore, the intensity is more spread out due to propagation in deep water.

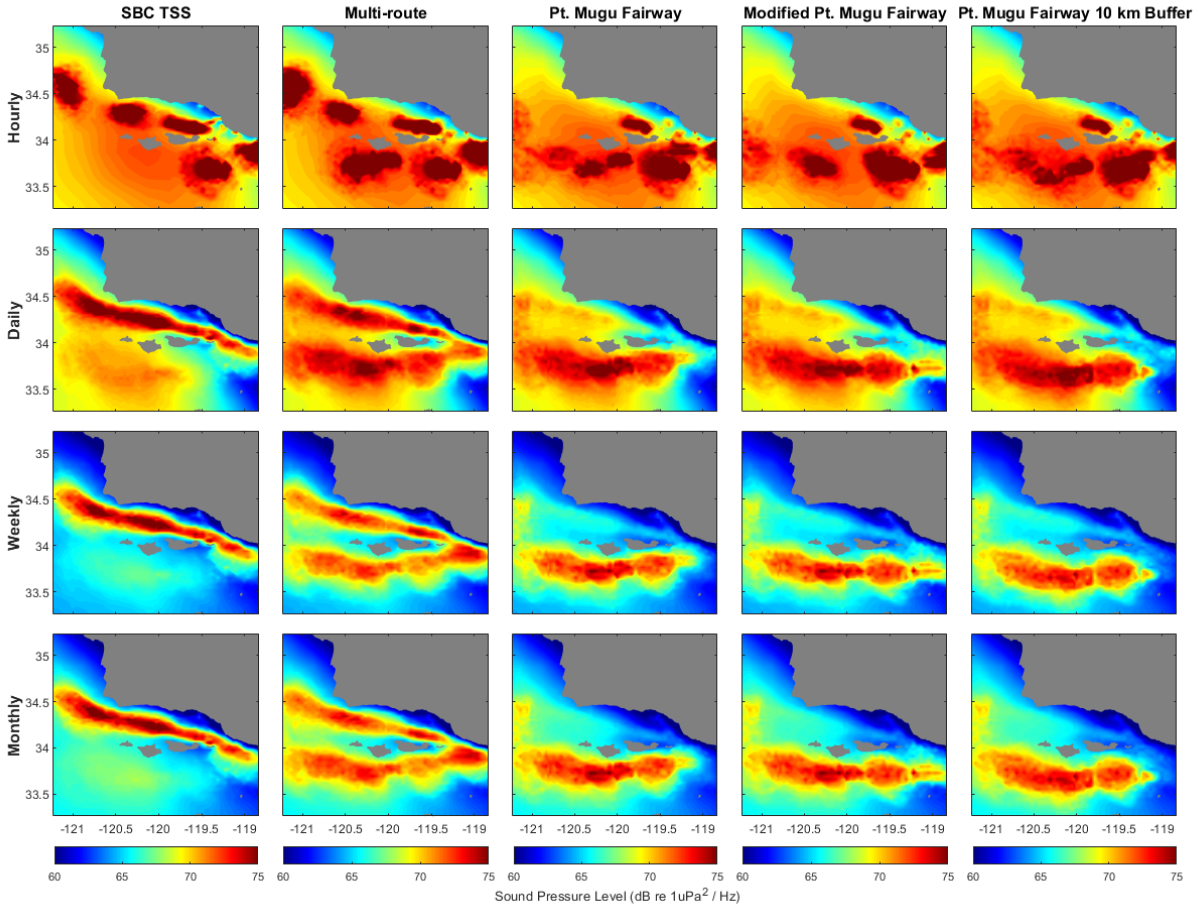

Figure 4. 12: Space-centric noise reduction approaches. 50 Hz sound pressure levels (modeled at 30 m) of five different routing options. Container ships were moved to the routes that were under investigation, small boats were mapped using the original AIS data.

The SPLs within the blue whale BIA and humpback whale BIA are shown to decrease with the removal of the SBC TSS (Figure 4.13). The CINMS showed an increase in SPL with the multi-route option. Pt. Mugu Fairway and modified Pt. Mugu Fairway allowed for some areas to reduce SPL, but the tails of high noise levels remained. The Pt. Mugu Fairway 10 km Buffer option allowed for the largest reduction in all three critical habitats and allowed for the closest SPLs to primeval.

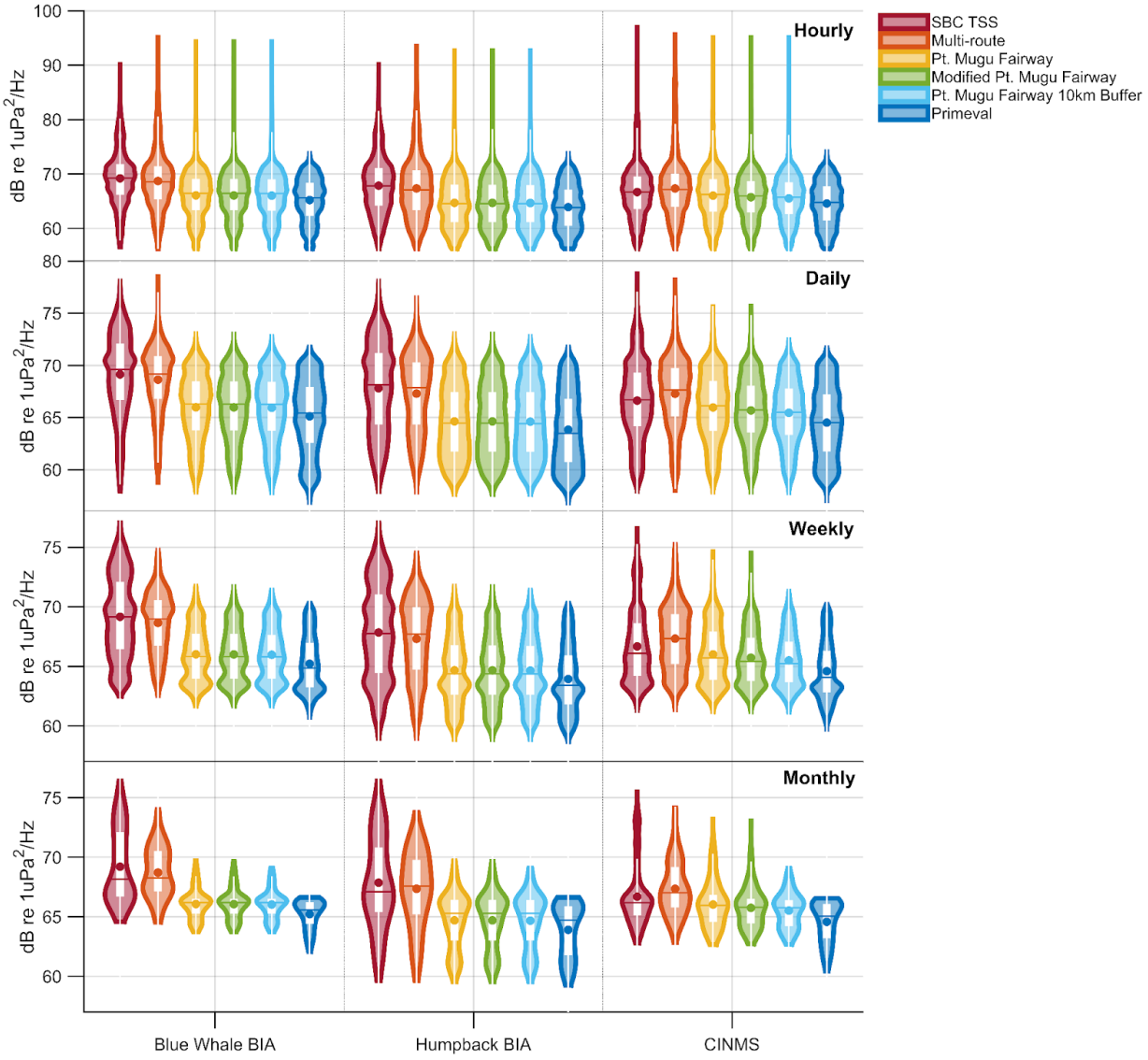

Figure 4. 13: Distribution of sound pressure levels within the blue whale BIA, humpback whale BIA, and Channel Islands National Marine Sanctuary (CINMS) for hourly, daily, weekly, and monthly temporal resolutions. Space-centric noise reduction simulations are shown with colors.

4.5 Discussion

The focus of our study was to understand how primeval noise levels compared to modern ocean noise levels in the ocean, which can aid in understanding which regions have been acoustically degraded and which regions have remained relatively pristine. Additionally, we sought to determine if noise reduction efforts were successful spatiotemporally and which noise reduction methods were most helpful in reducing noise in critical habitats. We modeled wind-drive noise which served as primeval noise and ship noise plus wind noise which served as modern ocean noise levels in two frequencies, 50 Hz and 1 kHz.

4.5.1 Limitations and Uncertainties

Although the model includes robust datasets and models including range-dependent sediment properties, sound speed, bathymetry, and sediment thickness, various assumptions and averaging are still included. In addition to the environment, errors in AIS data such as vessels without an AIS antenna or false AIS signals may lead to errors within our model. Because container ships are the dominant ship type in the region, we chose a propeller depth of 5 m. This may be deeper than propeller depths of smaller vessels, which may have a propeller depth of 1-2 m. Running the model for different source depths would potentially improve the model, however would also introduce more computational expenses. Additionally, our model utilized a source level model developed from ship measurements from the Enhancing Cetacean Habitat and Observation (ECHO) data set (Macgillivray and de Jong 2021). Although there were ample sample sizes of each of these ship types included in the model, the ships may be different from the ships that transit in the Santa Barbara Channel. The ships found within the Santa Barbara Channel were on average larger than the “average ship” used in the JOMOPANS model and also had different reference speeds for each ship type. Creating a source level model from the ships

within the Santa Barbara Channel for ship noise mapping in the same region may improve model accuracy. The JOMOPANS model includes ship type, ship speed, and ship length when estimating monopole source level (Macgillivray and de Jong 2021). Including additional variables that are known to affect source levels including oceanographic variables may be helpful in increasing source level model accuracy, however incorporating more variables may also introduce more complexities. In addition to ship noise, the wind-driven ocean wind model used was created by Hildebrand 2020 from HARP measurements from around the world. Modeling wind-noise at low-frequencies that are often dominated by shipping is difficult, and the wind model may do worse at the lower (50 Hz) frequencies. Wind noise for this reason may be overestimated for the lower frequency in this study.

To further understand model limitations and error, the model was validated at two sites within the region. Good agreement was identified when there were nearby ships present, or when ships were far away when wind noise was dominant. Poor agreement was found when there was additional human-made noise or marine mammal calling within the acoustic region.
Two-point validation was computed to compare modern ocean noise levels to measured data collected from High-frequency Acoustic Recording Packages. Good agreement (3-4 dB) was found between measured and modeled data at Site B which is located in the Santa Barbara Channel at 50 Hz and 1 kHz. Good agreement was also found at Site C, located off of point conception at 1 kHz. The modeled 50 Hz data off of point conception was approximately 9 dB lower than the measured data, which is due to long-range shipping that travels across the entire North Pacific Ocean. Low-frequencies travel further than high-frequencies, which is why the 50 Hz model is in poorer agreement to the measured data than the 1 kHz model. Inclusion of long-range shipping would improve the model at 50 Hz at Site C.

4.5.2 Primeval versus Modern Noise

Based on our model, modern noise levels were greater in many areas than wind noise alone. The excess noise levels extended beyond the traffic separation scheme and into the nearshore regions of the Santa Barbara Basin. The excess noise expanded more in deeper regions, such as off of Point Conception. The region between the mainland and Anacapa island had the highest intensity of excess noise in both frequency bands, most likely because of the bathymetry which echoes noise off of the shelves on either side of the land masses and the small corridor that yields congestion of ships in this area. Differences between primeval and modern ocean noise levels were greatest at the hourly time resolution for 50 Hz, and varied when averaging over different time resolutions. 50 Hz had higher modern noise levels than 1 kHz for all time resolutions, as ship noise is seen to decrease with increasing frequency (Farcas et al. 2020). Many marine organisms, including fish and mammals, are motile species and are not constrained to one location over the course of a month. Species may be transiting and therefore experiencing a variety of different acoustic soundscapes over the course of a month or season. Modeling noise levels in shorter time resolutions is important to capture the heterogeneity of the soundscape spatially over time (Sertlek et al. 2019). The changes in soundscape over shorter time scales (hours / days) may be important when answering questions about organisms' movement and behavior, while longer time scales (weeks / months) may be more helpful when investigating physiological questions such as stress hormone levels.

4.5.3 Noise Reduction

Noise reduction has been recognized as a priority of the International Maritime Organization, International Whaling Commission, and additional parties. Noise reduction in this study was investigated with speed reduction, retrofitting designs, and re-routing. We found that

re-routing was the most effective way to reduce noise within the three critical habitats that we studied. Speed reduction was able to reduce noise the most effectively without re-routing the shipping lanes. The retrofitting design shown here was based off of one retrofitting effort that was established to increase fuel efficiency, and not necessarily with the intent to reduce noise, although that was a co-benefit of the initiative. The reduction in noise from different vessel designs should be investigated to see if different design and retrofitting efforts are more effective in noise mitigation. However, the retrofit also included an increase in cargo capacity which may allow for reduced transit in total, which was not taken into account in this model.

Additionally, different combinations of these solutions could be investigated, such as a multi-route option with speed reduction required on the SBC TSS and normal speeds allowed on the Pt. Mugu Fairway. Temporal variations in routing may prove helpful when protecting different species. Dynamic management approaches, such as moving vessels to the Pt. Mugu Fairway in the summer when blue whales are in the region and allowing vessels to transit on the SBC TSS in the summer when blue whales are less frequent may be an option to allow for seasonal dependencies in regional use of the habitats.

Although biologically important areas exist for two endangered species within this region, additional species, such as fin whales and grey whales utilize these areas for a portion of their migration. Additional range estimates or habitat models for species of concern are needed to complete a full evaluation of the conservation benefits and tradeoffs of proposed routing plans.

4.6 Acknowledgements

This work was funded by the Dr. Nancy Foster Scholarship, the Office of National Marine Sanctuaries, the Green Family Fellowship, and the UCSD Science Policy Fellowship.

We would like to thank Bruce Thayre, Kieren Lenssen, John Hurwitz, Erin O'Neill, and Shelby Bloom from the Scripps Whale Acoustic Lab for help in data collection and processing. Thanks to the crew of the R/V Shearwater for help with HARP deployments and recoveries. Special thanks to all members of the Scripps Marine Bioacoustics Research Collaborative for guidance over the course of this project.

Chapter 4, in part is currently being prepared for submission for publication of the material. ZoBell, Vanessa M., John A. Hildebrand, and Kaitlin E. Frasier. The dissertation author was the primary researcher and author of this material.

References

Ahl, Celeste, Elaine Frey, and Seiji Steimetz. 2017. “The Effects of Financial Incentives on Vessel Speed Reduction: Evidence from the Port of Long Beach Green Flag Incentive Program.”

“AMERICAN NATIONAL STANDARD Quantities and Procedures for Description and Measurement of Underwater Sound from Ships-Part 1: General Requirements.” 2014.

Andrew, Rex K., Bruce M. Howe, and James A. Mercer. 2011. “Long-Time Trends in Ship Traffic Noise for Four Sites off the North American West Coast.” *The Journal of the Acoustical Society of America* 129 (2): 642–51. https://doi.org/10.1121/1.3518770.

Barlow, Jay. 1995. “The Abundance of Cetaceans in California Waters. Part I: Ship Surveys in Summer and Fall of 1991.” *Oceanographic Literature Review*.

Bass, Andrew H., and Jessica R. McKibben. 2003. “Neural Mechanisms and Behaviors for Acoustic Communication in Teleost Fish.” *Progress in Neurobiology*. Elsevier Ltd. https://doi.org/10.1016/S0301-0082(03)00004-2.

Benjamini, Yoav. Hochberg, Yosef. 1995. “Controlling the False Discovery Rate: A Practical and Powerful Approach to Multiple Testing.” *Journal of the Royal Statistical Society*.

Birney. 2015. “Protecting Blue Whales and Blue Skies: Report on the 2014 Vessel Speed Reduction Incentive Trial in the Santa Barbara Channel.”

Byrd, M. Flannigan, T. 2017. “Protecting Blue Whales and Blue Skies Expands to San Francisco Bay Area.”

“California Cooperative Oceanic Fisheries Investigations.” n.d. Https://Calcofi.Org/Data/Oceanographic-Data/Ctd-Cast-Files/.

Carey, W.M. 2009. “Lloyd’s Mirror-Image Interference Effects.” *Acoustics Today*.

Checkley, David M., and John A. Barth. 2009. “Patterns and Processes in the California Current System.” *Progress in Oceanography* 83 (1–4): 49–64. https://doi.org/10.1016/j.pocean.2009.07.028.

Chion, Clément, Dominic Lagrois, and Jérôme Dupras. 2019. “A Meta-Analysis to Understand the Variability in Reported Source Levels of Noise Radiated by Ships From Opportunistic Studies.” *Frontiers in Marine Science*. Frontiers Media S.A. https://doi.org/10.3389/fmars.2019.00714.

Chou, Emily, Brandon L. Southall, Martin Robards, and Howard C. Rosenbaum. 2021. “International Policy, Recommendations, Actions and Mitigation Efforts of Anthropogenic Underwater Noise.” *Ocean and Coastal Management* 202 (March). https://doi.org/10.1016/j.ocecoaman.2020.105427.

Conn, P. B., and G. K. Silber. 2013. “Vessel Speed Restrictions Reduce Risk of Collision-Related Mortality for North Atlantic Right Whales.” *Ecosphere* 4 (4): 1–16. https://doi.org/10.1890/ES13-00004.1.

Cooper, Geoffrey R, Julia Lewis, Benjamin Lozier, and Jay Golden. 2017. “DEMONSTRATING AIR EMISSIONS REDUCTIONS THROUGH ENERGY EFFICIENCY RETROFITS ON MAERSK LINE G-CLASS VESSELS.”

Croll, Donald A, Bernie R Tershy, Roger P Hewitt, David A Demer, Paul C Fiedler, Susan E Smith, Wesley Armstrong, et al. 1998. “An Integrated Approch to the Foraging Ecology of Marine Birds and Mammals.” *Deep-Sea Research II*. Vol. 45.

Erbe, Christine, Alexander MacGillivray, and Rob Williams. 2012. “Mapping Cumulative Noise from Shipping to Inform Marine Spatial Planning.” *The Journal of the Acoustical Society of America* 132 (5): EL423–28. https://doi.org/10.1121/1.4758779.

Erbe, Christine, Sarah A. Marley, Renée P. Schoeman, Joshua N. Smith, Leah E. Trigg, and Clare Beth Embling. 2019. “The Effects of Ship Noise on Marine Mammals—A Review.” *Frontiers in Marine Science*. Frontiers Media S.A. https://doi.org/10.3389/fmars.2019.00606.

Erbe, Christine, Renee P. Schoeman, David Peel, and Joshua N. Smith. 2021. “It Often Howls More than It Chugs: Wind versus Ship Noise under Water in Australia’s Maritime Regions.” *Journal of Marine Science and Engineering* 9 (5). https://doi.org/10.3390/jmse9050472.

Farcas, Adrian, Claire F. Powell, Kate L. Brookes, and Nathan D. Merchant. 2020. “Validated Shipping Noise Maps of the Northeast Atlantic.” *Science of the Total Environment* 735 (September). https://doi.org/10.1016/j.scitotenv.2020.139509.

Fiedlera’, Paul C, Stephen B Reillya, Roger P Hewitta, David Demera, Valerie A Philbricka, Susan Smitha, Wesley Armstronga, Donald A Croll, Bernie R Tershy, and Bruce R Mate’. 1998. “Blue Whale Habitat and Prey in the California Channel Islands.” *Deep-Sea Research*. Vol. 11.

Freedman, Ryan, Sean Herron, Mary Byrd, Kristi Birney, Jessica Morten, Brian Shafritz, Chris Caldow, and Sean Hastings. 2017. “The Effectiveness of Incentivized and Non-Incentivized Vessel Speed Reduction Programs: Case Study in the Santa Barbara Channel.” *Ocean and Coastal Management* 148: 31–39. https://doi.org/10.1016/j.ocecoaman.2017.07.013.

Frisk, George V. n.d. “Noiseonomics: The Relationship between Ambient Noise Levels and Global Economic Trends.” www.coltoncompany.com,.

Gassmann, Martin, Sean M. Wiggins, and John A. Hildebrand. 2017. “Deep-Water Measurements of Container Ship Radiated Noise Signatures and Directionality.” *The*

Journal of the Acoustical Society of America 142 (3): 1563–74. https://doi.org/10.1121/1.5001063.

"General Bathymetric Chart of the Oceans (GEBCO) 2023 Grid." n.d. 2023.

Gray, Leslie M, and David S Greeley. n.d. "Source Level Model for Propeller Blade Rate Radiation for the World's Merchant Fleet." http://acousticalsociety.org/content/terms.

Hildebrand, John A. 2009. "Anthropogenic and Natural Sources of Ambient Noise in the Ocean." *Marine Ecology Progress Series* 395: 5–20. https://doi.org/10.3354/meps08353.

Levesque, Peter. 2012. *The Shipping Point: The Rise of China and The Future of Retail Supply Chain Management*. John Wiley & Sons.

Linder, Alison. 2018. "Explaining Shipping Company Participation in Voluntary Vessel Emission Reduction Programs." *Transportation Research Part D: Transport and Environment* 61: 234–45. https://doi.org/10.1016/j.trd.2017.07.004.

Lindstad, Haakon, Bjørn E. Asbjørnslett, and Anders H. Strømman. 2011. "Reductions in Greenhouse Gas Emissions and Cost by Shipping at Lower Speeds." *Energy Policy* 39 (6): 3456–64. https://doi.org/10.1016/j.enpol.2011.03.044.

Macgillivray, Alexander, and Christ de Jong. 2021. "A Reference Spectrum Model for Estimating Source Levels of Marine Shipping Based on Automated Identification System Data." *Journal of Marine Science and Engineering* 9 (4). https://doi.org/10.3390/jmse9040369.

MacGillivray, Alexander O., Zizheng Li, David E. Hannay, Krista B. Trounce, and Orla M. Robinson. 2019. "Slowing Deep-Sea Commercial Vessels Reduces Underwater Radiated Noise." *The Journal of the Acoustical Society of America* 146 (1): 340–51. https://doi.org/10.1121/1.5116140.

Mackenzie, Kenneth V. 1981. “Nine-Term Equation for Sound Speed in the Oceans.” *Journal of the Acoustical Society of America* 70 (3): 807–12. https://doi.org/10.1121/1.386920.

“Maersk.” n.d. Https://Www.Maersk.Com/.

McDonald, Mark A., John A. Hildebrand, and Sean M. Wiggins. 2006. “Increases in Deep Ocean Ambient Noise in the Northeast Pacific West of San Nicolas Island, California.” *The Journal of the Acoustical Society of America* 120 (2): 711–18. https://doi.org/10.1121/1.2216565.

McKenna, M. F., S. L. Katz, S. M. Wiggins, D. Ross, and J. A. Hildebrand. 2012. “A Quieting Ocean: Unintended Consequence of a Fluctuating Economy.” *The Journal of the Acoustical Society of America* 132 (3): EL169–75. https://doi.org/10.1121/1.4740225.

McKenna, Megan F., Donald Ross, Sean M. Wiggins, and John A. Hildebrand. 2012. “Underwater Radiated Noise from Modern Commercial Ships.” *The Journal of the Acoustical Society of America* 131 (1): 92–103. https://doi.org/10.1121/1.3664100.

McKenna, Megan F., Sean M. Wiggins, and John A. Hildebrand. 2013. “Relationship between Container Ship Underwater Noise Levels and Ship Design, Operational and Oceanographic Conditions.” *Scientific Reports* 3. https://doi.org/10.1038/srep01760.

Mckenna, Megan F, Melissa Soldevilla, Erin Oleson, Sean Wiggins, and John A Hildebrand. 2009. “INCREASED UNDERWATER NOISE LEVELS IN THE SANTA BARBARA CHANNEL FROM COMMERCIAL SHIP TRAFFIC AND THE POTENTIAL IMPACT ON BLUE WHALES (BALAENOPTERA MUSCULUS).” http://www.coaa.co.uk/.

National Marine Sanctuary Foundation. 2018. “Partners Launch 2018 Program to Protect Blue Whales and Blue Skies.”

Organization International Maritime. 2014. “GUIDELINES FOR THE REDUCTION OF

UNDERWATER NOISE FROM COMMERCIAL SHIPPING TO ADDRESS ADVERSE IMPACTS ON MARINE LIFE." Vol. 44.

Raynolds, Laura. 2006. *Organic and Fair Trade Movements in Global Food Networks*. Edited by Routledge.

Redfern, J. V., M. F. McKenna, T. J. Moore, J. Calambokidis, M. L. Deangelis, E. A. Becker, J. Barlow, K. A. Forney, P. C. Fiedler, and S. J. Chivers. 2013. "Assessing the Risk of Ships Striking Large Whales in Marine Spatial Planning." *Conservation Biology* 27 (2): 292–302. https://doi.org/10.1111/cobi.12029.

Redfern, Jessica V., Leila T. Hatch, Chris Caldow, Monica L. DeAngelis, Jason Gedamke, Sean Hastings, Laurel Henderson, Megan F. McKenna, Thomas J. Moore, and Michael B. Porter. 2017. "Assessing the Risk of Chronic Shipping Noise to Baleen Whales off Southern California, USA." *Endangered Species Research* 32 (1): 153–67. https://doi.org/10.3354/esr00797.

Ross, Donald. 2005. "Ship Sources of Ambient Noise." *IEEE Journal of Oceanic Engineering* 30 (2): 257–61. https://doi.org/10.1109/JOE.2005.850879.

Rudnick, Daniel. 2016. "California Underwater Glider Network." Https://Spraydata.Ucsd.Edu/Projects/CUGN/. 2016.

Sertlek, Hüseyin Özkan, Hans Slabbekoorn, Carel ten Cate, and Michael A. Ainslie. 2019. "Source Specific Sound Mapping: Spatial, Temporal and Spectral Distribution of Sound in the Dutch North Sea." *Environmental Pollution* 247: 1143–57. https://doi.org/10.1016/j.envpol.2019.01.119.

Simard, Yvan, Nathalie Roy, Cédric Gervaise, and Samuel Giard. 2016. "Analysis and Modeling of 255 Source Levels of Merchant Ships from an Acoustic Observatory along St. Lawrence

Seaway." *The Journal of the Acoustical Society of America* 140 (3): 2002–18. https://doi.org/10.1121/1.4962557.

Simpson, S. D., M. G. Meekan, A. Jeffs, J. C. Montgomery, and R. D. McCauley. 2008. "Settlement-Stage Coral Reef Fish Prefer the Higher-Frequency Invertebrate-Generated Audible Component of Reef Noise." *Animal Behaviour* 75 (6): 1861–68. https://doi.org/10.1016/j.anbehav.2007.11.004.

Sornn-Friese, Henrik. 2019. "'Containerization in Globalization': A Case Study of How Maersk Line Became a Transnational Company." In , 103–31. https://doi.org/10.1007/978-3-030-26002-6_5.

"Southern California Coastal Ocean Observing System." n.d. Https://Hfradar.Msi.Ucsb.Edu/.

Star, J L, and M M Mullin. 1981. "Zooplanktonic Assemblages in Three Areas of the North Pacific as Revealed by Continuous Horizontal Transects." *Deep-Sea Research*. Vol. 28.

Straume, E. O., C. Gaina, S. Medvedev, K. Hochmuth, K. Gohl, J. M. Whittaker, R. Abdul Fattah, J. C. Doornenbal, and J. R. Hopper. 2019. "GlobSed: Updated Total Sediment Thickness in the World's Oceans." *Geochemistry, Geophysics, Geosystems* 20 (4): 1756–72. https://doi.org/10.1029/2018GC008115.

Tollefsen, Dag, and Stan E. Dosso. 2020. "Ship Source Level Estimation and Uncertainty Quantification in Shallow Water via Bayesian Marginalization." *The Journal of the Acoustical Society of America* 147 (4): EL339–44. https://doi.org/10.1121/10.0001096.

"Underwater Acoustics-Quantities and Procedures for Description and Measurement of Underwater Sound from Ships-Part 1: Requirements for Precision Measurements in Deep Water Used for Comparison Purposes Acoustique Sous-Marine-Grandeurs et Modes de Description et de COPYRIGHT PROTECTED DOCUMENT Copyright International

Organization for Standardization Provided by IHS under License with ISO.” 2016. www.iso.org.

“United Nations Conference on Trade and Development (UNCTAD): Navigating Stormy Waters.” 2022. New York.

Urick, R. 1975. *Principles of Underwater Sound*. McGraw-Hill.

US Coast Guard. 2023. “Pacific Coast Port Access Route Study,” no. May.

Veirs, Scott, Val Veirs, and Jason D. Wood. 2016. “Ship Noise Extends to Frequencies Used for Echolocation by Endangered Killer Whales.” *PeerJ* 2016 (2). https://doi.org/10.7717/peerj.1657.

Wales, Stephen C., and Richard M. Heitmeyer. 2002. “An Ensemble Source Spectra Model for Merchant Ship-Radiated Noise.” *The Journal of the Acoustical Society of America* 111 (3): 1211–31. https://doi.org/10.1121/1.1427355.

Walker, Tony R. 2016. “Green Marine: An Environmental Program to Establish Sustainability in Marine Transportation.” *Marine Pollution Bulletin* 105 (1): 199–207. https://doi.org/10.1016/j.marpolbul.2016.02.029.

Wartzok, Douglas, and Darlene R Ketten. 2014. “Marine Mammal Sensory Systems Blast Trauma in Marine Mammals View Project Investigations of Dolphin Echolocation and Auditory Scene Analysis: How Do Dolphins Extract Target Information from Return Echoes? View Project.” https://www.researchgate.net/publication/230691450.

Webb, Spahr C. 1998. “Broadband Seismology and Noise under the Ocean.” *Reviews of Geophysics* 36 (1): 105–42. https://doi.org/10.1029/97RG02287.

Weilgart, Lindy. 2018. “THE IMPACT OF OCEAN NOISE POLLUTION ON FISH AND INVERTEBRATES.”

Wenz, Gordon M. 1962. “Acoustic Ambient Noise in the Ocean: Spectra and Sources.” *The Journal of the Acoustical Society of America* 34 (12): 1936–56. https://doi.org/10.1121/1.1909155.

Wiggins, Sean M, and John A Hildebrand. n.d. “High-Frequency Acoustic Recording Package (HARP) for Broad-Band, Long-Term Marine Mammal Monitoring.” http://www.motorola.com.

Zhang, Ze guo, Jian chuan Yin, Ni ni Wang, and Zi gang Hui. 2019. “Vessel Traffic Flow Analysis and Prediction by an Improved PSO-BP Mechanism Based on AIS Data.” *Evolving Systems* 10 (3): 397–407. https://doi.org/10.1007/s12530-018-9243-y.

ZoBell, Vanessa M., Kaitlin E. Frasier, Jessica A. Morten, Sean P. Hastings, Lindsey E. Peavey Reeves, Sean M. Wiggins, and John A. Hildebrand. 2021. “Underwater Noise Mitigation in the Santa Barbara Channel through Incentive-Based Vessel Speed Reduction.” *Scientific Reports* 11 (1). https://doi.org/10.1038/s41598-021-96506-1.

ZoBell, Vanessa M., Martin Gassmann, Lee B. Kindberg, Sean M. Wiggins, John A. Hildebrand, and Kaitlin E. Frasier. 2023. “Retrofit-Induced Changes in the Radiated Noise and Monopole Source Levels of Container Ships.” *PLoS ONE* 18 (3 March). https://doi.org/10.1371/journal.pone.0282677.